RAINFALL ORGANIZATION AND ATMOSPHERIC CONDITIONS ASSOCIATED WITH FLASH FLOODING IN THE NORTHEASTERN UNITED STATES

A Dissertation

Presented to the Faculty of the Graduate School

of Cornell University

In Partial Fulfillment of the Requirements for the Degree of

Doctor of Philosophy

by

Stephen Michael Jessup

May 2011

RAINFALL ORGANIZATION AND ENVIRONMENTAL CONDITIONS ASSOCIATED WITH FLASH FLOOING IN THE NORTHEASTERN UNITED STATES

Stephen Michael Jessup, Ph. D.

Cornell University 2011

Heavy precipitation and flash flooding have been extensively studied in the central U.S., but less so in the Northeast. This study examines 187 flash flood events identified in *Storm Data* to better understand the organization and structure of the precipitation systems that cause flash flooding in the Northeast. Based on the organization and movement of these features on radar, the events are classified into one of four categories – back-building, linear, scalar, and scattered – and then further classified into one of four sub-types for each category. Ten of these sub-types were not previously recognized in the literature. The back-building events were the most common, followed by the scattered, scalar, and linear types. The linear event types appear to produce flash flooding less commonly in the Northeast than in other regions. In general, the sub-types producing the highest precipitation estimates are those whose structure is most conducive to a long duration of sustained moderate to heavy rainfall. Composite maps were constructed to analyze the atmospheric conditions associated with each event type. Different event types were found to be associated with a variety of upper and lower tropospheric features: long-wave troughs, short-wave troughs, cutoff lows, zonal flow, and long wave ridges. There was no clear preference for a specific atmospheric configuration to produce the heaviest rainfall; any atmospheric

configuration can produce heavy rainfall given the right ingredients. In general, the event types were found to be different from those in the central U.S. in that the events were more often found to be more disorganized in the Northeast. One event type in particular, back-building with merging features, while not more disorganized than the previously recognized event types, offers promise for improved forecasting because it makes the duration of sustained heavy precipitation potentially easier to predict.

BIOGRAPHICAL SKETCH

Steve Jessup has always been fascinated by the weather. An early obsession with snowstorms and the prospect of missing school evolved into the pursuit of a career in meteorology. Steve chose Cornell University for his undergraduate study because of its academic prowess, its natural beauty, and its matching of extracurricular activities with his interests. After earning his Bachelor's degree in Atmospheric Science, he stayed for a Master of Arts in Teaching, before deciding that public school education was not his true calling. He switched into the Master's of Science program in Atmospheric Science. His first year in the M.S. was supported by funding from the Cornell Science Inquiry Partnerships, where he was able to merge his love for teaching with his growing academic interest in atmospheric science. He has remained involved in teaching through teaching assistant positions in the Atmospheric Science department, as well as volunteer efforts with the Graduate Student School Outreach Project. This Master's project has inspired Steve to continue his education at Cornell, seeking a Ph.D. in Atmospheric Science and following up on his Master's work.

Steve has also had a long-lived interest in music, which keeps him sane when academic work becomes stressful. At one time or another, he played trumpet in practically every instrumental ensemble on campus, including the wind ensemble, jazz ensemble, marching band, pep band, symphony orchestra, chamber orchestra, pit orchestra for a musical production, and brass quintet. As a grad student, he keeps his trumpet chops intact as a full-time member of the jazz ensemble and the wind ensemble.

This dissertation is dedicated to my parents, Duane and Lois Jessup, for their steadfast love and unwavering support. It would not have been possible without them.

ACKNOWLEDGMENTS

Thanks to my parents, Duane and Lois, and to my sisters, Lori and Karen, for their constant love and support. Thanks to my mentors in the EAS department, especially Steve Colucci, Art DeGaetano, and Mark Wysocki, for their guildance and knowledge. Thanks to Brian Belcher for his computer skills. Thanks to Brian Belcher for his always-reliable computer expertise. Thanks to my musical mentors, Paul Merrill, and Cindi Johnston Turner, for giving me the opportunity to play in their ensembles. And last, but not least, thanks to my graduate student colleagues for their support, especially Christina Patricola, Emily Riddle, Mike Kelleher, and Marcus Walter.

Financial support for this project was provided by the National Science Foundation, Grant EAR 0911076.

TABLE OF CONTENTS

LIST OF FIGURES

LIST OF TABLES

LIST OF ABBREVIATIONS

NWS……National Weather Service

NOAA…….National Oceanic and Atmospheric Administration

MCC……..….Mesoscale Convective Complex

JJA…….June-July-August

HPD……Hourly Precipitation Dataset

CAPE…….convective available potential energy

LST……..…local standard time

LFC……...……..level of free convection

MBE……..….meso-beta scale element

MCS…….……..mesoscale convective system

LCL……lifted condensation level

MPS……...…..mesoscale precipitation system

LS…….leading stratiform

TS…….……trailing stratiform

PS……...…..parallel stratiform

TL/AS……...…training line/adjoining stratiform

BB……...……back-building

RUC-2…….…….Rapid Update Cycle Version 2

NCEP…… National Centers for Environmental Prediction

SPD…….…..Severe Precipitation Day

SYN…….synoptic

MULT……..multiple

SMISO……..…small mesoscale isolated

MM…….medium mesoscale

LM……..large mesoscale

SCTTR……...scattered training

SCTRAND……..…scattered random

SCTMERGE…….scattered merging

SCTSM……..scattered small

BBMERGE……...……back-building merging

BBMULT1……...……back-building followed by linear feature

BBMULT2……...…linear feature followed by back-building

LIN……...……linear

SCL…….....scalar

SCT…….scattered

AMBER……..…… Areal Mean Basin Estimated Rainfall

DHR……. Digital Hybrid Reflectivity

WSR-88D……... Weather Surveillance Radar - 1988, Doppler

NEXRAD……... Next-Generation Weather Radar

NCDC…….…… National Climatic Data Center

CODE…….…….Common Operations and Development Environment

NARR…….. North American Regional Reanalysis

NCL…….NCAR Command Language

LLJ……...….low-level jet

LIST OF SYMBOLS

θ_e…….Equivalent potential temperatur

CHAPTER 1

BACKGROUND

1.1 Introduction

Flash floods – floods occurring within six hours of the causative precipitation event (NWS, 2008) – remain one of the greatest weather hazards, despite decades of research. Flooding (including both flash floods and river floods) has resulted in more deaths in the United States since 1940 than either tornadoes or hurricanes. The 10-year average fatality rate due to flooding from 1999 to 2008 was higher than those for tornadoes and lightning, and was lower than that of hurricanes only due to the extreme death toll of Hurricane Katrina in 2005. Though flash floods remain the most hazardous form of extreme weather, improved scientific understanding and increased warning efforts have resulted in detectable improvements: flood-related deaths have begun to decrease. The ten-year average of 65 flood-related fatalities per year from 1999 to 2008 is markedly reduced from the thirty-year average of 93 flood-related fatalities per year from 1979 to 2008. (NOAA, 2010a) Besides the obvious threat to human life, flash flooding damages homes, businesses, and other structures overrun by flood waters and washes away bridges, culverts, and road surfaces. On agricultural land, rapid runoff can cause soil erosion and deprive the soil of minerals and nutrients.

Quantitative precipitation forecasting remains perhaps the greatest challenge in short-term weather forecasting (Fritsch et al., 1998). Numerical weather models have difficulty in predicting the intensity, duration, and location of heavy precipitation (Fritsch et al., 1998), making it difficult to anticipate where flash flooding will be most likely and how severe it may be. Because the atmospheric conditions on flash flood days often appear very similar to the conditions on innocuous, flood-free days (Doswell et al, 1996), it is difficult to improve the skill of the prognostications made by numerical models. Even the real-time detection of flash floods can be difficult, as

radar estimation of rainfall is inaccurate (Ciach et al., 2007) and real-time rain gauge observations are sparse compared to the spatial variability of precipitation. And finally, unlike other weather hazards such as tornadoes, lightning, and high winds, flash floods are not purely a meteorological phenomenon – the response of a stream or river to precipitation, and thus the severity of the flood's impact, depends on the hydrological response at the basin scale, which is determined not only by the intensity and duration of the precipitation itself, but also by a complex combination of spatially and temporally varying factors such as land use, soil composition, antecedent soil moisture, vegetation cover, and topography. Thus, even if it were possible to forecast accurately, or even to observe accurately in real time, the total precipitation to fall in a given basin, the hydrological response to that precipitation depends upon both the spatial and temporal distribution of that precipitation and the surface properties within the basin. For example, a small core of intense precipitation will produce a vastly different response depending on whether the precipitation falls on a highly urbanized area or on a patch of densely vegetated forest; and similarly, a broad, uniform area of long-duration moderate rainfall could generate a very different hydrological response as compared to a small, short-lived core of intense precipitation producing the same total precipitation amount over the area drained by a stream whose discharge is measured by a given stream gauge.

In the meteorological literature, there have been two common approaches to the study of flash floods. Case studies examine a single event in detail, often through a combination of observations and modeling. Cases are often selected for their severity, such as the Big Thompson Canyon, Colorado flood of 31 July 1976 (Maddox et al. 1978, Caracena et al. 1979, Yoshizaki and Ogura 1988), and the Johnstown, Pennsylvania flood of 19-20 July 1977 (Bosart and Sanders 1981, Zhang and Fritsch 1986, 1987, and 1988), which claimed 139 and 77 lives, respectively. Case studies

have the advantage of being able to pinpoint localized, event-specific features that contributed to the formation, maintenance, or dissipation of heavy precipitation. The second approach is to examine a relatively large number of cases and to describe patterns that are found to commonly arise. Maddox et al. (1979) examined 151 flash flood events throughout the United States and described four surface and upper-air patterns that generalize the most common atmospheric features of the events. More recently, Schumacher and Johnson (2006) classified 184 heavy precipitation events based on the organization of the precipitation and described the prominent surface and upper-air features associated with each type of event. This "climatological" approach provides a more general indication of the conditions that may be likely to produce flash flooding, based upon more general categories of organization of the atmospheric conditions and the rainfall.

1.2 Motivation

While many studies have examined flash flooding and heavy precipitation across the country (e.g. Maddox et al., 1979; Schumacher and Johnson, 2006; Brooks and Stensrud, 2000; Karl and Knight, 1998; Winkler et al., 1988), regional studies have focused on the southeastern United States (Konrad, 1997; Geerts, 1998), the midwest (Junker et al., 1999), the southern plains (Bradley and Smith, 1994), the western United States (Maddox et al., 1980), and the mid-Atlantic (Giordano and Fritsch, 1991), but have neglected the northeastern United States. Further, the Northeast contains a smaller percentage of events as compared with other regions in the national climatologies of Maddox et al. (1979) and Schumacher and Johnson (2006) (see Figures 1.1 and 1.2 below). Thus, there is a need for an expanded analysis of flash flooding in the northeastern United States.

Figure 1.1 Flash floods examined by Maddox et al. (1979).

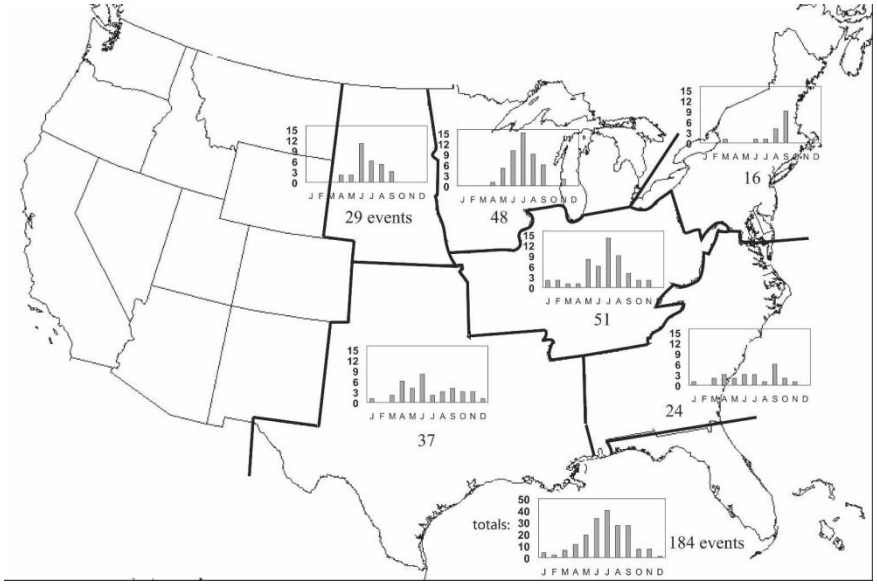

Figure 1.2 Extreme precipitation events studied by Schumacher and Johnson (2006), with histograms displaying the annual distribution of events for each region.

There is reason to suspect that the most common organizational modes of precipitation in the Northeast may differ from those in other regions of the country.

Fritsch et al. (1986) examined the precipitation resulting from mesoscale convective complexes (MCCs) as a percentage of the total precipitation and found that these systems accounted for anywhere from 30% to 70% of the precipitation from April through September over a large area spanning from the Rocky Mountains to the Mississippi River. These systems, however, rarely travel east of the Appalachian Mountains (Tollerud et al., 1987). The MCCs studied by Fritsch et al. (1986) tend to be overnight phenomena, while ordinary convection is most common in the late afternoon hours, fed by diurnal heating (Davis, 2001). In examining the timing of heavy rainfall, Winkler et al. (1988) found that the heaviest precipitation tends to occur in the late afternoon to early evening hours in the eastern United States, but in the overnight hours in the central United States, supporting the contention that the precipitation systems affecting the Northeast are different in structure than those affecting the central U.S. Schumacher and Johnson (2006) classified four of the seven mesoscale events that occurred in the northeastern United States as "other" events – events that could not fit the most common patterns of mesoscale organization that they had diagnosed. The combination of these findings suggests that heavy precipitation in the northeastern United States may be more commonly a product of localized, diurnally-forced convection, and less commonly associated with larger, more organized mesoscale features than in other regions of the country, especially the Midwest and Southern Plains. This study seeks to examine this hypothesis by classifying and describing the atmospheric conditions associated with flash flood events in the northeastern United States for the years 2003-2007. First, this chapter continues with a careful review of the literature.

1.3 Temporal characteristics of heavy precipitation

a) Annual Climatology

One of the ways to search for regional differences in the driving mechanisms of flash flooding is to examine the annual and diurnal climatologies. Local and regional differences in seasonal and diurnal processes – such as the monsoon in the Southwest and the nocturnal jet in the Midwest – may be reflected in the timing of flash floods. One of the earliest large studies of flash floods in the literature, by Maddox et al. (1979), examined the atmospheric conditions associated with 151 flash floods reported in *Storm Data* from 1973-1977. They found that July accounted for nearly 25% of the sample, and that approximately 86% of all events took place from April through September. Flash floods, at least when accounted for using *Storm Data* flash flood reports, appeared to be largely a warm-season (and especially mid-summer) phenomenon. Figure 1.1 (above) displays the flash flood events in this study, with one panel for each season. In the northeastern United States, the peak season for flash flood reports was June-July-August (JJA). However, even during this peak time of northeastern flash flood reports, no flash floods were reported for sparsely populated northern New York and northern New England. In the Northeast, all types of events are equally common during JJA, and very few events occurred during the rest of the year. Elsewhere in the country, the peak season was also JJA, but events were more common in other seasons than in the Northeast. Outside the Northeast, there appears to be seasonality to the most common types of events: "synoptic" events were more common in the non-summer seasons, while "mesohigh" events were most common in the summer. (These types of events will be discussed in section 1.4.)

Schumacher and Johnson (2006) studied heavy precipitation events, defined as events for which the 24-hour precipitation exceeded the 50-year recurrence interval, from 1999 to 2003. The seasonality of the events they studied (Figure 1.2 above) matches that of the Maddox et al. (1979) study (Figure 1.1 above) for most of the country, but not in the Northeast. Also, the sample size in the Northeast is notably smaller than in other areas of the country. The natural question arising from the disparity in the Northeast between these two studies (Figures 1.1 and 1.2) is whether this 24-hour selection criterion is less suited to capturing typical flash-flood-producing events in the Northeast than in other regions. In other words, in the central U.S., it may be more likely that the storms producing the greatest 24-hour precipitation totals are the same storms producing the greatest six-hour (and shorter) precipitation totals, while this may not be true for the Northeast. Although this specific question is not the focus of this dissertation, examining the regional differences between flash flood events will be an important objective, to be discussed later.

Brooks and Stensrud (2000) examined rainfall reports exceeding 1 in/hr in the Hourly Precipitation Dataset (HPD) from 1948-1993. Their annual climatology produces similar results to those in Maddox et al. (1979): the peak month for heavy precipitation is July, with approximately 20% of all cases, and more than 81% of all heavy precipitation events occurred between April and September. They also plotted the frequency of hourly rainfall eclipsing hourly thresholds from 1 to 6.5 inches per hour (Figure 1.3). They found that the number of heavy precipitation events decreases log-linearly as the precipitation rate increases, with approximately 50 events of 2 in/hr and only one event of 3.5 in/hr, on average, across the United States each year. They attribute the inaccuracy of the log-linear fit at high precipitation totals to bad data. Finally, they also plotted maps of 1 in/hr or larger rainfall totals for each month objectively analyzed to a regular grid. While a large portion of the country is expected

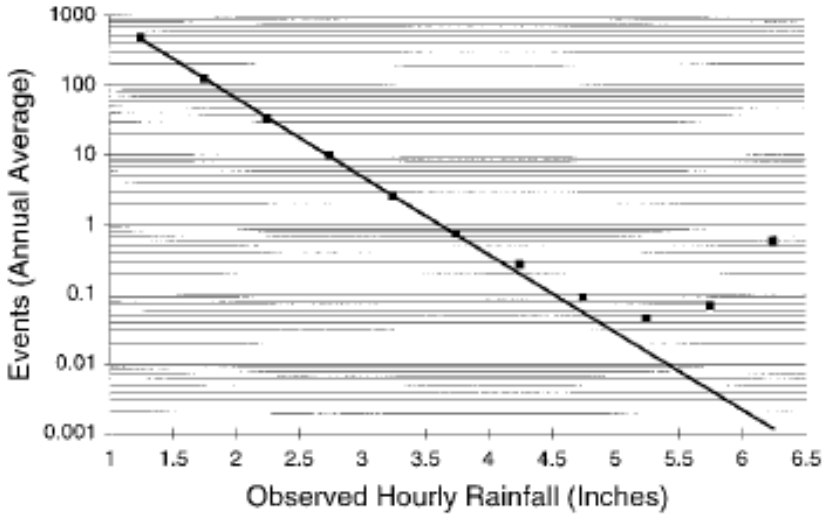

Figure 1.3 Average number of heavy rainfall events in July in United States reported in HPD. Events are binned in half-inch intervals, with all events greater than 6 inches in last bin. Black squares represent reports. Solid diagonal line is a least squares fit to the binned data from 1 to 4 inches.

to experience an event of 1 in/hr or greater precipitation in the summer months (JJA) approximately once every three years or less, for the Northeast, the frequency is no higher than once every four years, and for much of the Northeast is once every five years or more. Thus, extreme precipitation was found to be less common in the Northeast than in other parts of the country.

Ashley and Ashley (2008) examined flash flood fatalities in the United States from 1959-2005 as reported in *Storm Data* and confirmed by Rappaport (2000). They found that flash flood fatalities are most common from May through September, with a peak in June. Not only do flash flood fatalities occur more frequently from late spring through early fall, but those months also contain some of the most devastating single-day events. For the Northeast, fatalities are most common from June through September. This finding is more in line with the results of Maddox et al. (1979) and

Brooks and Stensrud (2000), and in less agreement with those of Schumacher and Johnson (2006). Ashley and Ashley (2008) attribute the high flood fatality rates in June and July to convective thunderstorms in the central and eastern U.S., and the high flood fatality rates in August and September to tropical systems in the Southeast and "monsoon" rains in the Desert Southwest.

Bradley and Smith (1994) studied heavy precipitation events in the Southern Plains (most of Oklahoma, plus adjacent portions of Kansas and Texas) from 1948 to 1990. Figure 1.4 shows the annual climatology (bottom) and a conceptual model (top) for the occurrence of heavy precipitation, which is defined to be events for which the daily rainfall (from local noon to noon) equals or exceeds 25 mm over an area of 12,500 km^2 or greater and at least one rain gauge reporting a daily rainfall accumulation of at least 125 mm. The extreme precipitation climatology peaks in May and September, with a decline during the summer months. The conceptual model attempts to explain these seasonal peaks in the context of the major contributors to the production of heavy rainfall: atmospheric moisture (median precipitable water at Oklahoma City), convective instability (median convective available potential energy (CAPE) at Oklahoma City), and large scale dynamical forcing (average number of observed 500 hPa cyclones in the central United States, Bell and Bosart, 1990). The combination of these three variables – high moisture availability, strong dynamical forcing, and moderate CAPE – overlaps for the Southern Plains during May and September, the two months that also coincide with the most frequent extreme rainstorms in the climatology. A high CAPE is not necessary for (and may, in fact, impede) widespread heavy rain; as Davis (2001) and others point out, a moderate CAPE is typically associated with a higher precipitation efficiency than a high CAPE, as large amounts of CAPE can eject moisture to the hail growth layer. The physical mechanisms behind flash-flood- producing rainstorms will be discussed in greater

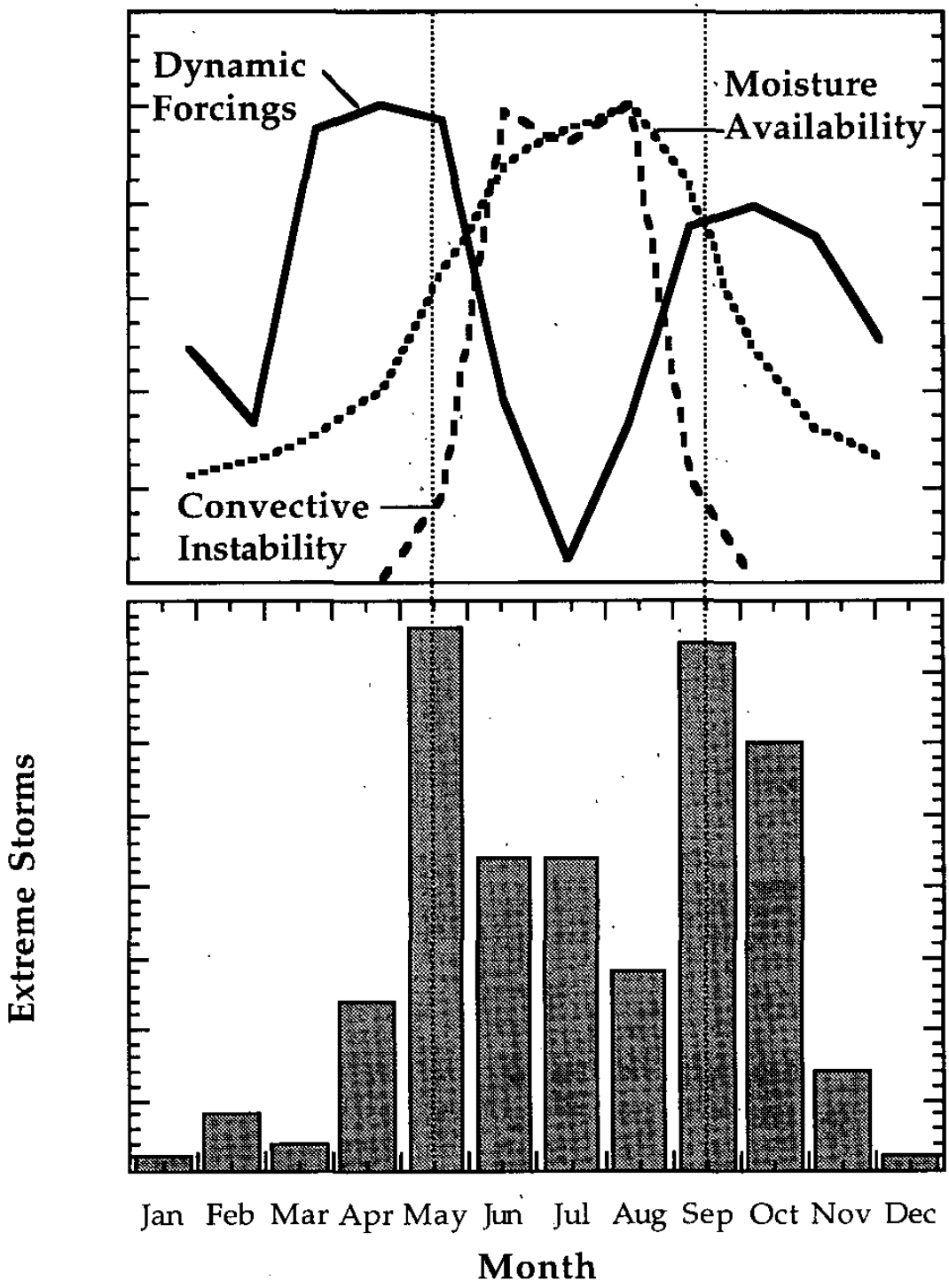

Figure 1.4 Annual climatology of precipitation and diagram of atmospheric forcings for the southern plains, from Bradley and Smith (1994).

detail in the next section.

Several studies have focused on the climatology of flash flooding in parts of the northeastern U.S. Most recently, Cope (2009) examined all flash flood reports for the National Weather Service Eastern Region from 1986 – 2007. The Eastern Region was divided into four sub-regions: New England, Mid Atlantic, Ohio Valley, and South. Across the Eastern Region, flash flooding is most common in June, and the warm season from May through September experiences the majority (68%) of the flood events. The westernmost sub-region, the Ohio Valley, experiences an earlier flash flood season, with a large percentage of its events in May through August, while the other 3 sub-regions have a larger percentage of events from June through September.

Giordano and Fritsch (1991) studied 63 intense rainstorms (defined as events for which the peak rainfall exceeded 19 cm (7.5 inches) within 12 hr, excluding events associated with a tropical depression) in the mid-Atlantic region from 1942 through 1986. Nearly half of the intense rainstorms occurred in July, and half of the July rainstorms occurred in an eight-day period from July 18 to July 25. Overall, 78% of these rainstorms occurred in June, July, and August, and all but one occurred from May through September, showing good agreement with other studies. Jessup and DeGaetano (2008) examined flash floods reported in *Storm Data* for the Binghamton, NY Weather Forecast Office's County Warning Area (which comprises parts of central New York and northeast Pennsylvania) from 1986-2003. They found that flash floods were most common in June, with a broader peak during the summer months of June, July, and August.

b) Diurnal Climatology

Figure 1.5 (from Maddox et al. (1979)) displays the time of onset of heavy rains (plotted in 6-hour intervals) for flash flood events as reported in *Storm Data* from 1973-1977. The heavy rain associated with frontal and mesohigh classes of events begins most often in the evening to overnight hours. In contrast, the events occurring in the western United States, which were typically associated with diurnally-forced convection, saw the onset of heavy rain most often in the afternoon hours. For the hypothesis that flash flood-producing precipitation in the northeast U.S. is more often less well-organized than in the central portions of the country as a result of diurnal convection, one would expect a higher percentage of events in the Northeast to initiate in the afternoon hours. This hypothesis will be examined in chapter 4.

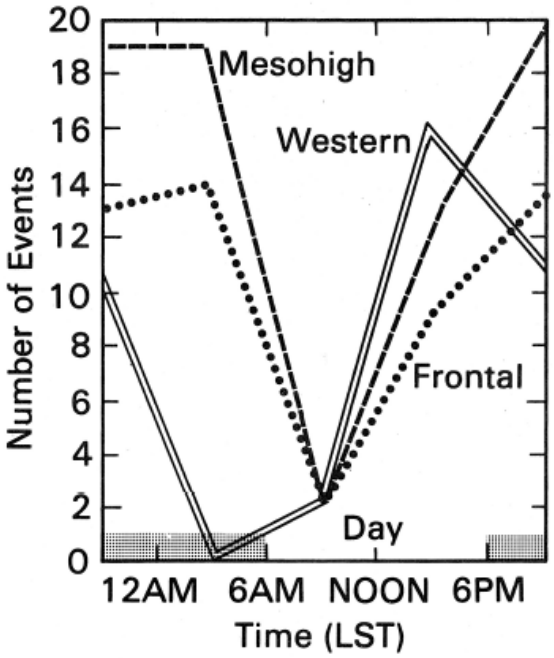

FIG. 3. Timing of the onset of heavy rains for three types of flash flood events. The number of events that began in each 6-hour interval is plotted at the midpoint of the interval.

Figure 1.5 Timing of the onset of heavy rains for three types of flash flood events. The number of events that began in each 6-hour interval is plotted at the midpoint of the interval. (Figure 3 from Maddox et al., 1979)

Winkler et al. (1988) performed a harmonic analysis on hourly precipitation data (HPD) from 1967 to 1983 across the U.S. Observations from the HPD were interpolated to a 75 km x 75 km grid, such that the maximum hourly precipitation total within each grid box was used to represent the value of the corresponding grid point. Figure 1.6 below displays the normalized amplitude and phase of the first harmonic during summer for various precipitation rates. From the figure, it is apparent that the heavier precipitation amounts (lower half of the figure) tend to occur late in the evening or overnight in the upper Midwest but during mid-afternoon in the Northeast. This regional dependence suggests that different types of forcing mechanisms or convective organization may occur in these regions, but to what extent will be examined in section 1.5.

Rogash and Racy (2002) examined flash flood events (defined as significant flash flood reports in at least 3 counties) occurring in proximity to strong or violent tornadoes (2 or more F2 tornadoes or one or more F3 tornado) across the U.S. from 1992-1998. The majority of events (79%) occurred between local noon and local midnight. Although in 65% of cases the tornadoes developed before the flash floods, for many of these cases (35% of all cases), the tornadoes overlapped with the flash flooding, creating an especially difficult forecasting and emergency management response scenario.

Giordano and Fritsch (1991) found that intense rainstorms in the mid-Atlantic region were most common in late afternoon and early evening, while they were least common in the early morning hours. They found that the peak time of the most frequent intense rainstorm occurrence was longer than the peak time of the most frequent tornado occurrence, as tornadoes are most common from late in the afternoon until approximately sunset. They point out that the peak at local 1900 (0000 UTC)

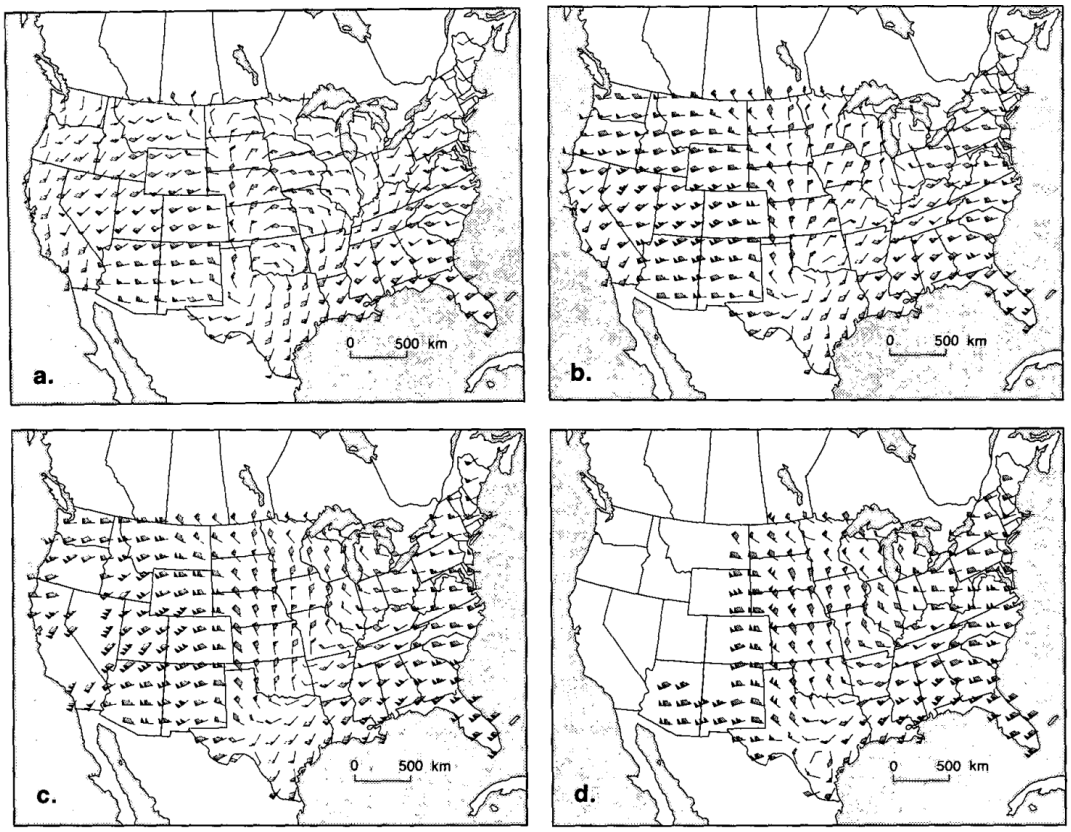

Figure 1.6 Normalized amplitude and phase of the first harmonic during summer for precipitation rates of (a) 2.5 – 6.2 mm/hr, (b) 6.3-12.6 mm/hr, (c) 12.7-25.3 mm/hr, and (d) 25.4 mm/hr or more. The harmonic analysis was performed only for grid points with at least 48 events for a particular category. An arrow directed from the north represents a phase angle of midnight local standard time (LST), an arrow from the east represents 0600 LST, and so on. The normalized amplitude is represented by the flags and barbs on the arrows, with each flag indicating a value of 0.5, each full barb 0.10, and each half barb 0.05.

coincides with a synoptic station reporting time, and, as a result, events may be reported more frequently at this hour.

Flash floods in the Northeast are most common in the late afternoon through

early evening and least common from midnight to early morning (Cope, 2009). The time of maximum flood occurrence is earliest in New England and latest in the South sub-region, with the Ohio Valley and Mid Atlantic sub-regions in between. In short, flash floods and heavy precipitation appear to occur earlier in the day in the northeast U.S. than in the central U.S., but during approximately the same time of year as much of the country.

1.4 Atmospheric Conditions Associated with Flash Flooding

Flash floods are the products of extreme rainfall; as Chappell (1993) noted, the heaviest rainfall occurs where the rainfall rate is the highest for the longest period of time. Doswell et al. (1996) presented this concept as the fundamental method for forecasting heavy precipitation (and thus flash flooding):

$$P = R\ D$$

where P is the total precipitation, R is the average rainfall rate, and D is the duration of the rainfall. How do heavy rainfall rates arise, and how are they sustained? Are there common ingredients to all heavy precipitation events that can aid in their identification? This section will explore the most common atmospheric conditions and patterns associated with flash flooding.

Doswell et al. (1996) identified the fundamental meteorological ingredients of flash flooding by expanding upon the above equation. They showed that the average rainfall rate, R, is the product of the vertical velocity (w) of the ascending moist air, and the specific humidity (q) of the air, modified by a variable that describes the efficiency with which the inflowing moisture is converted to precipitation:

$$R = Ewq$$

Theoretically, the precipitation efficiency (E) is the ratio of the mass of water falling

as precipitation (m_p) to the influx of water vapor into a cloud (m_i):

$$E = \frac{m_p}{m_i}$$

At a given moment, the precipitation efficiency can range from zero (non-precipitating) to infinite (precipitating despite a lack of inflowing moisture). Figure 1.7 illustrates this concept – in the beginning of the hypothetical storm, the precipitation is zero while the input precipitation increases, the precipitation efficiency approaches unity during time period 5, when the input water and output precipitation briefly become approximately equal, and it becomes infinite at the end of the storm,

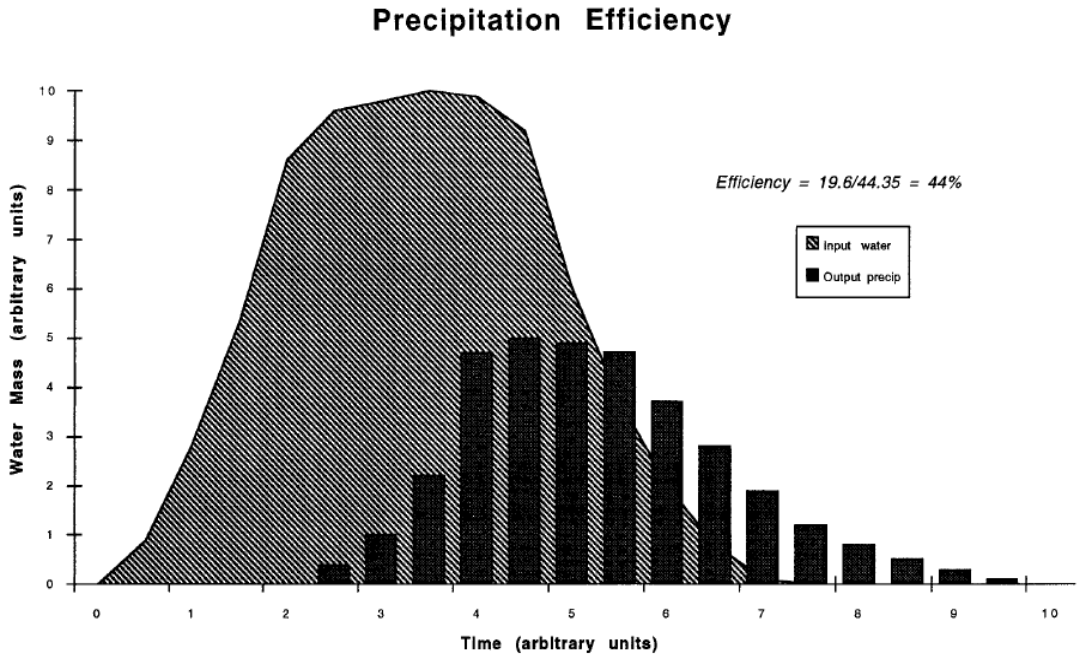

Figure 1.7 Schematic illustration of the time variation of water vapor input (cross-hatched area) and the precipitation output (vertical bars) over the lifetime of a precipitation system. The units are arbitrary, so the system being portrayed can be any precipitating process with a developing phase (time 0–3 units), a mature phase (time 3–6 units), and a dissipating phase (time 6–10 units). For this example, the areas under the respective curves give a precipitation efficiency of about 44%. From

Doswell et al. (1996).

when there is no more input water, but the storm is still precipitating. The precipitation efficiency of a given precipitating system is affected by the entrainment of dry air into a cloud, and from the perspective of measurable environmental variables, the entrainment rate can be best estimated by environmental relative humidity and vertical wind shear: a high environmental relative humidity and low vertical wind shear indicate that there is less likely to be entrainment of dry air into the precipitating system. To achieve sufficient ascent (w) for large rainfall rates requires storm-scale processes, rather than synoptic-scale lifting mechanisms. These small-scale processes involve parcel theory, which maintains that a conditionally unstable lapse rate, along with sufficient moisture for a level of free convection (LFC) and a process to lift a rising parcel of air to the LFC, are all required to support and maintain deep, moist convection**.** Parcel theory can be described with an analogy to balloons. Conditional instability is somewhat like a balloon filled with air – an air parcel in a conditionally unstable environment cannot rise unless a force pushes it upward. Once an air parcel reaches the LFC, though, the air parcel acts like a helium balloon, rising until it encounters a layer of stable air, which is often the tropopause.

While cloud scale processes are important in understanding precipitation processes at the macroscale, cloud physics affect the formation of precipitation at both the macroscale (over the depth of the cloud) and microscale (the interactions among raindrops) (Davis, 2001). Clouds with a deep warm cloud layer and a relatively long droplet residence time in this layer (that is, moderate updraft speeds) are more efficient rainfall producers than clouds with a thinner warm cloud layer (lower freezing level) and stronger updrafts. A longer residence time in the warm cloud layer provides more time for droplets to interact in the collision-coalescence (warm rain) process, which converts inflowing moisture to precipitation relatively low in the cloud.

In contrast, clouds that have low freezing levels and, thus, thin warm cloud layers, tend to produce the majority of their precipitation through ice processes, especially if the convective potential available energy (CAPE) is relatively high, as this accelerates droplets through the warm cloud layer, ejecting them to higher levels of the storm where ice processes dominate (Young, 1993). Thus, for efficient microphysical processes, a thick warm cloud layer and moderate CAPE are required.

Much like the fundamental processes that contribute to the rainfall rate, the fundamental processes that contribute to rainfall duration are simple in concept but more complex in reality (Doswell et al., 1996). Conceptually, the duration of a given rainfall system is the system's speed, C_s, divided into the length of the system along the motion vector, L_s:

$$D = L_s \left(|C_s|\right)^{-1}$$

Thus, long durations of heavy rainfall may result from slow system movement, a large area of high rainfall rates along the system's motion vector, or both. Predicting system movement is relatively straightforward for single-celled systems, as they typically move with the mean wind computed through a relatively deep tropospheric layer. When both the movement of individual cells and the propagation effects of newly forming cells are important, as in multicellular systems, the system movement is more difficult to predict. Corfidi et al. (1996) found that the movement of individual cells correlates well with the mean wind in the cloud layer (estimated to extend from 850 to 300 hPa), and that the propagation of new cells is roughly equal in magnitude but opposite in direction to the low-level jet (Figure 1.8). Thus, the motion of a meso-beta scale element (MBE) was found to be approximately equal to the vector difference of these two contributions:

$$v_{MBE} = v_{CL} - v_{LLJ}$$

where v_{MBE} is the net system motion, v_{CL} is the mean cloud layer wind, and v_{LLJ} is the speed of the low level jet (typically taken at 850 hPa). Thus, with an estimate of the net system motion and the size of the system, one can approximate the duration of a rainstorm.

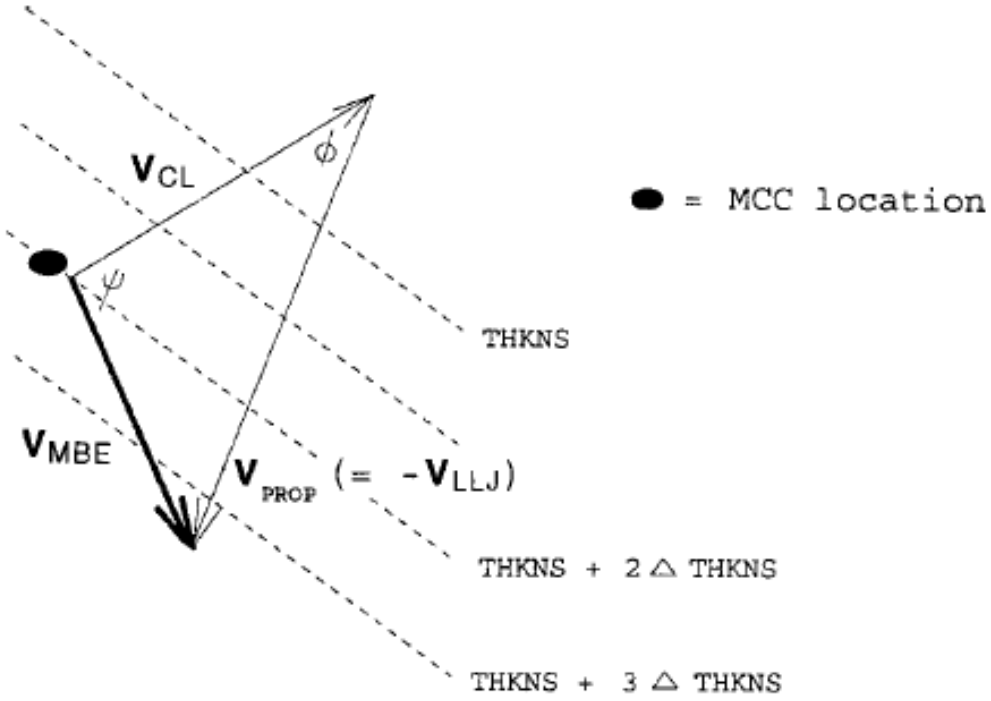

Figure 1.8 Conceptual model of MBE movement (V_{MBE}) as the vector sum of the mean flow in the cloud layer (V_{CL}) and the propagation component (V_{PROP}). The magnitude and direction of V_{PROP} are assumed to be equal and opposite to those of the low-level jet (V_{LLJ}). The angles φ and ϕ are used to calculate V_{MBE} given observed values of V_{CL} and V_{LLJ}. Dashed lines (labeled THKNS) indicate a typical relationship of the 850–300-mb thickness pattern to the environmental flow and MBE movement during Mesoscale Convective Complex (MCC) events. From Corfidi et al. (1996).

Junker et al. (1999) studied 85 rainfall events that produced 2 inches (50.8 mm) or greater precipitation in 24 hours during the midwestern U.S. floods of 1993. They found that the largest and most extreme rainfall events occur when an elongated pattern of low-level moisture flux convergence intersects a low-level quasi-stationary boundary oriented approximately parallel to the mean wind. This is associated with a veering wind profile with height, providing (often southerly) low level moisture on the flank of convection that is traveling with the mean wind (often westerly) and helping to further destabilize the environment (Davis 2001; Figure 1.9). This provides for a long duration of training precipitation and provides, in many ways, an ideal situation for flash flood potential.

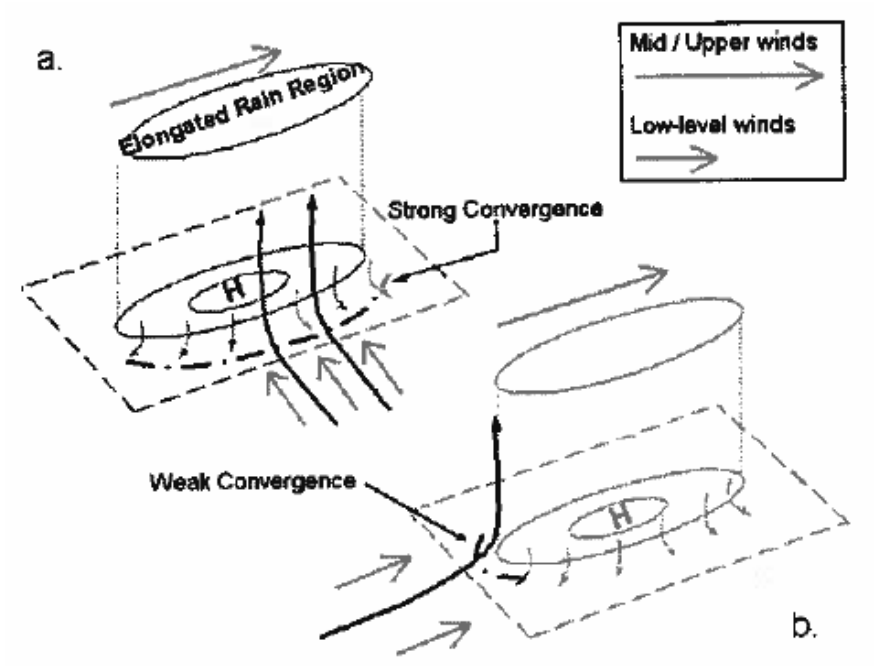

Figure 1.9 Illustration of a multicellular storm growing in an environment where (a) the low-level winds are perpendicular to the mid- and upper-level winds, and (b) the low-level winds are parallel to the mid- and upper-level winds. (Figure 12.19 from Davis (2001), originally from Cotton (1990).)

In addition to the meteorological environment, the physical environment, in the form of terrain, can impact the formation and duration of heavy rainfall (Davis, 2001). The terrain itself can produce orographic lifting and gravity waves, which may influence local and downwind clouds and precipitation. As air approaches elevated terrain, it may slow down, producing mass convergence on the windward side of the terrain. The elevated vegetation and soil of relatively high terrain can serve as an elevated source of heat and moisture that may help to destabilize the air (Orville, 1968). Synoptic-scale flow that persistently pushes weakly stable air over hilly terrain can produce potentially several days of heavy rainfall. Terrain can also help to anchor precipitation when a persistent flow of low-level moisture remains in place near a topographic feature (mountain or hill), especially if an outflow boundary or front coincides with the feature. New cells will be continually generated and move away (slowly, if the environmental flow is weak) as long as the low level moisture source remains in place. A flash flood in Madison County, Virginia produced rainfall totals of nearly 600 mm in 18 hours, proving that the Appalachian Mountains are sufficiently large to support this anchored precipitation (Pontrelli et al., 1999).

A natural question in light of the basic ingredients to produce flash flooding is what types of weather systems help to put these ingredients in place? At the synoptic scale, short wave troughs produce moistening and destabilization, providing low-level moisture and instability ahead of the trough, which increases the probability of deep, moist convection (Doswell et al., 1996). Many floods have been observed near mid-tropospheric ridges (Maddox et al., 1979). Though ridges are typically associated with fair weather, their suppression of convection can lead to the accumulation of low-level moisture and destabilization through surface heating; eventually this “cap” on the convection can be broken from below. The thermal boundaries on the margins of a ridge can also be regions for focusing convection.

One of the principal functions at the mesoscale, Doswell et al. (1996) argue, is to provide lift to enable parcels to reach the buoyant level. Many of the heavy precipitation events that lead to flash flooding are organized at the mesoscale, specifically in the form of mesoscale convective systems (MCSs). These MCSs may be organized with a leading line of brief, heavy rainfall followed by sustained moderate rainfall; the common structures of MCSs will be examined in section 1.5. MCSs can also play a role in the mesoscale environment by affecting system propagation, by generating outflow boundaries that can become focal points for new convection, and by changing the wind field and thus the wind shear, which can affect the advection of moisture and entrainment of dry air for new convective cells.

Finally, at the storm-scale, Doswell et al. (1996) point out that storm-scale cold outflow increases evaporation, which reduces the precipitation efficiency of the storm. In some cases, new cells regenerate close to their "parent" cell; in cases with weak environmental wind shear, the precipitation cascade can be located close to the updraft and, provided that the low level outflow is weak enough that it does not cut off inflowing moisture from the updraft (as occurs in environments with high relative humidity), then new cells will form near old ones, forming what is known as a quasi-stationary system.

With an understanding of the ingredients necessary for flash floods and how these ingredients are put in place, the next step is to consider the common patterns that arise to create flash flooding. Maddox et al. (1979) classified 151 flash flood events based on their surface and upper air conditions. They grouped the 120 events east of 104 ºN into three categories: synoptic, frontal, and mesohigh. All events west of this longitude, which were typically associated with storm-scale events and lower precipitation totals, were given their own classification.

Synoptic events feature a deep trough, a quasi-stationary surface boundary, and

a strong low-level jet. Because the storm is associated with a strong cyclone, winds tend to be fast and storms move rapidly. Winds aloft are parallel to the front, favorable for the training of multiple storms over periods of hours to days. These events can be associated with severe weather in addition to flash flooding, complicating the forecasting problem.

Frontal events typically have precipitation on the cool side of an east/west oriented boundary (warm front), with weak large scale forcing. Warm air advection (typically from the south) plays a role in providing lift for these events. Like the synoptic events, a (usually southerly) low level jet is present to supply warm, moist air for new cell formation. Winds aloft are approximately parallel to the front, causing system motion parallel to the front. Flash floods tend to form along and to the north of the frontal boundary. This description is very similar to the "training line/adjoining stratiform" events described in section 1.5, and to the multicellular storms illustrated in Figure 1.9 above.

Unlike Maddox et al.'s (1979) other types of events, which are forced by large-scale surface boundaries, the mesohigh class of events is a product of mesoscale outflow boundaries generated by ongoing or previous convection. These events can occur in a variety of scenarios, from the vicinity of large-scale frontal boundaries to nondescript conditions. The Johnstown, Pennsylvania flash flood of 19-20 July 1977 was a mesohigh type of flood. The convection persisted north of a preexisting outflow boundary, and the outflow from each cell reinforced the boundary, providing continued forcing for the persistence of the heavy rainfall. This description, particularly of the Johnstown event, is very similar to the "back-building/quasi-stationary" category of events described in section 1.5.

Finally, the "western" category of events is comprised of convective events that occur in the absence of large-scale or mesoscale forcing. The environment is

conditionally unstable, with high precipitable water and light winds. A weak trough is often present upstream to destabilize the atmosphere and provide low-level moisture. Maddox et al. (1980) found that outflow boundaries, surface fronts, and terrain can interact to provide the lifting needed to initiate deep moist convection.

In summary, there are several basic ingredients that are common to most flash flood events (Davis, 2001). Most flash floods are the result of deep, moist convection, often at night in the central U.S. and more often in the late afternoon in the western and eastern U.S. This convection is sustained by a deep layer of moisture, which is typically reinforced by a low-level jet. The low-level jet helps to focus the convection, and its width determines the extent of heavy rainfall. Large-scale forcing mechanisms are typically non-existent or weak, but low-level boundaries (such as fronts or outflow boundaries) are often present and aligned parallel to upper-level winds. Aloft, there is typically an upwind meso-α-scale wave approaching a long wave ridge. Due to the relative orientation of the low-level jet and the winds aloft, individual cells form and train over the same area, producing long-duration heavy rainfall. Upper air soundings for flash flood events also have many commonalities (Chappell, 1993). The sounding displays high precipitable water; moderate values of CAPE, which are often distributed in a long, narrow vertical distribution; a low, warm cloud base; a high equilibrium level; and relatively weak vertical wind shear with a veering wind profile. This combination of environmental properties helps to produce long-duration heavy rainfall.

1.5 Organization of Heavy Precipitation

Several studies have sought to describe the organization of MCSs that produce heavy precipitation, flash flooding, and/or other types of severe weather. Rather than

first examining the atmospheric conditions to classify the events (the approach taken by Maddox et al., 1979), these studies typically examine radar reflectivity and describe the relative positions and movement of rainfall based on the categories of "convective", or high reflectivity, and "stratiform", or moderate to low reflectivity, rainfall. As Doswell et al. (1996) have pointed out, the "stratiform" region is not necessarily due to stratiform rain processes, but the name has been used as a convention to distinguish between regions of heavy and moderate precipitation.

Bluestein and Jain (1985) examined the organization of approximately 150 squall lines in Oklahoma over an 11 year period. They reduced this sample to 52 squall line cases that were associated with severe weather reports in *Storm Data* (tornado, funnel cloud, strong wind, or large hail) and that had reliable images of the radar reflectivity. They defined squall lines as linearly oriented mesoscale convective systems with a length-to-width ratio of at least five-to-one, a length of a least 50 km, a width less than 50 km, for a duration of at least 15 minutes. Figure 1.10 shows the four categories of squall lines that they identified, which were based on the squall lines' depiction on radar. The most common classes were the broken line and back building types, while the embedded areal type was least common. Twelve of the 52 cases could not be classified according to this scheme.

After classifying the events based on their radar signatures, Bluestein and Jain (1985) described the synoptic surface boundaries associated with each type of event. Most broken line cases occurred in close proximity to a surface cold front. The back-building scenarios resulted from an approximately equal number of cases in close proximity (70 km or less) to each of the following: a dry line, a cold front, and the intersection of a dryline with a cold front. Broken areal cases were either within close proximity (90 km or less) to a quasi-stationary front or 80-200 km east of a dryline. The five embedded areal cases occurred with four different synoptic scenarios. From

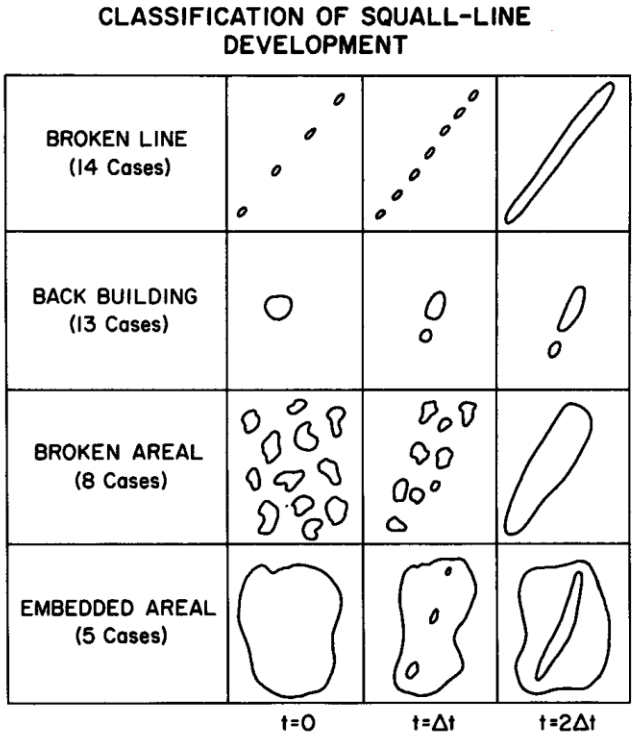

Figure 1.10 Idealized depiction of squall-line formation. (Figure 1 from Bluestein and Jain (1985)).

these results, it is clear that surface boundaries appear to be a key ingredient for the formation of a severe squall line, and the type of boundary may play some role in determining how the convection will be organized.

Although they had different appearances, all storm types studied by Bluestein and Jain (1985) exhibited some common features. The vertical wind shear was greatest below the lifted condensation level (LCL), that is, the pressure level of the cloud base. The wind substantially veers with height in the subcloud layer and more weakly backs with height aloft. The orientation of the vertical shear in the lowest kilometer is roughly parallel to the orientation of the squall line. The squall lines are oriented at a large angle to the shear vector in the lower part of the middle tropophere, and at an angle of 30-40 degrees from the shear in the upper tropopshere. The overall

moisture content as exhibited by the precipitable water and the tropospheric humidity (ratio of precipitable water to saturation precipitable water) is nearly identical for all storm types.

Bluestein et al. (1987) expanded the study of squall lines, looking into how squall lines that produce severe weather differ from those that do not produce severe weather. They found that severe squall lines are associated with high CAPE, strong updrafts, and a variety of surface boundaries (though severe broken-line squall lines tend to form along cold fronts). In contrast, non-severe squall lines are associated with moderate CAPE and weaker updrafts, and they tend to form along cold fronts (though non-severe broken-line squall lines tend to form along a variety of surface boundaries).

Rather than focusing specifically on squall lines, Houze et al. (1990) studied 55 major rain events (events with at least 25 mm of precipitation in 24 hours over an area of at least 24,500 km^2) in central Oklahoma from April, May, and June for the years 1977-1982. The 63 mesoscale precipitation systems (MPSs) associated with the 51 events with adequate radar data were classified according to the relative position and movement of convective and stratiform regions of precipitation, which were defined based on the magnitude and gradient of radar reflectivity. They found that 48 of 51 events with adequate radar data had a substantial stratiform region covering at least 10% of the study area (about 12,500 km^2 or more) and that most of the events with stratiform rainfall covering at least 30% of the study area occurred in the overnight hours. Most of these events had a similar appearance, with a leading convective line and a trailing broader area of stratiform precipitation.

Houze et al. (1990) further classified the leading line/trailing stratiform cases into three types: symmetric, asymmetric, and unclassifiable. These types were further described as being strongly, moderately, or weakly classifiable, based on the

agreement of the radar signatures with the schematic illustrations shown in Figure 1.11 below. These schematic illustrations (Figures 7 and 8 from their paper) illustrate the differences between the symmetric and asymmetric leading line/trailing stratiform cases described in their paper. For the symmetric schematic, the stratiform region follows the center of the convective line, which is (in the ideal case) where the strongest convective echoes are located. In the asymmetric schematic, the stratiform region is located farther to the north and/or east relative to the convective line, while the strongest convective echoes are located on the southern or southwestern end of the convective line.

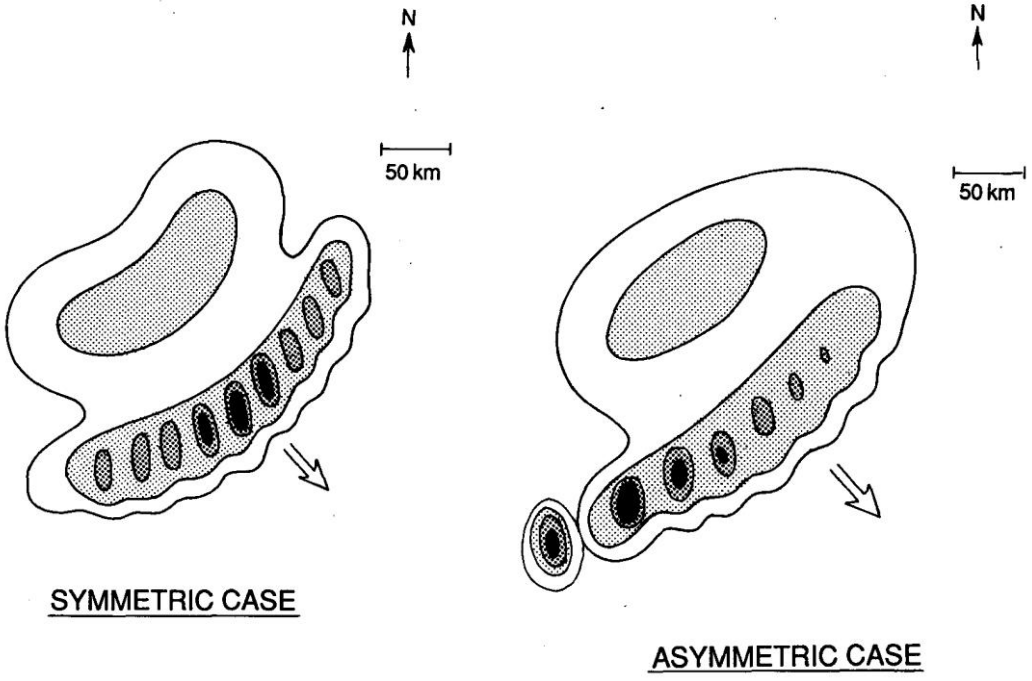

Figure 1.11 Schematic diagrams of leading-line/trailing-stratiform MCSs (Figures 7 and 8 from Houze et al., 1990).

Twenty-one of the 63 MPSs with adequate radar data were unclassifiable; 11 were classified as symmetric; 15 were classified as asymmetric; and 16 were classified as intermediate between the symmetric and asymmetric archetypes. The symmetric

cases tended to be moderately to strongly classifiable, while the asymmetric cases tended to be weakly to moderately classifiable. Of the cases with flooding reported in *Storm Data*, the symmetric cases most commonly associated with flooding were strongly classifiable events, while flooding was equally distributed for the asymmetric cases between the weakly, moderately, and strongly classifiable events.

Houze et al. (1990) also examined the environmental conditions associated with the events as a whole and with each class of events. The composite sounding (not shown) for all major rain events in the sample shows a stable layer near 800 hPa, which can be interpreted as a cap on the top of the boundary layer; below this stable layer, conditions were well-mixed throughout the boundary layer. Aside from the relatively thin stable layer at 800 hPa, the profile is conditionally unstable throughout most of the troposphere. The mean tropopause is located at a pressure level of approximately 200 hPa. The wind profile features veering winds and generally increasing speeds with height through the troposphere. There is a southerly low-level jet in the composite sounding, but this feature was not found in all cases. For the asymmetric events as opposed to the symmetric events, the wind shear was stronger, which may be favorable for supercell development, particularly near the southwestern end of a convective line. For the asymmetric events, a mesoscale vortex sometimes formed at mid-levels, leading to asymmetry by ingesting dry air into the south and advecting clouds and precipitation from the convective line to the northern part of the startiform region.

In comparing the features of strongly organized leading-line/trailing stratiform organization with weakly organized mesoscale features, they found that the strongly organized events had a large bulk Richardson number (ratio of CAPE to wind shear) as a result of weak wind shear and higher instability in comparison to the weakly organized events. Thus, strongly organized events had an environment favorable for

multicell development, with the formation of new cells at the front of the convective zone and the dissipation of cells at the rear of the mesoscale systems. In contrast, the weakly organized systems were in an environment favorable for individual cells to last longer, making these systems less likely to form new cells; therefore, the trailing-stratiform structure tends to last for a shorter period of time in the weakly organized systems.

They also compared systems based on how well they matched the classification prototypes. They found that the height of the stable layer decreases from strongly to moderately and then to weakly classifiable systems. Less classifiable systems are also associated with: a cooler, more stable boundary layer; less directional shear of the wind with height; little evidence of a low-level jet in the weakly classifiable composite as compared with the strongly classifiable composite; and greater vertical speed shear in the lower to middle troposphere.

Parker and Johnson (2000) examined 88 linear MCSs in the central United States during May 1996 and May 1997. Figure 1.12 below depicts schematically the organization of different types of linearly organized MCSs based on radar reflectivity. The classification scheme is based upon the positions of convective and stratiform precipitation relative to the motion of the system as a whole. The stratiform region is either "leading" (LS), "trailing" (TS) or "parallel" (PS) to the convective line (Figure 1.12). Of the 88 cases studied, 58% were of the TS type. The LS and PS types each accounted for 19% of the cases and the remaining 4% of cases were deemed unclassifiable according to their classification scheme. In addition to being most common, the TS cases also persisted for approximately twice as long as the LS and PS cases and, thus, traveled much farther than the LS and PS cases.

Parker and Johnson (2000) further examined the difference in synoptic conditions between active periods and inactive periods. They deemed a period active

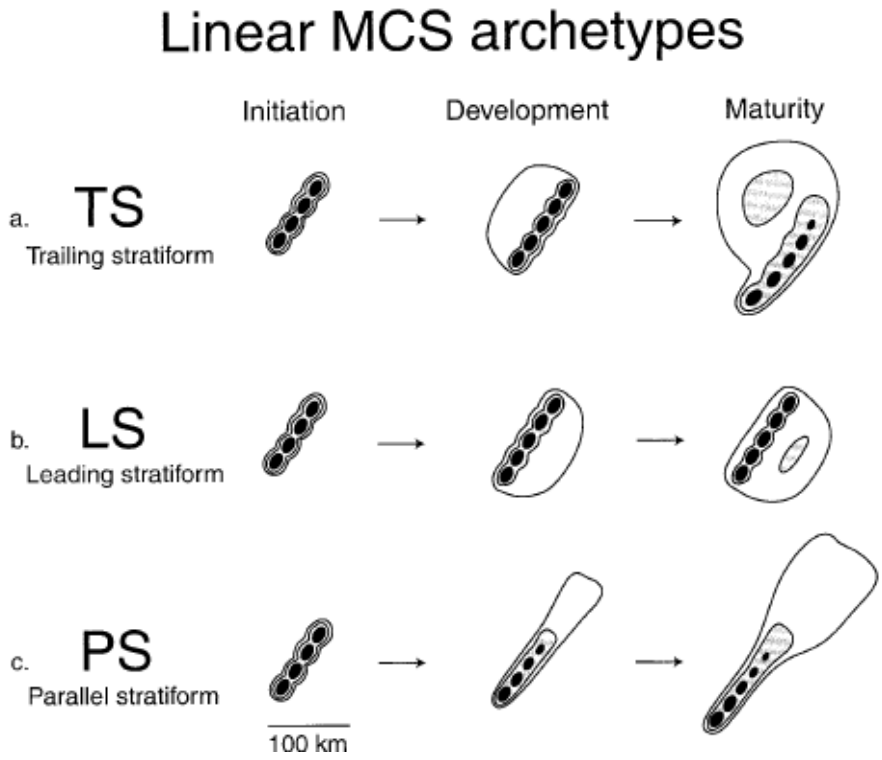

Figure 1.12 Schematic drawings of radar reflectivity for three types of linear organization observed to be common to mesoscale convective systems in the central United States. Levels of shading correspond to 20, 40, and 50 dBZ. (Figure 4 from Parker and Johnson, 2000).

if it 1) produced at least one MCS per day during a contiguous series of two or more days, or 2) produced at least two MCSs during an individual day. A period was deemed inactive if it was not active. Active periods tended to be associated with lower sea level pressure and an approaching surface cyclone. There was also a tendency for an approaching short-wave trough during active periods, as indicated by lower 500 hPa heights during active periods. Linear MCSs were observed to occur in the right entrance region of an upper tropospheric jet. In contrast, a ridge tends to be located over the eastern U.S. during active periods (to the east of the study area),

which helps to put warm air in place prior to the occurrence of the linear MCSs. At the surface, active periods are associated with a tongue of warm, moist air as indicated by the equivalent potential temperature: strong southerly flow helps to advect warm, moist air into the study region.

The 57 classifiable MCSs (33 TS, 12 LS, and 12 PS) with good quality radar data that occurred in the warm sector of an extratropical cyclone were analyzed in greater detail. Wind profiler data were composited to diagnose the wind patterns associated with each type of MCS. The TS class had negative line-perpendicular storm-relative winds at every level and significantly larger rearward storm-relative winds above 2 km than those for the LS and PS classes. As a result, the TS class of storms moved more rapidly than the other classes. The LS and PS classes exhibited a very similar line-perpendicular structure, with weak mid-tropospheric storm-relative winds and modest upper-level rear-to-front winds. The notable exception to the similarity between the LS and PS classes is in the boundary layer, where the mean PS line-perpendicular winds were stronger than those in the mean TS profile, while the mean LS low-level winds were notably weaker. As a result, the LS systems were the slowest-moving systems. The 5-8 and 3-10 km mean line-perpendicular storm-relative winds were found to be the most statistically significant differentiators among the three classes studied. Ground-relative winds (i.e. u and v components) were also found to be statistically significantly different for the 0-6, 3-10, 5-8, and 9-10 km layers.

Doswell et al. (1996) show in Figure 1.13 that the speed and direction of a given linear MCS help to determine how much precipitation a given location will receive. Thus, it is not only the structure of a given linear feature that determines the total precipitation at a point, but also the direction of motion relative to the orientation of the components of the system as a whole: the convective line and the stratiform

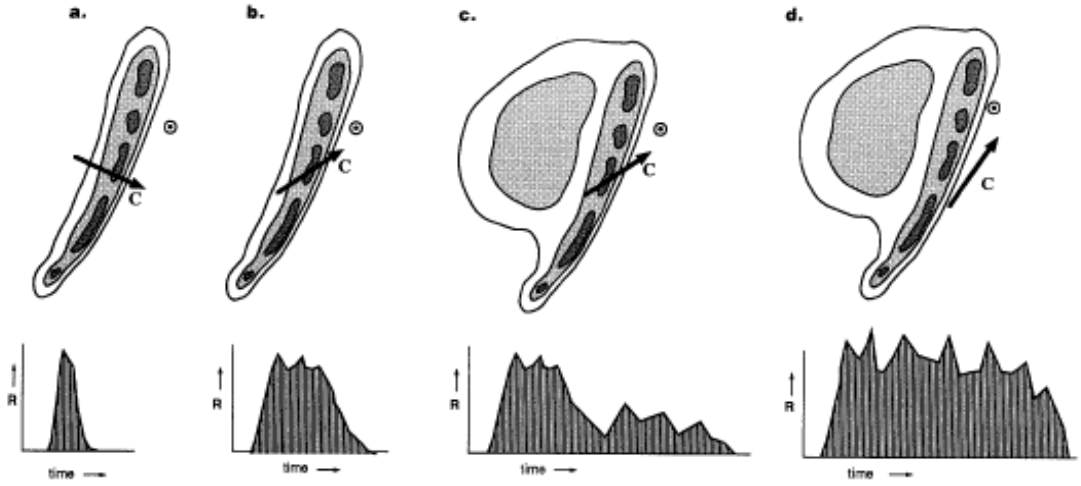

Figure 1.13 Schematic drawing showing how different types of linear mesoscale convective systems with different motions affect the rainfall rate (*R*) at a point (circled dot) as a function of time. Contours and shading indicate radar reflectivity. (Figure 3 from Doswell et al. 1996.)

region. As Figure 1.13 shows, the more parallel the motion is with respect to the orientation of the convective line, the more rainfall a given location that intersects the convective line will receive. Similarly, the more perpendicular the motion is with respect to the orientation of the convective line, the less rainfall a given location that intersects the convective line will receive.

In addition to the three linear types of MCSs diagnosed by Parker and Johnson (2000), Schumacher and Johnson (2005) identified two additional types of linear organization. In the training line/adjoining stratiform (TL/AS) events (Figure 1.14(a)), many cells train over the same area, with cell motion typically parallel to an adjacent surface boundary (often a stationary front). For these events, the stratiform rain shield travels parallel to the convective line, rather than following or leading the convection. In the back-building/quasi-stationary (BB) events (Figure 1.14(b)), new cells typically

form on the rear flank of old cells, producing a train of cells over the same area. Figure 1.15 shows the locations of heaviest rainfall for these two classes of events. Both classes of events are concentrated in the central portion of the United States, with most events in the upper Midwest and eastern plains states. No events of these types were observed along the East Coast of the U.S. (Figure 1.15, below). Overall, TL/AS events comprised 20.7% of all events studied (31.6% of all MCSs), and BB events comprised 12.9% of all events (19.7% of all MCSs).

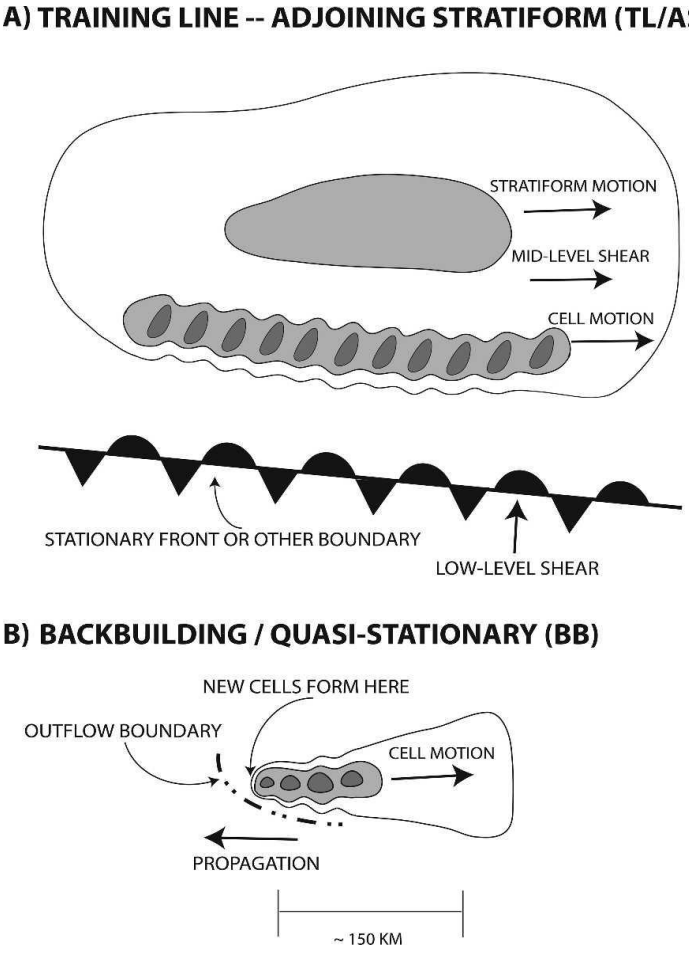

Figure 1.14 Schematic diagrams for the training line – adjoining stratiform (TL/AS) and back-building/quasi-stationary (BB) classes of events. Shading represents approximate radar reflectivity values of 20, 40, and 50 dBZ. (Figure 3, Schumacher and Johnson, 2005)

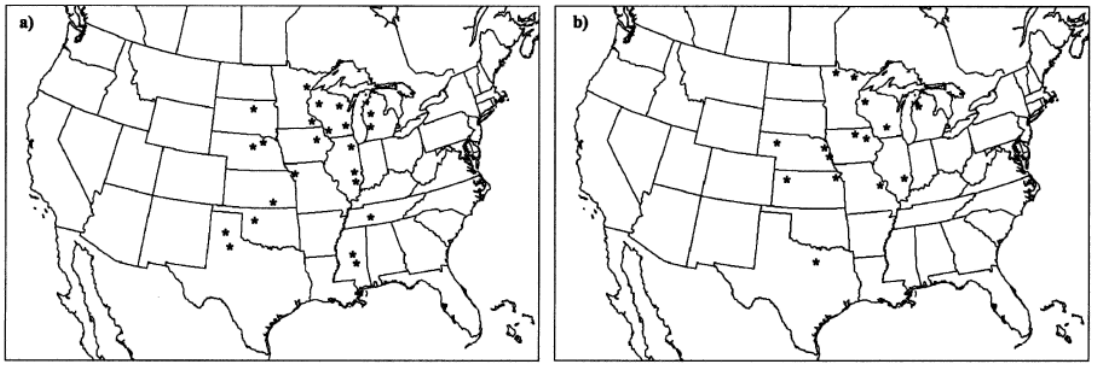

Figure 1.15 Approximate locations of highest rainfall totals for (a) TL/AS and (b) BB MCS events. (Figure 4, Schumacher and Johnson, 2005)

To describe the environments associated with these new classes of events, Schumacher and Johnson (2005) analyzed the environmental conditions prior to and during the MCS events using the Rapid Update Cycle Version 2 (RUC-2) analyses. Over 70% of the TL/AS events corresponded to Maddox et al.'s (1979) "frontal" pattern, forming on the cool side of a warm front or stationary front. This frontal boundary is visible in the surface composite (not shown), with a tight equivalent potential temperature gradient and a wind shift located near the site of maximum rainfall. Other TL/AS events formed on the cool side of a long, preexisting outflow boundary. For a few cases, TL/AS structures also appeared in the absence of any boundary. A cross section through the extreme rainfall center shows warm, moist air being lifted over the boundary from the south to the north. This suggests that the convection in TL/AS events is typically elevated. A maximum in low-level convergence is co-located with this low-level instability, providing a favorable environment for cell development. The cross section also indicates a maximum area of upper-level divergence just north of the heavy rainfall location, which is consistent with the northward shift in precipitation and the stratiform rain shield to the north of

the convective line in the conceptual model in Figure 1.14. The vertical profile of the mean wind for TL/AS events shows veering at low levels and approximately unidirectional flow with height in the middle and upper troposphere. The 925-500mb wind shear vector is oriented approximately parallel to the convective line, while the surface to 925 hPa shear is oriented approximately perpendicular to the convective line. This finding is similar to the results of Houze et al. (1990) and reflects the more general findings from section 1.4 that point out the role of a veering profile in providing a favorable environment for training cells with low-level moist inflow on their flank. To the south of the center of maximum rainfall, a maximum in wind speed at 850 hPa appears, suggesting the presence of a low-level jet. Finally, there is a maximum of 850 hPa equivalent potential temperature advection to the north and northeast of the heavy rainfall location, which indicates the advection of warm, moist air away from the location of heavy rainfall and toward the broader stratiform region of rainfall.

Like the TL/AS events, BB events were found to occur in a variety of surface environments, some of which did not have any well-defined features according to the National Centers for Environmental Prediction (NCEP) analysis. It appears that many of these events did have storm-scale or mesoscale boundaries that, perhaps because of their smaller size, were not indicated by the NCEP analysis. The greatest difference in the BB surface composite (not shown) from the TL/AS surface composite (not shown) is that the features that are prevalent across the whole domain in the TL/AS composite – the wind shift from southerly to easterly and the tight equivalent potential temperature gradient - are present only near the heavy rainfall location in the BB composite. This suggests, as does the absence of NCEP-analyzed boundaries in several cases, that the boundaries which help to focus the convection in BB cases may be relatively small-scale features with different storm-relative positions from case to

case. Above the surface, the BB events were also found to be very similar to the TL/AS events. Like the TL/AS cross section, the BB south-north cross section (not shown) contains a sloping area of warm, moist air co-located with strong low-level convergence. Unlike the TL/AS cross section, the upper level divergence is directly over the center, rather than displaced to the north. This yields a smaller, more focused area of precipitation for the BB events. The vertical wind profile for BB events is similar to that for TL/AS events, except that the upper level winds are a bit weaker and more westerly. Like the TL/AS cases, there is a pronounced low-level jet advecting warm, moist air into the heavy rainfall location, but this jet is a bit lower in the troposphere for the BB composite. In short, despite some subtle differences, the environmental conditions associated with TL/AS and BB event types were found to be very similar in their mean appearance.

Doswell et al. (1996) illustrate how a storm-scale process can produce back-building/quasi-stationary mesoscale systems (Figure 1.16). As cells move away (to the right in the figure above), new cells form on the rear flank of the storm, lifted by a cold outflow boundary (indicated by the frontal symbol). While the cells move away, advected by the wind, the outflow boundary remains in place to continually generate new cells. The result is a long duration of heavy rainfall over a small area.

Schiesser et al. (1995) categorized the organization of MCSs in Switzerland from 1985-1989, year-round. They defined a severe precipitation day (SPD) as a day on which at least 5 Swiss communities suffered damage by water and/or at least 20 communities were damaged by hail. Their 5-year sample included 120 SPDs, 94 of which had adequate radar data for their study, and 82 of which were classified as "intense SPDs" and subject to further study. They used the strength and organization of the convective cells, as well as the relative position of the convective line compared with the stratiform rain that may have accompanied it to classify the MCSs that

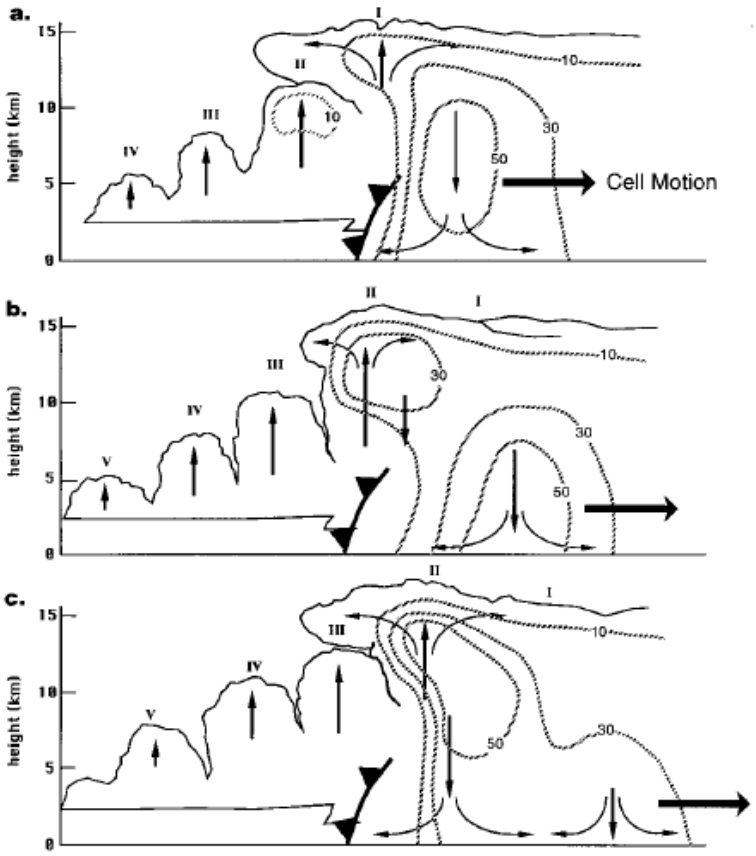

Figure 1.16 Schematic illustrating three stages in the evolution of a multi-cell thunderstorm system. Cells are labeled with Roman numerals; thin arrows indicate updrafts, downdrafts and divergence at the storm top and surface associated with each cell the frontal symbol indicates the low-level boundary; the cell motion is indicated by the bold arrow; and hatched lines show radar reflectivity, labeled in dBZ. (Figure 7 from Doswell et al. 1996).

contributed the heavy precipitation and/or hail (see Figure 1.17 below). Note that the broken line category was most common, and that leading line/trailing stratiform events comprised roughly a third of the sample. Thus, their findings show a less frequent occurrence of leading-line/trailing stratiform events than Houze et al. (1990) found for the southern plains region of the U.S.

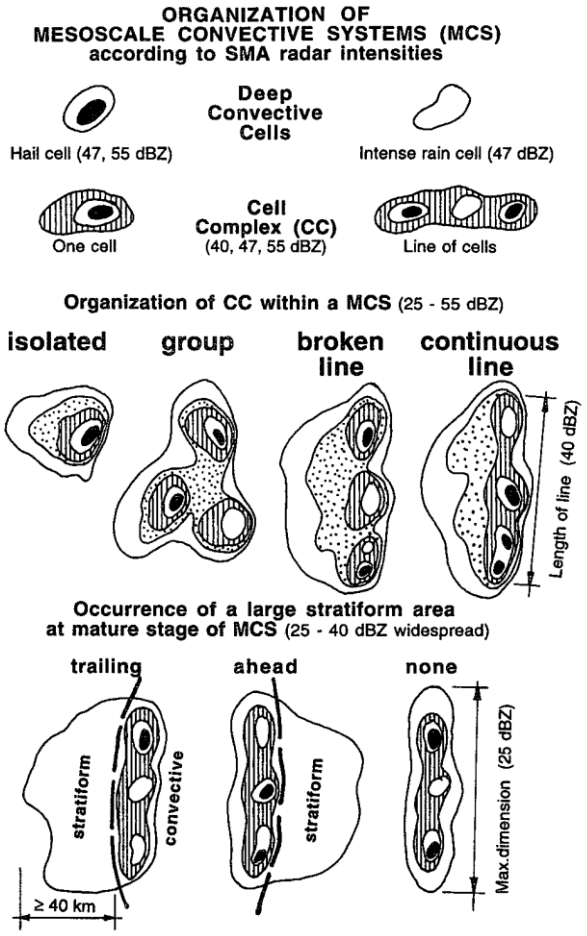

Figure 1.17 Schematic illustrations of the organization of MCSs as categorized by Schiesser et al. (1995). Contours are radar intensities in dBZ. System movement is from left to right.

This survey of the literature on the organization of mesoscale convective systems has yielded some similarities and differences between the different classifications of mesoscale systems, most of which were located in the central portion of the United States. Virtually all precipitation systems studied in the literature featured a high content of moisture in the atmosphere and veering winds in the lower troposphere. However, at upper levels the winds backed for some types of systems or individual cases but veered or remained unidirectional with height in others. Most, but

not all, of the systems occurred along or near a surface or low-level boundary. A major difference, though, was in the type of boundary most commonly associated with each type of event; some events were most commonly found near a cold front, while others typically coincided with a warm front or a stationary front. The composites of most types of events were associated with a low-level jet, but some individual cases were exceptions to this general rule. Finally, a key difference between different categories of events was in the magnitude of the bulk Richardson number. These parameters will be examined for events in the northeastern U.S. in chapter 4.

1.6 Flash flooding and heavy precipitation in the northeastern United States

A few studies have sought to describe flash flooding in the northeastern U.S. and how it differs from flash flooding in other parts of the country. LaPenta et al. (1995) describe the most common types of events contributing to flash floods in the eastern U.S. – synoptic, convective, and tropical systems. Synoptic-scale storms affect large river valleys over a period of several days. They are often associated with either a quasi-stationary (usually north-south oriented) synoptic front or a large extratropical cyclone. Though flooding due to storms at the synoptic scale is usually due to extratropical systems, they may also result from a tropical cyclone or the interaction of a tropical cyclone with an extratropical cyclone. Extreme synoptic-scale flooding is most common in springtime, associated with extratropical cyclones, and in late summer and early autumn, associated with tropical cyclones. Mesoscale extreme flood events in the northeast U.S. tend to be associated with abundant low level moisture, tropical plumes of mid and upper level moisture (Thiao et al., 1993), veering winds with height, a surface boundary, and a diffluent thickness pattern, which often results from low-level speed convergence and upper-level diffluent flow (Funk, 1991).

The orographic effects of the Appalachian Mountains can generate convection via upslope flow, and mountains, hills, or water bodies (such as the Great Lakes) can produce mesoscale boundaries that provide lift for convection.

While the synoptic and mesoscale processes producing flash floods in the northeastern U.S. are not terribly different from those findings for other parts of the country, at the storm scale LaPenta et al. (1995) point out that the Northeast appears to have a unique feature. Warm-top thunderstorms (Scofield et al., 1980) can produce quick bursts of heavy rainfall in the Northeast; these storms were found to occur more often in the eastern U.S. than in other parts of the country (Spayd and Scofield, 1983). Warm-top thunderstorms, which have cloud-top temperatures warmer than -62 ºC, form in environments with a low equilibrium level due to either stable upper levels of the troposphere or a low tropopause, and are often found near a deep trough or low aloft. The storms are associated with significantly less CAPE than cold-top storms producing similarly heavy rainfall. It is likely that the microphysical processes associated with precipitation generation in these storms are similar to the warm rain process described by Davis (2001).

Giordano and Frisch (1991) examined 63 extreme rainstorms in the mid-Atlantic region that dropped at least19 cm (7.5 inches) of rain in a period of 12 hours or less. They found that these events tended to be associated with an upstream long wave ridge over the Plains for events in the Ohio Valley and with an upstream trough over the Appalachians for events located along the East Coast. As a result, winds for summertime extreme rainstorms over the Ohio Valley (including western Pennsylvania) are commonly from the northwest, while winds were found to be typically southwesterly for extreme rainstorms along the East Coast. The authors surmise that the summertime ridge over the Plains helps to transport moisture from the Gulf to the northeast U.S., enabling the genesis of heavy rainfall. As has been shown

for other regions, the events were associated with high moisture from the surface to 700 hPa, strongly veering winds, and wind speeds about one-third faster than normal for the summer. Every northwest flow event was found to be associated with diffluent flow aloft or a jet stream maximum, while these features were not present for approximately a quarter of southwest flow events.

Jessup and DeGaetano (2008) compared 50 flash flood events in northeastern Pennsylvania and central New York with a set of 34 heavy precipitation events that did not produce flooding. They found that these heavy rain events were more common on days with small to moderate values of CAPE, suggesting warm rain processes, abundant low-level moisture, and a large upwind area of near constant equivalent potential temperature (θ_e) as compared to the summertime climatology. Unlike in the Schumacher and Johnson (2005) study, which found MCSs to be located downwind of a tongue of high θ_e air, it appears that in the Northeast, flash flooding commonly occurs in the middle of a broad area of warm, moist air. If such a feature is found to be consistent in this study, it would suggest that forecasting the likely location of flash flooding in the Northeast may be even more difficult than in other regions. Jessup and DeGaetano (2008) also found that antecedent soil moisture was the most significant discriminator between flash flood events and heavy rain events that did not produce flooding, and that point values of other environmental variables were less meaningful predictors of the likelihood of flooding given that heavy rainfall occurred.

1.7 Research Questions and Objectives

The literature review in this chapter has shown that a great deal of work has gone into investigating the atmospheric conditions and convective organization

associated with flash flooding and heavy precipitation. However, much of this work has been done in the central United States, and comparatively little has been done in the Northeast, especially New England. This dissertation seeks to explore the properties of flash flooding in the northeast U.S. in greater detail, in order to examine whether those properties of flash flooding that have been described for other regions are equally applicable in the Northeast. Certainly, the basic ingredients of heavy precipitation – moisture, a source of lift, and a means to prolong the precipitation, among others – must be present, but it is possible that the processes bringing these ingredients together may differ from region to region. The following research questions drive the exploration of this possibility.

1. Are the predominant patterns of organization of flash-flood-producing precipitation different in the Northeast than in the Midwest, Southern Plains, and other parts of the U.S.?

2. Do those events whose radar signatures have been identified in the literature share similar environmental characteristics in the Northeast?

3. Are there new classifications of the precipitation organization of flash flood events that have not been identified in the literature, and, if so, do the new classifications of events have distinctive environmental characteristics as compared to the environmental characteristics of the types already identified in the literature?

4. How do events producing heavy or extreme precipitation compare to events of the same type that produce more moderate amounts of precipitation?

CHAPTER 2

CASE SELECTION

2.1 Methodology

The overarching objective of this dissertation is to study flash floods in the Northeast that result from warm-season convection in order to understand how the organization and environmental conditions associated with the precipitation differs from the organization and environmental conditions of flash-flood producing convection in other regions. For this study, the Northeast is defined as the states of Pennsylvania, New York, New Jersey, Connecticut, Rhode Island, Massachusetts, Vermont, New Hampshire, and Maine. A five-year sample (2003 to 2007) was selected to provide a representative sample of events. Before 2003, radar data were often missing, and at the beginning of the study, the final complete summer of *Storm Data* was 2007.

Identifying a representative sample of flash floods or heavy precipitation events is more difficult than it may seem. One approach is to use hourly or daily precipitation data and to select a precipitation threshold; this was the approach of Schumacher and Johnson (2006). Another approach is to select events from flash flood reports in the National Climatic Data Center's *Storm Data* database (NOAA, 2010b). The seminal paper on flash floods by Maddox et al. (1979) used this selection criterion. This was also the approach used in this study, as it allowed for the detection of smaller scale events that are less likely to be observed by the precipitation gauge network. (Note: at this juncture, daily radar precipitation estimates are not available, so radar data make for an inconvenient starting point.) The *Storm Data* reports are

provided by local offices of the National Weather Service, using reports collected from local, county, state and federal emergency management officials, law enforcement officials, trained spotters, NWS damage surveys, newspaper clipping services, the insurance industry, and the general public (NOAA, 2010b). Typically containing the start and end time of the event, its location, and a brief description of the meteorological scenario as well as the impact of the flood, each flash flood report contains enough information to assemble a climatology of events that generated potentially life-threatening conditions from a combination of meteorological and hydrological causes. The reports specify whether the flooding was due to stream flooding, urban flooding, a dam failure, or other causes. Flash floods are classified separately from river floods, following the National Weather Service definition of a flash flood: that is, a flood occurring within six hours of the causative event (NWS, 2008).

To assemble a climatology of flash flooding for the northeast U.S. from May through September for the years 2003-2007, all *Storm Data* flash flood reports were recorded for the region of interest during this period, including the start and end times, location, type of flooding, and any reported precipitation observations or estimates. Flash floods attributed to dam failures on days with fair weather were excluded from the sample, as these events were likely due to mechanical failure rather than a meteorological or hydrological cause. To limit the climatology to flash floods resulting from warm-season convection, event days during which a named tropical system or its remnants were affecting the northeastern US were excluded from the sample. The desired end result was a climatology consisting of only one event per diurnal cycle – one flash flood per event day.

In general, an "event day" was defined to extend from 8 am local time on one day to 8 am local time on the following day. When a series of flood reports in the

same region began before 8 am and continued after 8 am, rather than strictly applying the 8 am time limit to separate flash flood reports in one event day from the next, these reports from before and after 8 am local time were classified as being part of the event day spanning the larger time interval relative to 8 am. For example, if the flash flood reports began at 6:30 am and continued until 11:00 am, all of these reports were classified as belonging to the event day that began at 8:00 am.

To determine which report to select on multiple-report event days, 24-hour precipitation data from cooperative observing stations archived by the Northeast Regional Climate Center were used to select the county containing the highest observed 24-hour precipitation total. If more than one flash flood was reported in that county, the flash flood location selected to represent the "event day" was determined later as the location receiving the highest radar-estimated precipitation total.

Once the flash flood report was selected to represent each flash flood day based on the total observed precipitation, the specific flash flood locations were determined through the event descriptions in *Storm Data*. The flood's location was often described as a road or a stream, or more broadly as occurring in the vicinity of a town or city. In the more recent flash flood reports, latitude/longitude coordinates were also given, but these locations were often found to disagree with the stated road or stream location of the flood; in these cases, the stated location, rather than the latitude/longitude point, was used. For some cases, the report clearly stated that the flooding was the result of one to several streams overflowing their banks, but the specific location of the flooding – a named stream or a road – was not cited in the report. In these instances, the more general locations named in these descriptions were viewed with Google Maps, Google Earth, and ArcGIS software to locate potential flooding locations – points where a stream intersected or ran closely alongside a road. From among the potential flood locations, the stream/road intersection point in the

basin with the highest radar-estimated precipitation total was then identified as the most likely flash flood location. For urban or road flooding reports in which no specific roads were mentioned, a road within the basin with the highest basin-estimated precipitation total within the town or city named in the flash flood report was identified as the most likely flash flood location.

2.2 Event Climatology

A survey of the flash flood reports in Storm Data revealed a total of 1251 flash flood reports on 201 event days for the Northeast from May through September 2003-2007, excluding events associated with named tropical storms and fair-weather dam breaks. Of these 201 event days, eleven were missing radar data, leaving 190 events whose radar signatures could be classified. A further three events were eliminated because they were the continuation of precipitation from the previous event day or represented the same type of organization in the same type of environment as the previous day. Thus, the total number of events analyzed in this study is 187.

Flash flood reports were most common during the summer months of June, July, and August, with a pronounced peak in the second half of July (Figures 2.1 and 2.2). Flash flood reports were less common in September, especially in comparison to the September peak for heavy precipitation events reported by Schumacher and Johnson (2006) for the Northeast. This difference in results is partially due to the exclusion of tropical storm event days from this study, many of which occurred in the month of September. In addition, Schumacher and Johnson's (2006) use of 24-hour precipitation data as the basis for selection criteria may place a greater emphasis on long duration events of lower intensity that may induce river flooding without generating flash flooding – events that may be more common in the spring and autumn

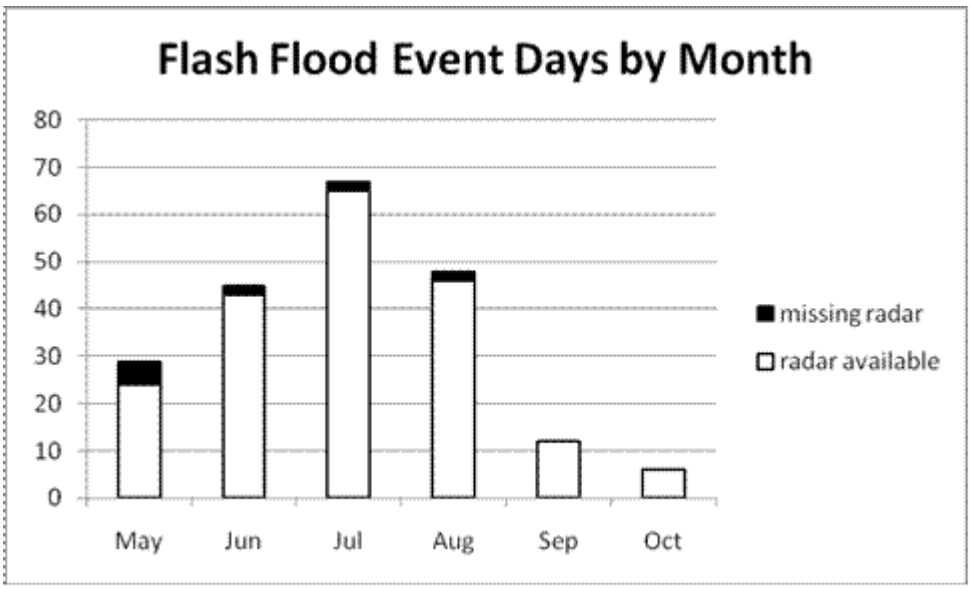

Figure 2.1 Flash flood event days by month, May-Sept. 2003-2007

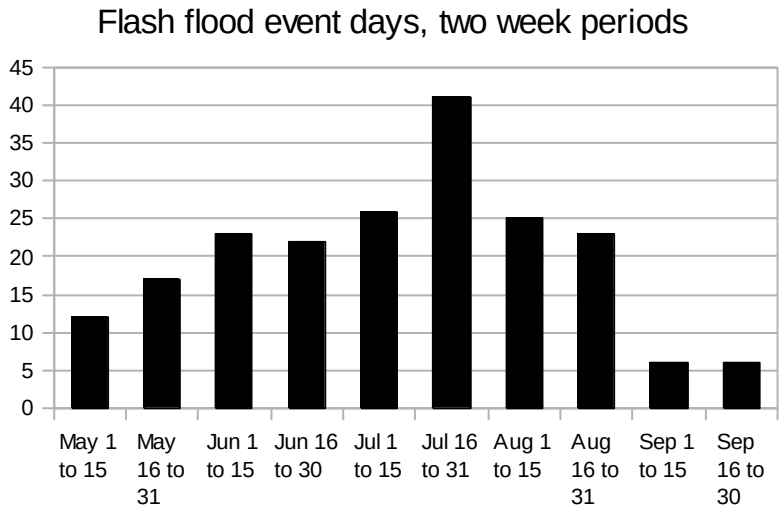

Figure 2.2 As above, but for the first and second half of each month.

months rather than during the summer. The monthly climatology found in the current study is much more similar to the results of Maddox et al. (1979) and Jessup and DeGaetano (2008), both of which used flash flood reports as selection criteria, and both of which found event frequency maxima in July over the Northeast, similar to what Schumacher and Johnson (2006) had found for most regions outside the

Northeast. The sharp peak in flash flood reports (Figure 2.2) during the last two weeks of July, consistent in the five years of this study, has not been previously noted in the literature. As pointed out in section 1.3(a), Bradley and Smith (1994) described pronounced peaks in the occurrence of extreme precipitation events for the southern plains during the spring and fall, and they attributed these peaks to the confluence of three critical factors: dynamical forcing, convective instability, and moisture. Applying this logic to the late-July peak in the northeast shown in Figure 2.2, while it is unlikely that large-scale dynamics are significantly stronger than in the remainder of the summer, it is possible – though not likely – that there is increased convective potential or increased moisture advected from the Gulf of Mexico or Atlantic Ocean during this short period of time. Giordano and Fritsch (1991) argue that a long wave ridge is necessary to advect substantial moisture north from the Gulf of Mexico to the Midwest and then east from the Midwest to the Northeast. It is possible that such a ridge is more common during the second half of July, but the July climatology of geopotential height (not shown) suggests that such a pattern is not persistent over a thirty year span during this portion of the summer. A second – and perhaps the more likely – reason for the maximum in flash flood frequency during the second half of July is that this is simply a statistical anomaly resulting from the relatively small sample of five years that was used to select the events.

The diurnal climatology displays an increase in flash flood reports from the early afternoon hours through mid-evening, with a pronounced peak in the late afternoon (Figure 2.3). This suggests that many flash flood events in the Northeast result from convection associated with daytime heating. The diurnal distribution of the first report for each event day (not shown) is similar, but with relatively fewer reports in the overnight and early morning hours and proportionally more reports in the early afternoon. Consequently, most nighttime flash flood reports in the Northeast

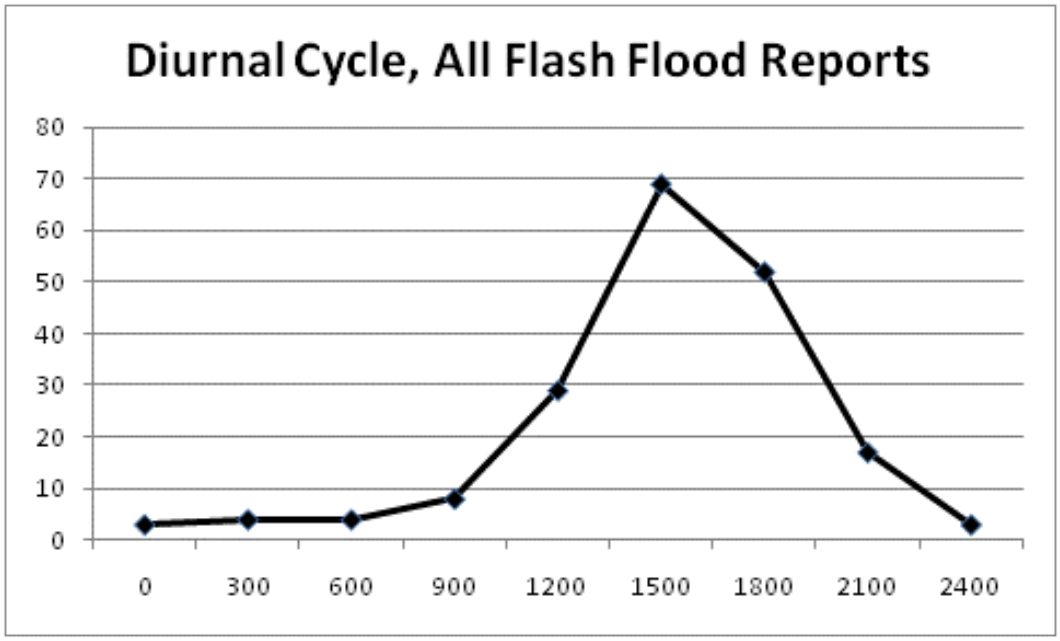

Figure 2.3 Reported time of all flash flood events, local time

result from convection that was likely initiated by daytime heating. The diurnal distribution of the first report for each event day (not shown) is similar, but with relatively fewer reports in the overnight and early morning hours and proportionally more reports in the early afternoon. Consequently, most nighttime flash flood reports in the Northeast appear to be a continuation of convection that initiated during the afternoon or earlier, rather than the more recent product of convection that developed later in the day. This differs from the findings of both Maddox et al. (1979) and Schumacher and Johnson (2006), who found that the onset of heavy rain associated with flash-flood-producing MCSs occurred most often from the late afternoon through the early evening hours, with the peak precipitation (which most likely corresponds best with the timing of flash flood reports) occurring late in the evening, from 8:00 pm to midnight local time. Whether this difference is due to regional differences in the types of storms and their accompanying environmental conditions will be examined in greater detail later in this paper.

The diurnal timing of flash flooding tends to remain relatively consistent throughout the warm season (Figure 2.4). Because synoptic scale systems can produce significant amounts of precipitation without diurnally-driven convection, one might expect a secondary peak in flash flood occurrence in the overnight or early morning hours in May and September, as the dynamics associated with features tend to be more common on the fringes of the warm season rather than in the middle of it (Bradley and Smith, 1994). However, there is very little difference in the timing of flash floods: the peak time for flash flood occurrence is in the mid-afternoon during June, August, and September, and the peak tends to widen to include the late afternoon or early evening hours in May and July.

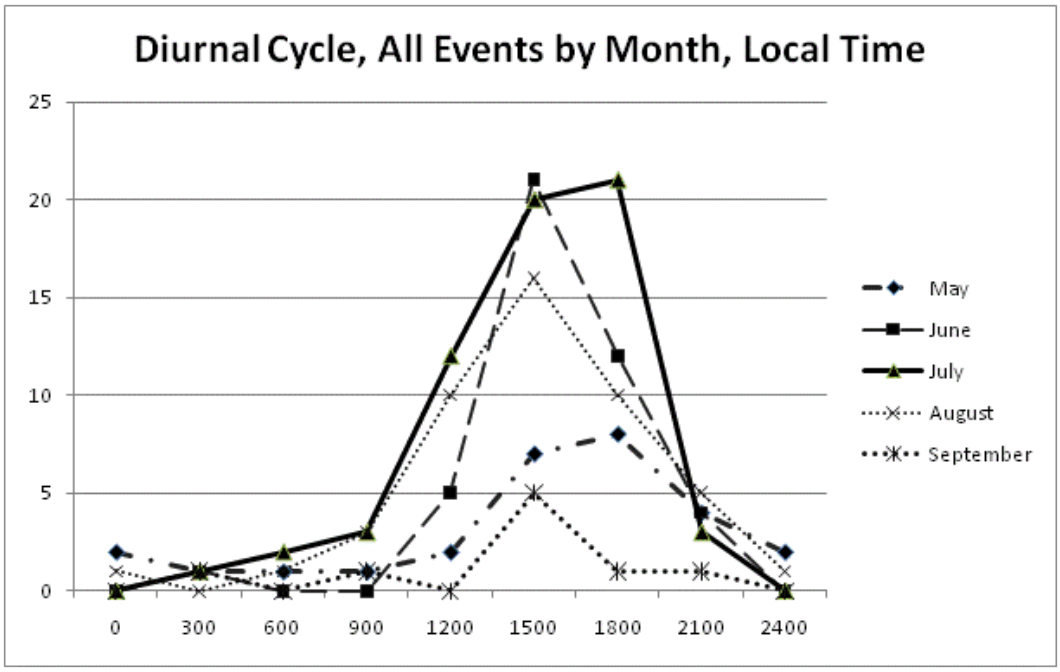

Figure 2.4 Reported time of all flash flood events, by month.

In terms of the spatial distribution of the flash flood reports, flash floods were most common in Pennsylvania, followed by New York and New Jersey, and considerably less common in the New England states. This is very similar to the

finding of LaPenta et al. (1995), except that they found New York to have approximately 1/3 more flash flood events than Pennsylvania from 1955-1988. A map of the flash flood locations (Figure 2.5) shows that the flash flood events in Pennsylvania tend to be focused in the eastern and western thirds of the state, with relatively few flash flood events in the central third, which comprises a large portion of the Susquehanna River basin. Other areas lacking in flash flood reports examined in this study include southern New Jersey, northern Vermont and New Hampshire, and eastern Maine. This represents only the 187 events selected from the overall total of 1251 flash flood reports during the time period of this study, so it is quite possible that events occurred in these areas but were not identified to represent an event day via the selection criteria described above. Along with the potential concern about spatial

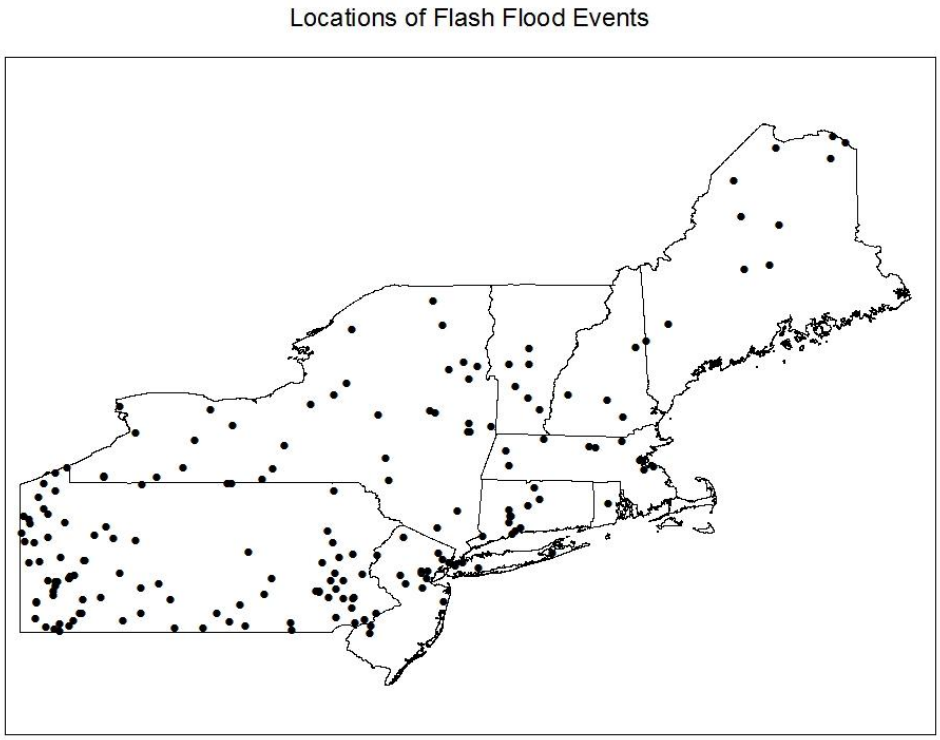

Figure 2.5 Locations of the 187 flash flood events in this study.

consistency in event selection using flash flood reports to select flash flood events, there may be concern over whether reporting bias may lead to an overabundance of flash flood reports in urban areas. Figure 2.5 shows that there do tend to be clusters of flash flood events in the vicinity of major cities, including Pittsburgh and Philadelphia, and to a lesser extent, Hartford, New York City, and Boston. Still, there are also many events in isolated areas of New York, Vermont, New Hampshire, and Maine – events which may not have been identified had rain gauge data been used to select events. On the whole, the selection criteria appear to have selected a set of events that adequately represents the temporal and spatial properties of flash flooding in the Northeast.

CHAPTER 3

CLASSIFICATION OF PRECIPITATION ORGANIZATION

3.1 Development of Classification System

Crucial to achieving the overarching objective of determining whether flash-flood producing rainstorms in the northeastern U.S. are qualitatively different from those in other areas of the country is determining how well the archetypes of heavy precipitation in the literature describe the observed organization of heavy precipitation in the Northeast. The classification of events in this study began with the types of events described by Parker and Johnson (2000) and Schumacher and Johnson (2006), and described in this paper in section 1.5. These included the leading stratiform (LS), parallel stratiform (PS), trailing stratiform (TS), and training line/adjoining stratiform types (TLAS), as well as the back-building/quasi-stationary (BB) class of events. Schumacher and Johnson (2006) also classified events as "synoptic" (SYN) if the radar signature persisted for more than 24 hours, and as "multiple" (MULT) if more than one distinct mesoscale feature on the radar contributed to the daily precipitation total. Events not meeting the description of any of the above categories were classified as "Other".

Schumacher and Johnson's (2006) results (Figure 3.1), which found a maximum of events in the Northeast in August and September due to synoptic and tropical events (tropical events are not shown), suggested that while the above classification scheme was robust for much of the country, this classification scheme appeared to be insufficient to describe mesoscale heavy precipitation events in the Northeast, which generally did not fit their classification scheme and were classified as "other". However, the sample size of only 13 events (with only four classified as

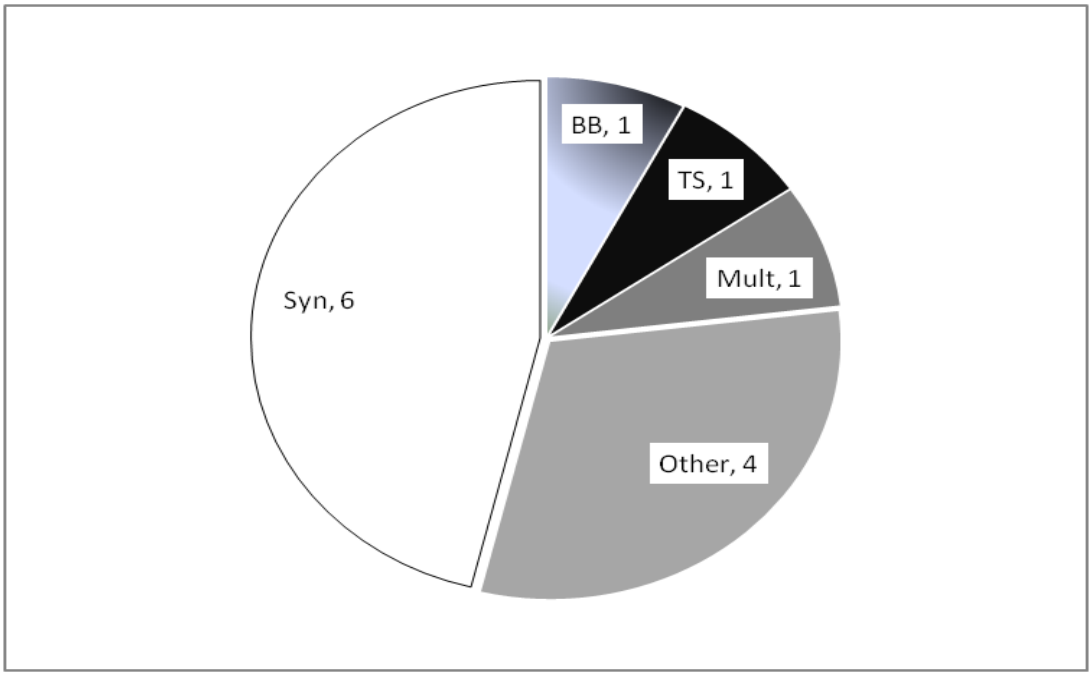

Figure 3.1 Frequency of northeast U.S. flash flood events by event type, Schumacher and Johnson (2006).

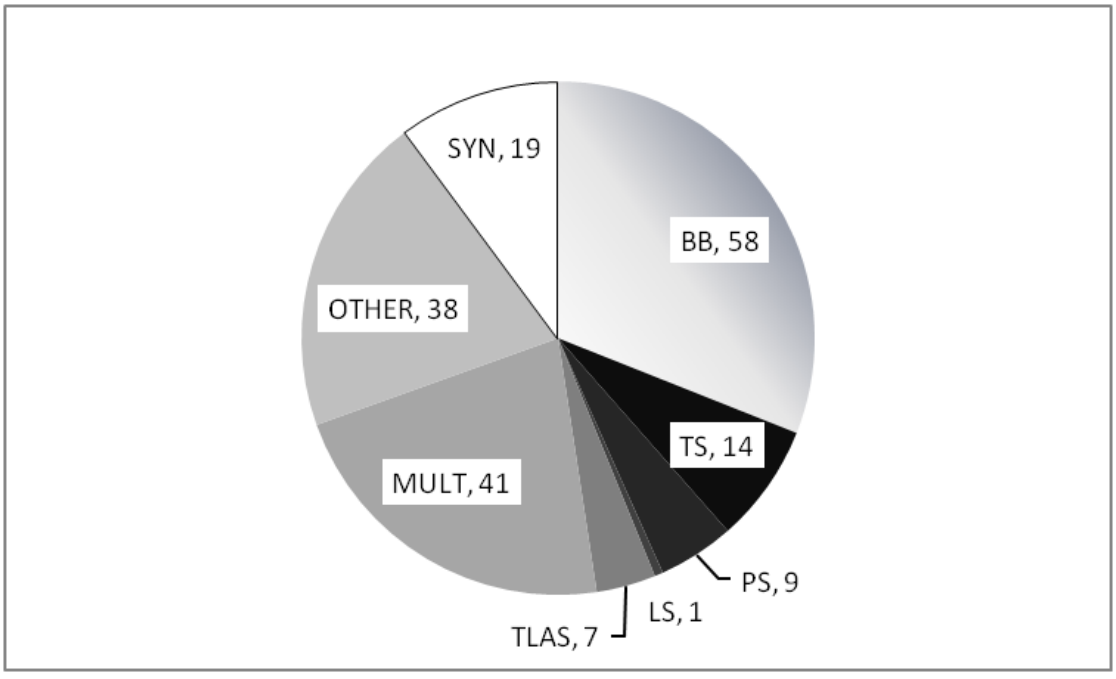

Figure 3.2 Frequency of northeast U.S. flash flood events, 2003-2007, by event type, following the scheme of Schumacher and Johnson (2006).

"other") limited the applicability of this conclusion. In examining 187 flash flood events in the Northeast, the current study found that these classifications were not sufficient to describe the configurations of precipitation organization for flash-flood producing rainfall in the northeast U.S., as illustrated in figure 3.2. In both Schumacher and Johnson's (2006) limited sample and the larger sample of events in this study, a sizable proportion of events fit none of Schumacher and Johnson's (2006) descriptions of linear organization, and were thus classified as "multiple" or "other" events.

In the present study, the back-building events comprised the most frequent classification of events. This suggests that back-building events are more common in the Northeast than Schumacher and Johnson's (2006) results had implied. Because Schumacher and Johnson (2006) based their classification on 24-hour rain gauge measurements, it is possible that the relatively small scale of the heavy precipitation cores produced by back-building events in the Northeast as observed on radar for the events in this study means that this type of event often escapes detection by the rain gauge network in the Northeast, while these events may form at a larger scale elsewhere. Similarly, Schumacher and Johnson (2006) found that nearly half of the non-tropical extreme precipitation events in the Northeast were of the SYN type, while in this study they comprised just over 10% of the events. This difference may again be due to the differences in selection methods for the two studies. The 24- hour precipitation thresholds used by Schumacher and Johnson (2006) may have preferably selected the long-duration moderate rainfall rates produced by synoptic events as compared to the shorter duration, more intense rainfall rates of smaller systems, while the flash flood report selection criteria used in this study may have reduced the number of SYN events producing large rainfall totals because these events may have

been more likely to produce delayed response river flooding rather than rapid response small basin flash flooding. The latter may be more likely to be a result of smaller but more intense systems which may be more capable of producing rapid runoff in smaller watersheds. Schumacher and Johnson (2006) found that events with linear organization of intense convection appear to be rarer in the Northeast than in most other areas of the country. Though this finding was limited by a small sample size, Figure 3.2 suggests that a reduced frequency of linearly organized events in the Northeast is likely to be true, as the linear events comprise less than 20% of all cases examined in this study, fewer than the "other", "multiple", and back-building groups.

Because these three most common classifications of "other", "multiple", and back-building events comprised such a large proportion of the events, yet at the same time provided little description as to their particular organization, these broad categories were examined to determine sub-categories that would more accurately reflect the similarities of the events within these groups. The "other" events, which all resulted from individual features ranging from thunderstorms to broad swaths of rain up to several hundred kilometers long, were partitioned by their length scale – the maximum length of each individual area of precipitation exhibiting approximately uniform motion. Those events having a length scale of 50 km or less (ostensibly thunderstorms) were classified as "small mesoscale isolated" (SMISO) events. In these cases, only one thunderstorm, often traveling relatively slowly, was responsible for the flash flood. Few, if any, other thunderstorm cells were detected on the radar's field of view during these events, and if they were detected, they were located at least 100 km from the isolated mesoscale feature that caused the flooding. Events with a length scale of 50 to 150 km were classified as "medium mesoscale" (MM) events. These events were approximately the same size as the mesoscale convective features described by Parker and Johnson (2000) and Schumacher and Johnson (2006), but

they lacked the organization – specifically, the well-defined lines of heavy convection – of the mesoscale features that these studies had identified. Features with a length scale of greater than 150 km that dissipated after less than 24 hours were classified as "large mesoscale" (LM) events. These events looked very similar to the "synoptic" events, and similarly produced flash flooding as a result of an extended duration of moderate to heavy rainfall, but the shorter lifetime of these precipitation systems placed them in a different sub-category. Figure 3.3 schematically display the four scalar classes of flash flood events.

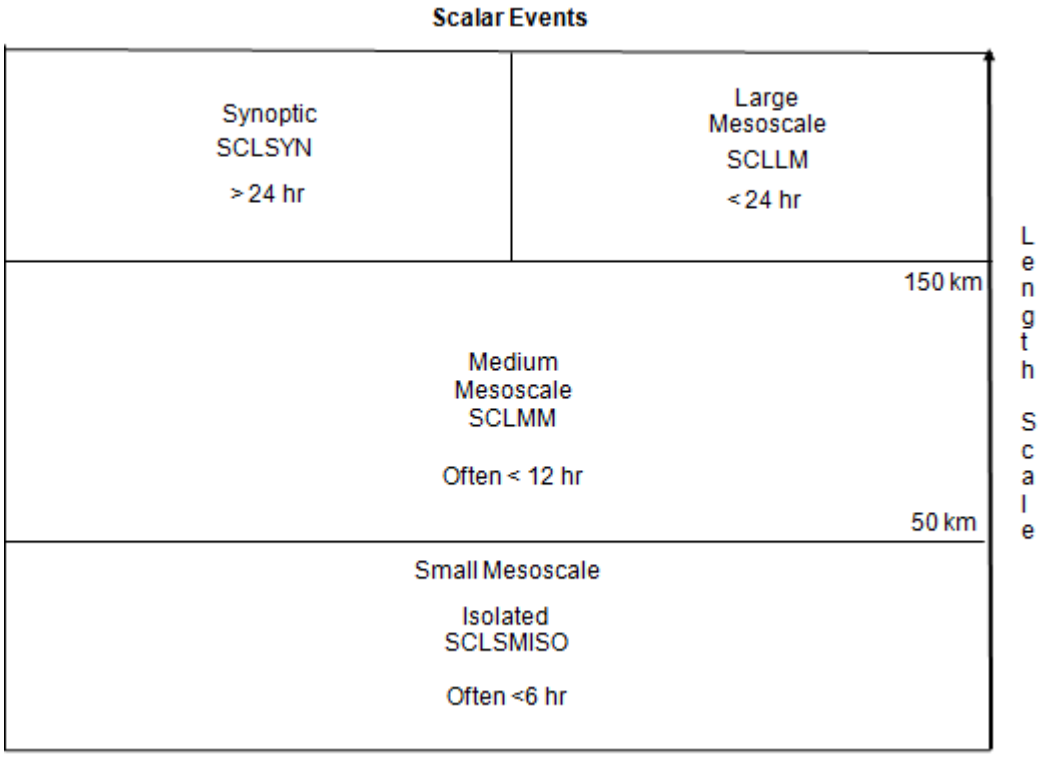

Figure 3.3 Schematic illustration of scalar flash flood events. Sub-classes are determined by the size and duration of events.

Like the single-feature events that did not fit into any classification, the events for which the flash flooding resulted from multiple radar features were divided into

sub-classes, which were based not on the appearance or size of the features themselves, but on the relative movement of the individual features on the radar. It was believed that this approach would best segregate the events based on the three-dimensional wind field, providing a physical basis for the different classes of "multiple" events. The "multiple" events featured what could best be described as "scattered" convection – thunderstorms, squall lines, and small MCSs, which on some occasions matched the descriptions of linear organization identified by Parker and Johnson (2000) and Schumacher and Johnson (2006) and on other occasions appeared not to be organized. These events with "scattered" precipitation were classified into one of three groups based upon the relative movement of the thunderstorms, squall lines, and other MCSs for the duration of the event. If the cells and MCSs traveled in the same direction at approximately the same speed, resulting in a series of features traversing the flood location via roughly the same path, these events were classified as "scattered training" (SCTTR) events. These events have a different appearance from the back-building class of events in that the individual cells and MCSs do not necessarily share the same genesis location and in that the individual features are separated by a much greater distance than the cells in a back-building event. Whereas the back-building events appear to be sustained by a positive feedback process which generates new convective cells on the rear flank of old cells, the training in SCTTR events appears to be coincidental, or at the very least, the product of an external, rather than internal, forcing mechanism. On some occasions, scattered thunderstorm cells (and usually not larger features such as squall lines or MCSs) were moving in seemingly random directions and at different speeds, as Figure 3.4 implies; the flash flooding was the fortuitous result of several cells randomly traversing the same location at different times. These events were classified as "scattered random" (SCTRAND) events. The slow movement typically exhibited by the cells suggests

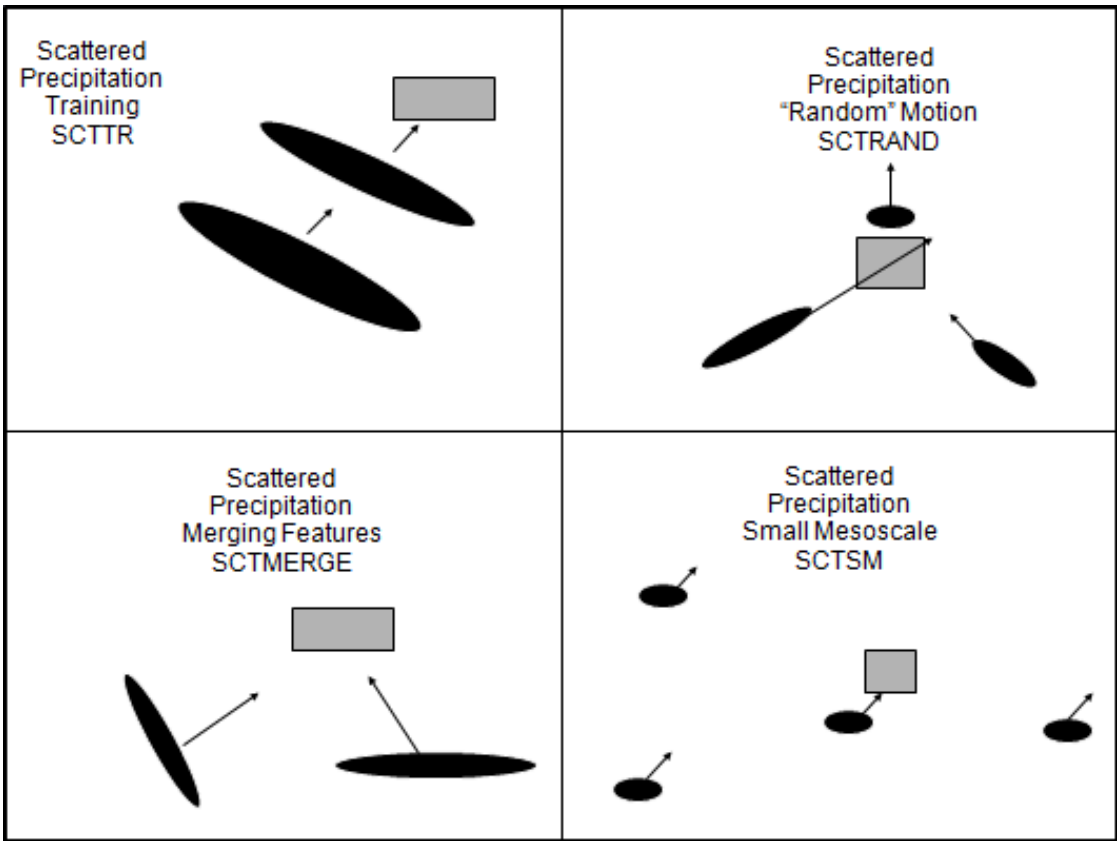

Figure 3.4 Schematic diagram of the four "scattered" sub-classes of events. Sub-classes are determined by the relative motion of cells and MCSs. Gray boxes indicated the area of highest flooding potential for each type.

that light upper-level winds were likely present, and the non-uniform movement of the individual cells suggests the presence of directional wind shear. Whether these features were present will be examined in chapter 5. The third class of "scattered" events consists of events in which two or more broad MCSs with moderate to heavy precipitation rates, traveling toward the same location from different directions, ultimately merge to form one larger MCS (typically merging just before reaching the eventual flood location). These events were different from SCTRAND events both in the behavior of the individual features, leading to the merger usually near the flood area, and the size of the individual features, which was often (but not always) larger

than in the SCTRAND events. These events were classified as "scattered merging" (SCTMERGE) events. The most common scenario for scattered merging events was for one MCS traveling approximately south-to-north to merge with another MCS traveling approximately west-to-east, and for the resulting combined MCS to continue on toward the northeast. A fourth and final sub-category of "scattered" events included small-scale thunderstorms which were scattered across the area, but only one of which traversed the flood location. Unlike the SMISO events, these "scattered small" (SCTSM) events were events in which a relatively large number of thunderstorms were present, and only one or a few of them in different places produced flash flooding. Figure 3.4 displays schematic diagrams of these four "scattered" types of events.

The most common category of events was that of back-building events. There was originally no intent to divide these back-building events into sub-groups, as they had been adequately been described by Schumacher and Johnson (2006) and had ostensibly been well-known in the forecasting community for quite some time. However, careful examination of a severe flash flood event in Delaware County, New York in June, 2006 revealed that the back-building feature remained in place while a trailing stratiform (TS) MCS approached from the southwest and dissipated after the MCS merged with the back-building cells. After re-examining the back-building cases, it was determined that nearly half of them had this same sequence of a back-building MCS which persisted until a linear MCS, often of the TS type, merged with it. These events were referred to as "back-building merging" (BBMERGE) events.

For several of the events that had originally been classified as "multiple" or "back-building" events, the flood location was affected by both back-building cells and one or more linear MCSs. Unlike in merging back-building cases, the features occurred independently of one another, with a time interval between the back-building

MCS and the linear MCS(s). In the first type of "multiple back-building" cases (BBMULT1), back-building convection forms and then dissipates, followed eventually by the passage of one or more linear MCSs. In the second type (BBMULT2), one or more linear MCSs traverses the flood area, and later back-building convection sets up over the flood area. Figure 3.5 displays schematic diagrams for the four back-building sub-classes of events. Table 3.1 lists all event types used in this study, which will be referenced throughout this paper.

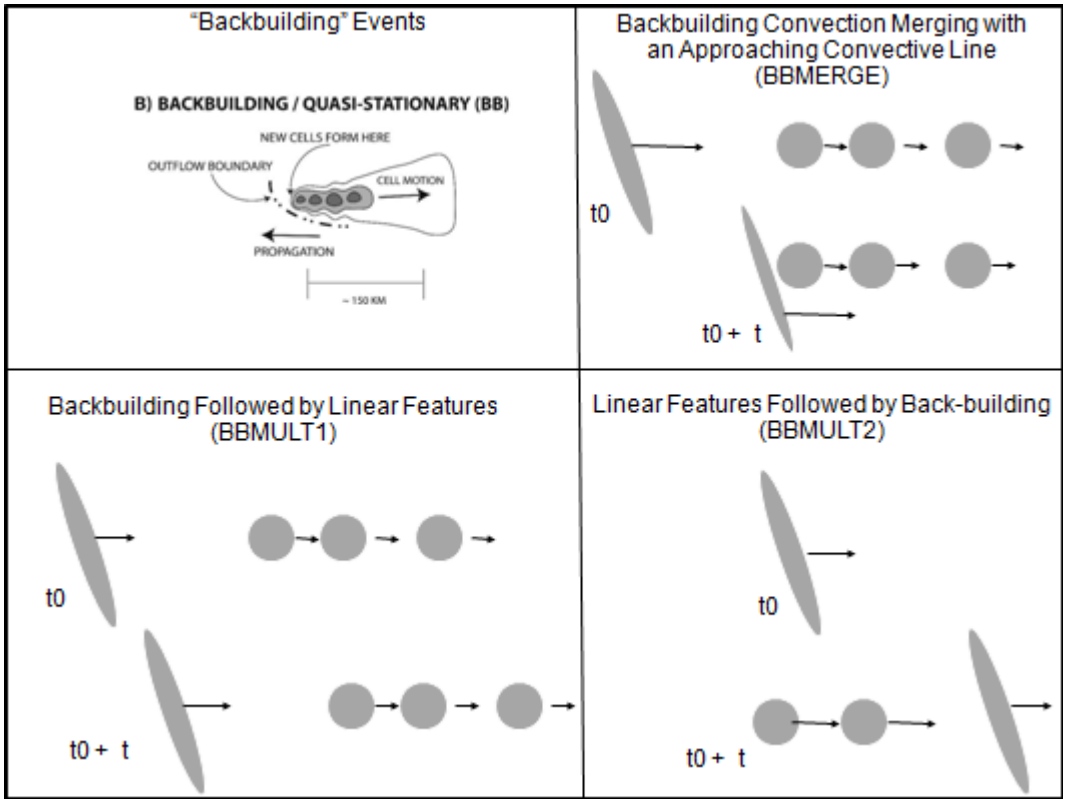

Figure 3.5 Schematic diagram of the four "back-building" sub-classes of events. Sub-classes are determined by the relative motion of back-building cells and MCSs and their relative transit across the flood area.

There are four categories of precipitation organization outlined in this study: back-building (BB), linear (LIN), scalar (SCL), and scattered (SCT), each of which

Table 3.1 List and description of all categories of precipitation organization associated with flash flood events examined in this study.

Name	Category	Description
BB	Back-building	Single back-building feature
BBMERGE	Back-building	Back-building feature merging with linear feature
BBMULT1	Back-building	Back-building feature later followed by linear feature
BBMULT2	Back-building	Linear feature later followed by back-building feature
LINTS	Linear	Convective line with trailing stratiform precipitation
LINPS	Linear	Convective line surrounded by stratiform precipitation
LINLS	Linear	Trailing convective line with leading stratiform precipitation ahead of it
LINTLAS	Linear	Training line of convective cells with stratiform precipitation adjoining it
SCLSYN	Scalar	Large scale (>150 km), long-lived (>24 hr) area of precipitation
SCLLM	Scalar	Large scale (> 150 km), relatively short-lived (<24 hr) area of precipitation
SCLMM	Scalar	Medium scale (50 km < MM < 150 km), nondescript areas of precipitation
SCLSMISO	Scalar	Small scale (<50 km), isolated areas of precipitation (usually thunderstorms)
SCTTR	Scattered	Scattered thunderstorms cells and or MCSs training over the same path in succession
SCTRAND	Scattered	Scattered thunderstorms moving slowly in arbitrary directions; several pass over the flood location
SCTMERGE	Scattered	Two MCSs moving toward the same area merge to form one larger entity
SCTSM	Scattered	Within an area of scattered thunderstorms, one storm travels slowly enough and drops enough precipitation in a watershed to produce a flash flood report

have four sub-categories describing their structure, size, and/or movement. The

following section will describe how frequently each of these categories occurred.

3.2 Observed Frequency of Storm Types

Using this new classification system, Figure 3.6 displays the relative frequency of the occurrence of each event type. The most common event types were the BB and BBMERGE types of organization, which each comprised approximately 15% of all events. This is a plausible result, as these events feature an internal positive feedback mechanism via the re-generation of new convective cells that ensures the persistence of heavy rainfall for an extended duration. Among the *scale* events, the events at the largest length scale (SYN and LM) were most common. A given SYN or LM event has the potential to cause flash flooding owing to the long duration of moderate to heavy rainfall that events of this type tend to produce.

The sub-categories of the *scattered* events that occurred most frequently were the SCTTR and SCTSM groups. Given the descriptions of the three *scattered* types of rainfall organization resulting from multiple features, the SCTTR group is the type which could be considered, purely from inferences made from observing the movement of cells and MCSs on radar, the most likely to occur under conditions most similar to the long-term mean summertime atmospheric environment. That is, the radar display for the SCTTR events displayed the scenario most commonly associated with summertime conditions in the warm sector of an extratropical cyclone. Unlike the SCTRAND events, which appear to be associated with abnormally light and variable winds, and SCTMERGE events, which appear to require convergent winds in the middle to upper troposphere, the SCTTR events appear to be possible in environments with moderate wind speeds and moderate amounts of wind shear, and,

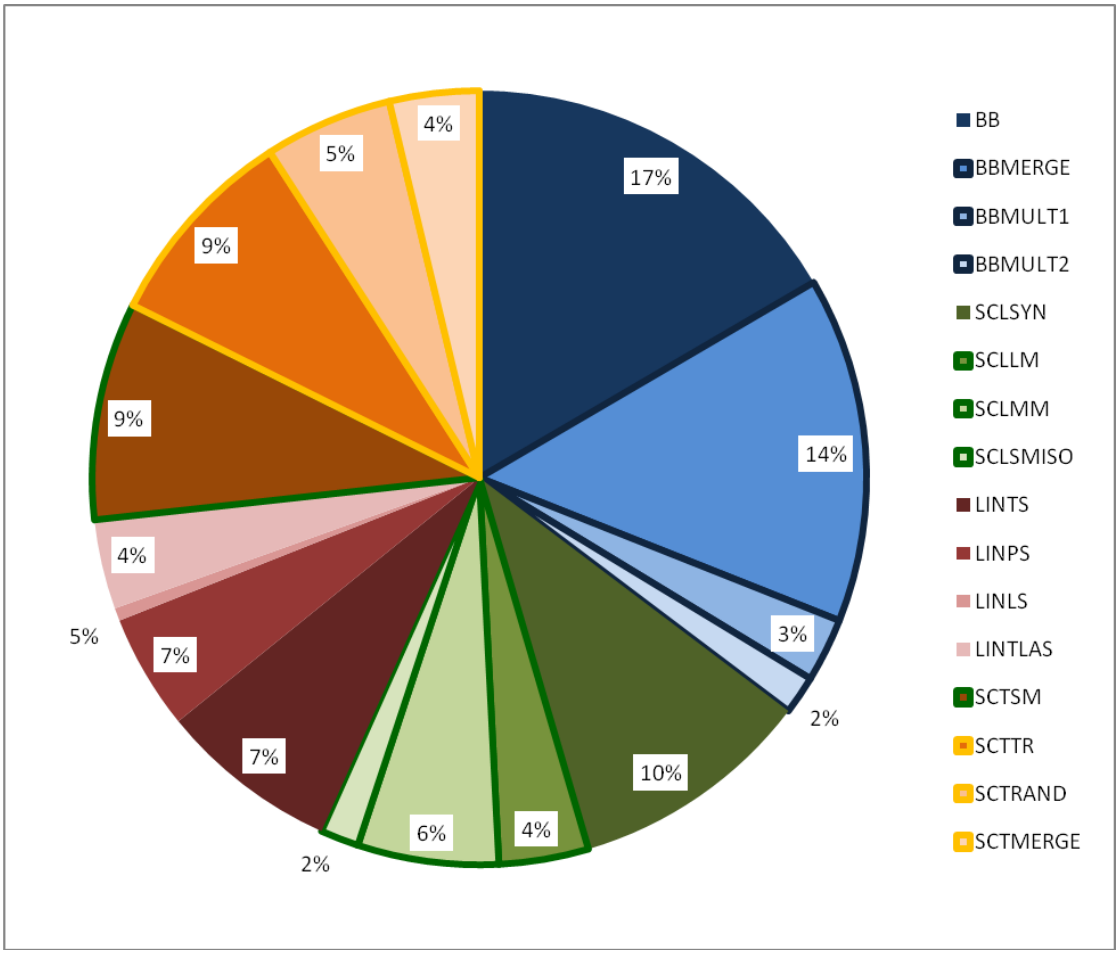

Figure 3.6 Pie chart displaying the relative frequency of events by storm type. The colors of the pie slices are based upon the groups of event types: back-building events, blue; scale events, green; linear events, red; scattered events, orange. Slices with a blue border were originally in the "back-building" class; slices with a green border were originally in the "other" class; and slices with an orange border were originally in the "multiple" class.

thus, are likely to occur more often than these types that seem to occur within a more unique environment. Meanwhile, the SMSCT events would also be likely to occur under seemingly common and benign conditions, especially in the warm sector of a mid-latitude cyclone. A single thunderstorm moving slowly enough and producing

intense rain rates over a hydrologically primed watershed could plausibly produce minor flash flooding.

Much like Parker and Johnson (2000) had found for the southern Plains region, the TS events were the most common among the *linear* groups of events. Of the linear types of events, the TLAS category could be described as the scenario that is theoretically most likely to generate flash flooding, as its training line of heavy rainfall provides a mechanism for sustained high rainfall rates (rather than the convective lines of the other linear archetypes, which tend to have a sizable component of motion perpendicular to the orientation of the line). However, the TLAS types of events were observed with only half of the frequency of TS events. While Schumacher and Johnson (2006) described TLAS events as often having a roughly west-to-east training line, there was no such consistency in the orientation of the TLAS events observed in the Northeast for the events in this study. It is possible that the environmental conditions which produce TLAS events with greater frequency in the Midwestern U.S. occur less often in the Northeast.

To make a meaningful comparison between the frequency of event types examined in this study and the results of other studies, such as that of Schumacher and Johnson's (2006), requires that only the events which meet similar selection criteria are used. As such, from the 187 events in the Northeast sample, only those events producing a radar-estimated 24-hour precipitation total meeting the precipitation threshold used by Schumacher and Johnson (2006) were selected, and Figure 3.7 displays the results for these 23 events. In comparison to Schumacher and Johnson's (2006) results for the Northeast, a much higher percentage of events was found to feature back-building convection, a much lower percentage of events was found to be the large-scale, SYN events, and a similarly small proportion of events was found to

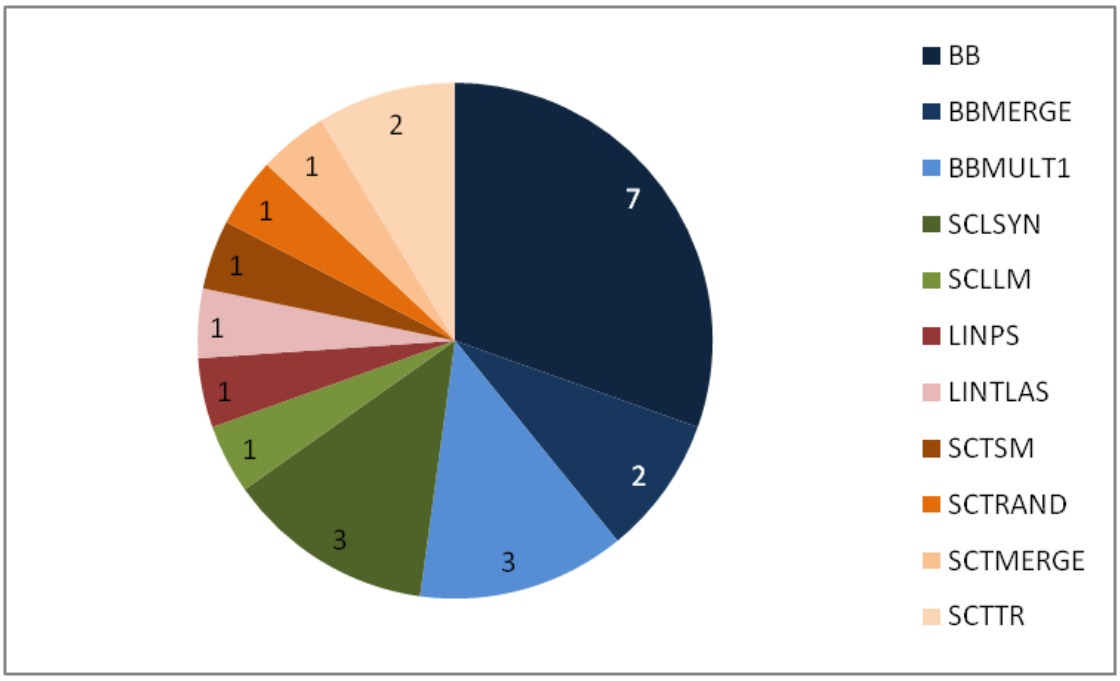

Figure 3.7 Pie chart displaying the relative frequency by storm type of events whose maximum radar-estimated precipitation totals meet or exceed the 24-hour precipitation threshold used by Schumacher and Johnson (2006). A total of 23 events (of the 187 events in this study) meet these criteria.

be of the linear type. More than half of the events in this study that met the precipitation threshold come from the back-building group of event types. Unlike in the overall climatology, here the "pure" BB events were more common than the BBMERGE and BBMULT events combined. The "scale" events were represented by the events at the largest scale, with both the SYN and LM types. Each of the four scattered types of events produced one or two flash flood events meeting the precipitation threshold. The group with the smallest representation among these extreme heavy precipitation events, though, was the linear group. Only the PS and TLAS types produced one event each that with an estimated 24-hour precipitation total meeting the 50-year precipitation frequency threshold. Perhaps a bit surprising,

while the TS event type was by far the most common linear event type in the overall climatology, it did not produce a single event that reached the extreme precipitation criteria defined by Schumacher and Johnson (2006).

3.3 Summary

This study has identified several new archetypes of precipitation organization associated with flash flood events in the northeastern U.S. Among these are special cases of back-building mesoscale precipitation systems that either merge with an advancing linear MCS or occur at some time interval before or after the passage of a linear MCS. Another series of events was classified by scale, with the largest extending over hundreds of kilometers and persisting for over a day, while the smallest are small thunderstorms with a lifetime of typically two hours or less. A third new group of events not discussed in the literature was the scattered class, in which events were classified based on their singularity (the SCTSM events) or the relative motion of the individual features appearing on the radar. Of these four general classes of events, the back-building group comprised approximately 35% of all events; the scattered group comprised approximately 27% of all events; the scalar group comprised approximately 21% of all events, and the linear group comprised nearly 17% of all events.

Do the results presented in this chapter support the hypothesis that flash flood-producing heavy rain events in the northeast differ from flash flood-producing heavy rain events in other areas of the country? The evidence suggests that the organization of precipitation for extreme precipitation events does differ in the Northeast as compared to other regions of the country, most significantly in terms of the much smaller frequency of linear MCSs that produce flash flooding and high precipitation

totals. Instead, flash flooding in the Northeast appears to more frequently result from events which are organized on smaller scales or not organized at all, including back-building events and events which can best be characterized as being the result of scattered precipitation, whether the flooding results from one slow-moving storm or a succession of several thunderstorms or MCSs. It also appears that, compared to other regions, flash floods in the Northeast are more often the result of larger-scale, longer-lived precipitation systems which have no clear tendencies for the organization of bands of heavier rainfall.

A brief characterization of how flash-flood producing precipitation appears to differ in the Northeast is that the precipitation systems appear to be less organized. While the storm types associated with flash flooding appear to differ regionally, including this apparent tendency to result from more disorganized precipitation in the Northeast, the methods used in this study cannot identify how frequently these storm types occur on non-flood days either in or outside of the Northeast, and, as a consequence, it cannot be determined whether a given storm type is more likely either to be present more often in one region than in another or to produce heavy rainfall and flash flooding in one region as compared to another. Similarly, the methodology cannot evaluate the question of whether either heavy precipitation or flash flooding occurs in other regions as a result of the small-scale features, such as scattered thunderstorms and thunderstorm-scale back-building features, which may be overlooked in the literature given the dependence in other studies upon rain gauge data. What this chapter has not resolved about the storm types identified for the Northeast are the unique precipitation properties associated with each storm type (to be addressed in chapter 4) and the environmental characteristics associated with each storm type (to be addressed in chapter 5).

CHAPTER 4

PRECIPITATION ESTIMATES

4.1 Methodology

Because the events in this study were selected using flash flood reports that often did not specify the amount of precipitation contributing to the flood, it was necessary to approximate these precipitation totals using the available data. Twenty-four-hour precipitation data were collected from the Northeast Regional Climate Center's archive of cooperative observer precipitation totals for each event day. For each station, precipitation totals are recorded each day at the same time; however, the observation time may differ from station to station, with most stations observing the 24-hour precipitation total sometime between 7:00 am and noon local time. These daily precipitation data served two purposes: first, to identify the county receiving the greatest precipitation amounts, as described in section 2.1; and second, to provide ground-truth precipitation measurements against which the radar-estimated precipitation could be compared, as described below.

Because rain gauges were rarely located within the flooded watersheds, precipitation totals for the location of flash flooding were estimated from radar. Radar functions by transmitting an electromagnetic wave and recording the proportion of this energy that is reflected back to the radar by raindrops, insects, and any other objects which the emitted radiation happens to intercept. It then aggregates this reflectivity in "bins" measuring one kilometer perpendicular to the beam by one degree in the radial direction. This radar reflectivity can be converted to a precipitation estimate using the reflectivity-to-rainfall conversion equation, $Z = AR^b$, where Z is the radar reflectivity, R is the rainfall rate, and A and b are constants that govern the relationship between

these two physical variables. For a standard Z/R conversion, A = 300 and b = 1.4. In this study, the radar reflectivity was converted to a rainfall estimate using the Areal Mean Basin Estimated Rainfall (AMBER) program, which is used operationally by the National Weather Service (NWS) to monitor potential flash flood situations in real time (Davis, 1993). To compute rainfall estimates, AMBER utilizes the Digital Hybrid Reflectivity (DHR) product generated by the Weather Surveillance Radar - 1988, Doppler (WSR-88D) Next-Generation Weather Radar (NEXRAD). Each one degree by one kilometer radar bin is associated with a hydrological basin (such that larger basins include multiple radar bins, which are averaged to determine the estimated precipitation for the basin), and the AMBER algorithm computes the mean estimated rainfall for each basin by converting the DHR product to an estimated rainfall rate using the above equation with the constants A and b specified in a configuration file used by the program.

Because the DHR product is not readily available for download from the National Climatic Data Center (NCDC), the raw reflectivity (Level II data) was downloaded and converted into the Level III DHR product that AMBER requires using the NWS's WSR-88D Common Operations and Development Environment (CODE) program. The DHR product was then input into AMBER, and AMBER was subsequently run using two different sets of basins, depending on the location. For the Pittsburgh-based WSR-88D, a set of basins that has been developed for local use by the NWS Pittsburgh forecast office was used (R. Davis, personal communication). For all other WSR-88D sites, the basins derived by the National Basin Delineation Project were used (Arthur et al., 2005).

Storm-total rainfall amounts were first computed using the standard Z/R relationship, described in the above paragraph. These totals were then compared with the cooperative observer 24-hour precipitation totals and with any precipitation

observations or estimates cited in the flash flood report. If the radar estimates significantly underestimated the observed rainfall totals and nearby atmospheric soundings detected a warm, near-saturated lower troposphere, the rainfall estimates were recomputed in AMBER using a tropical Z/R conversion, with constants A = 250.0 and b = 1.2. These updated radar-based precipitation estimates were again compared with the observed precipitation totals, and if they were found to be more accurate compared to the observations than the precipitation estimates derived from the standard Z/R relationship, these new estimates were used to represent the rainfall estimate for this case. Otherwise, the standard Z/R relationship was used for the given case. Once this process was completed for all cases, these best-estimate basin-averaged rainfall totals for the flash flood location and, in the case of flash floods identified as stream flooding rather than street or urban flooding, the rainfall totals including the contributing upstream basins were recorded to represent an approximate precipitation total for each flash flood event. Furthermore, because the highest precipitation totals were often found in the vicinity of the reported flash flood location but not within the flooded watershed itself, the maximum basin-averaged precipitation estimate in the vicinity of the flood location was also recorded. Throughout this paper, the entire area contributing to the flash flood will be referred to as the "watershed", while the smaller areas within and nearby the watershed over which the precipitation was averaged will be referred to as "basins".

4.2 General Precipitation Properties of Flash Flood Events

The median radar-estimated precipitation total for the basin with the highest precipitation estimate in the vicinity of the flash flood location was 85.09 mm (3.35 inches). Figure 4.1 displays a histogram of maximum radar-estimated precipitation

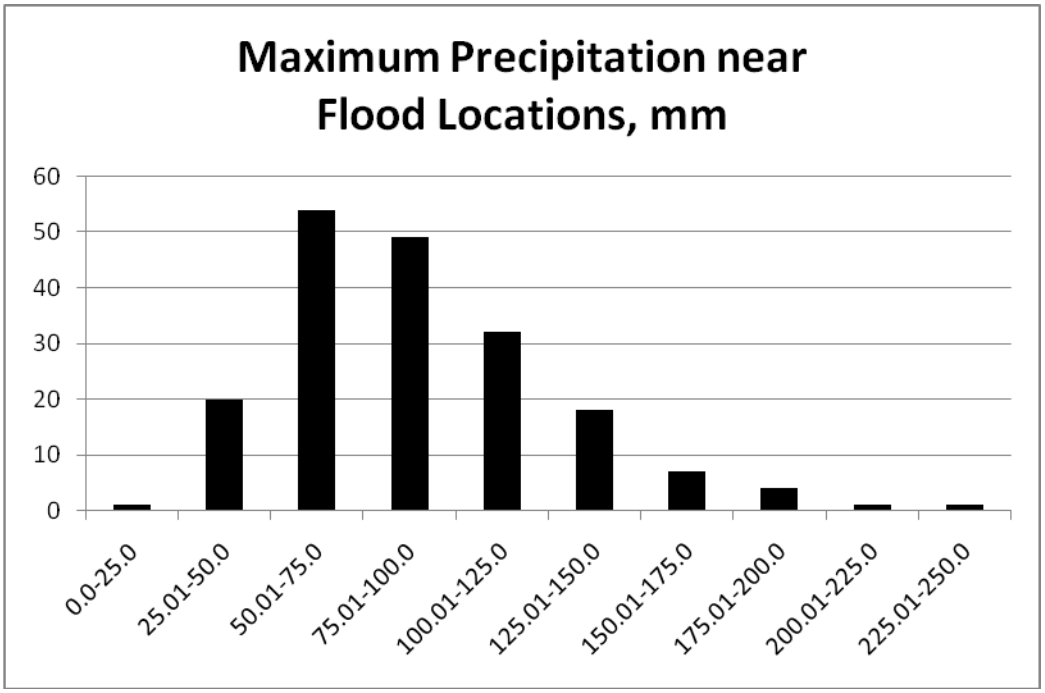

Figure 4.1 Histogram of Maximum Basin-Averaged Precipitation Estimates.

totals for the 187 events in this study. The majority of events (87.8%) included at least one basin with a precipitation estimate exceeding 50 mm (1.97 in), and a substantial minority (32.6%) included at least one basin with a precipitation estimate exceeding 100 mm (3.94 in). Only one case had a maximum precipitation estimate of less than 25 mm (0.98 in).

The remainder of this chapter will be dedicated to examining these precipitation data in more detail to seek trends in the characteristics of the events that produce larger or smaller rainfall totals. To investigate some of the spatial properties of the flash flood events, Figure 4.2 displays the maximum basin-averaged, radar-estimated precipitation totals within each flooded watershed (shaded) and the approximate size of each watershed (size of circles). One might expect to find flooding of smaller watersheds or street flooding in urban areas, owing to the rapid response of runoff to impervious areas, and flooding of larger watersheds in more

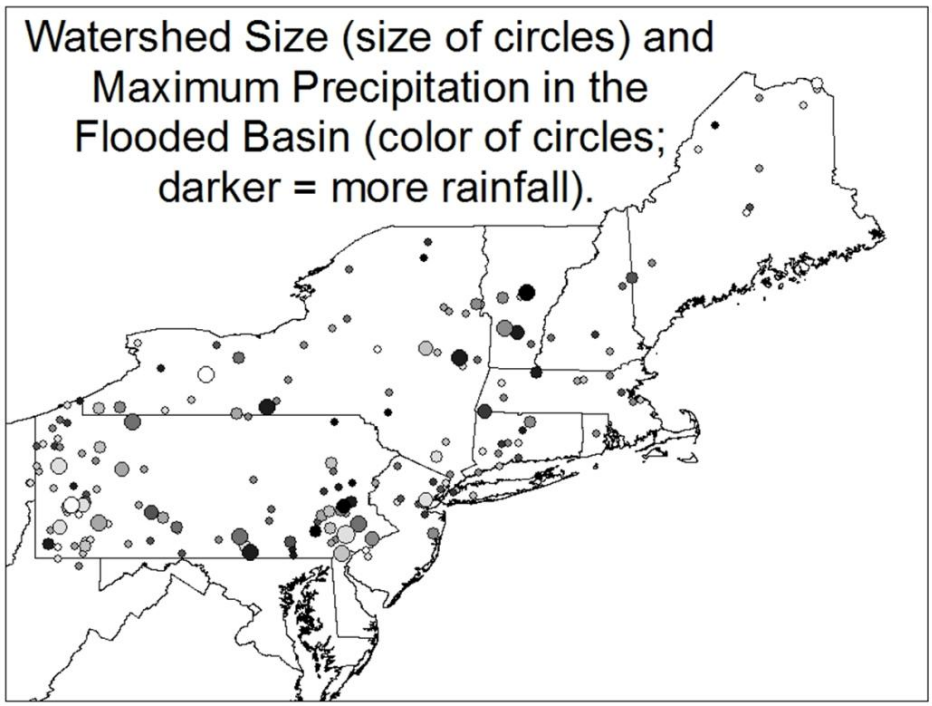

Figure 4.2 Map of the 187 flash flood events in this study. Size of circle indicates watershed size and shading of circles indicates maximum basin-averaged precipitation estimate near the flash flood location.

rural areas, as there is less impervious area and, as a consequence, runoff may be slower to accumulate in rural areas, thus favoring larger watersheds. In reality, the opposite is true. Larger watershed floods appear to be more common in urban or suburban areas (especially in and around Philadelphia and Pittsburgh), and floods of smaller watersheds appear to be more common in rural areas. It may be that the larger amount of impervious area in urban and suburban settings tends to channel precipitation over a large area, which overwhelms the natural or man-made channels farther downstream. In more rural areas, flash flooding more commonly occurs in association with smaller watersheds likely because the time scale of basin response for flash flooding – six hours or less – selects these smaller basins which respond more

rapidly. It is also more likely that the smaller channels have scoured the land surface less than larger streams, so they are thus more likely to run out of their banks in response to a given amount of rainfall over a relatively small area. The heavy precipitation cores associated with flash flood producing rainfall tend to be relatively small (Davis, 2001), so it is, in retrospect, probably not unexpected that most of the rural basins that reported flash flooding tended to be relatively small. In fact, all flash floods east of the Vermont/New Hampshire border were associated with relatively small basins, even in the urban areas around Boston and Worcester, Massachusetts.

Turning to the precipitation totals (shaded on Figure 4.2), there is no clear tendency for areas within the Northeast to favor larger or smaller maximum rainfall totals. There are no clusters of either high or low precipitation totals and there are no relatively large areas devoid of events with either high or low total precipitation. Both urban and rural locations contain both heavy and light precipitation. In short, the maximum precipitation associated with flash flooding is similar across the Northeast.

In looking at the precipitation totals in conjunction with the size of the watershed, a "meteorological" explanation might expect that the highest precipitation totals would be associated with the smallest watersheds because the cores of heaviest precipitation tend to be at this scale. A "hydrological" explanation, on the other hand, might expect a larger watershed to be associated with a higher precipitation total, as the larger watersheds tend to be associated with larger channels, and thus might be more difficult to overrun unless larger precipitation totals were present for a large portion of the basin. In reality, it appears that neither of these explanations by itself is adequate to explain the majority of events with the highest precipitation totals, as the highest precipitation amounts lead to flooding of both large and small watersheds. The Pearson correlation coefficient for the total drainage area and the maximum precipitation total in the vicinity of the flash flood site is -0.0024, with an R^2 value of

5.76×10^{-6}. The argument developed in the last two paragraphs is statistically confirmed: the variance in the size of the watershed explains none of the variance in the maximum precipitation values. The shortcoming of this analysis in capturing the precipitation amounts associated with flooding in the corresponding watershed is that these maximum precipitation totals, as pointed out earlier in this chapter, were in many cases only one of several or many basins contributing to the flooding in the larger watershed that flooded. However, the correlation coefficient between the total precipitation falling in the entire watershed and the total drainage area of the entire watershed was 0.64, with an R^2 value of 0.415, suggesting that in general, larger watersheds tend to accumulate more total rainfall. Whether the area-averaged precipitation total is larger when the watershed is larger, however, will be addressed in the next paragraph.

Figure 4.3 shows a plot more indicative of the relationship between the size of a flooded watershed and the precipitation that fell in that watershed to induce flooding. In this figure, the precipitation is not the maximum precipitation in the flooded watershed, as used before, but instead, it represents the area-averaged precipitation for the flooded watershed as a whole. For watersheds up to about 25 mi^2, there appears to be little correlation between watershed size and mean precipitation, but above this threshold, there is a pronounced decline in mean precipitation as the watershed size increases. The Pearson correlation coefficient for the entire dataset between these two variables is -0.275, with an R^2 value of 0.076. As a result, the variance of the size of the flooded watersheds does not explain a considerable amount of the variance in the mean precipitation, but the correlation between these two variables suggests that it does contribute a piece to the puzzle, unlike the wholly inconclusive result from using only the basin receiving the maximum precipitation within the watershed. Other properties of a given watershed, such as its land use, soil type, and vegetation,

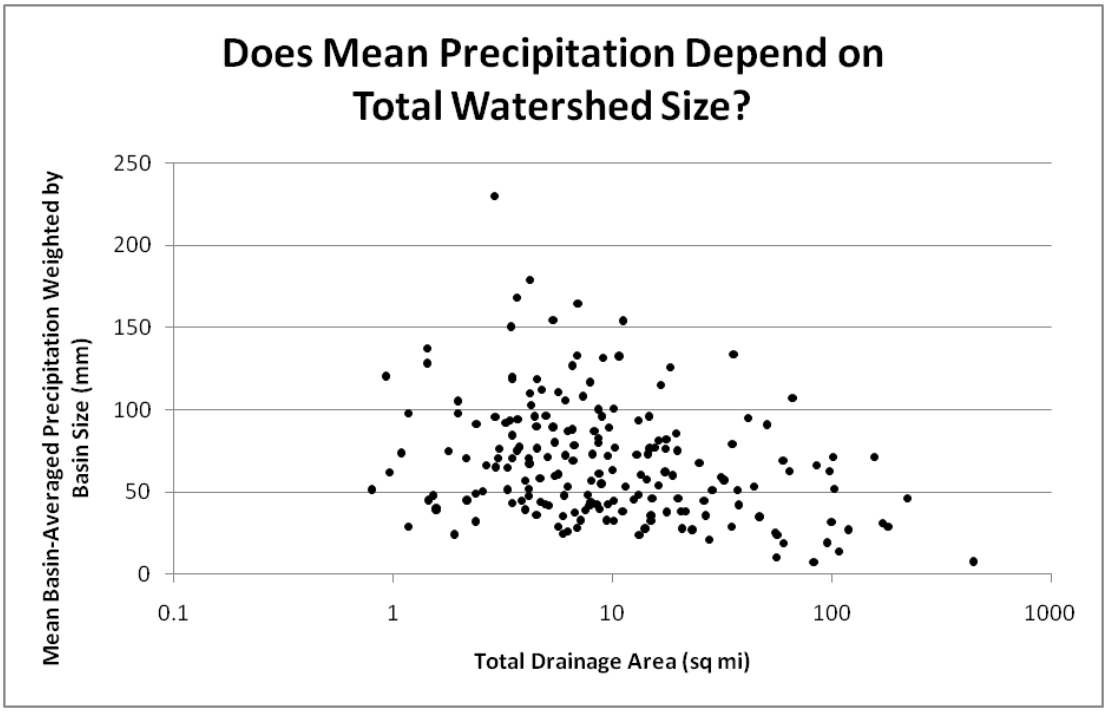

Figure 4.3 Watershed Mean Basin-Averaged Precipitation Weighted by Basin Size (mm) as a Function of Total Drainage Area (mi^2)

certainly play a role in determining a given watershed's response to precipitation (and these properties are likely more important in determining whether a given precipitation system will induce flooding than the size of the watershed), but such an analysis is outside the scope of this paper.

What can be determined from the analysis to this point is that those flash floods that affect the largest watersheds (defined here as greater than 25 mi^2) tend to occur in urban or suburban watersheds where the effects of urbanization may have altered the watershed's ability to concentrate (through the addition of impervious surfaces) or to channel (through changes to the channel itself) the floodwaters, supporting the hydrological argument that urbanization increases the likelihood of flooding. These larger watershed flash floods tend to be associated with smaller area-averaged precipitation totals than flash floods in smaller watersheds, suggesting that

the precipitation for these larger watershed flash floods are the product of heavy precipitation over only a portion of the total watershed area. This supports the meteorological argument that the heaviest precipitation occurs in relatively small cores of intense precipitation. An interesting question, not addressed in this study, would be to investigate whether those heavy precipitation cores in large watershed flash floods tend to fall on hydrologically-sensitive portions of the watershed area. In contrast to the large watershed flash floods, those events with smaller watersheds appear to be largely in response to small precipitation cores which persist for varying amounts of time, accounting for the variability in precipitation totals. Later in this chapter, an analysis of precipitation totals as related to storm type will analyze this assertion.

In addition to understanding the spatial properties of flash flood response with respect to watershed size, flash flood forecasters could benefit from knowing the temporal characteristics of heavy precipitation and flash flood events, both at a seasonal and diurnal time scale. A pronounced peak in the seasonal frequency of extreme precipitation events could suggest the presence of a recurring, anomalous weather pattern which might reveal itself in a climatological analysis. Similarly, a pronounced peak in the diurnal frequency of extreme-precipitation events could reflect a feature which operates on short space and time scales: for example, the influence of daytime heating on convection. Figure 4.4 shows the maximum basin-averaged precipitation estimate (size of circle) compared to the month and time of day (abscissa and ordinate, respectively). The purpose of this figure (and the other "bubble" charts in this chapter) is to show relative trends in the temporal characteristics of the precipitation totals, not to focus on individual precipitation amounts. From this figure, it is difficult to detect one clear preferred time of year or time of day for the heaviest flash-flood producing rainfall. Several trends, however, are present. The afternoon and early evening hours, from approximately noon to 9:00 pm local time, contain the

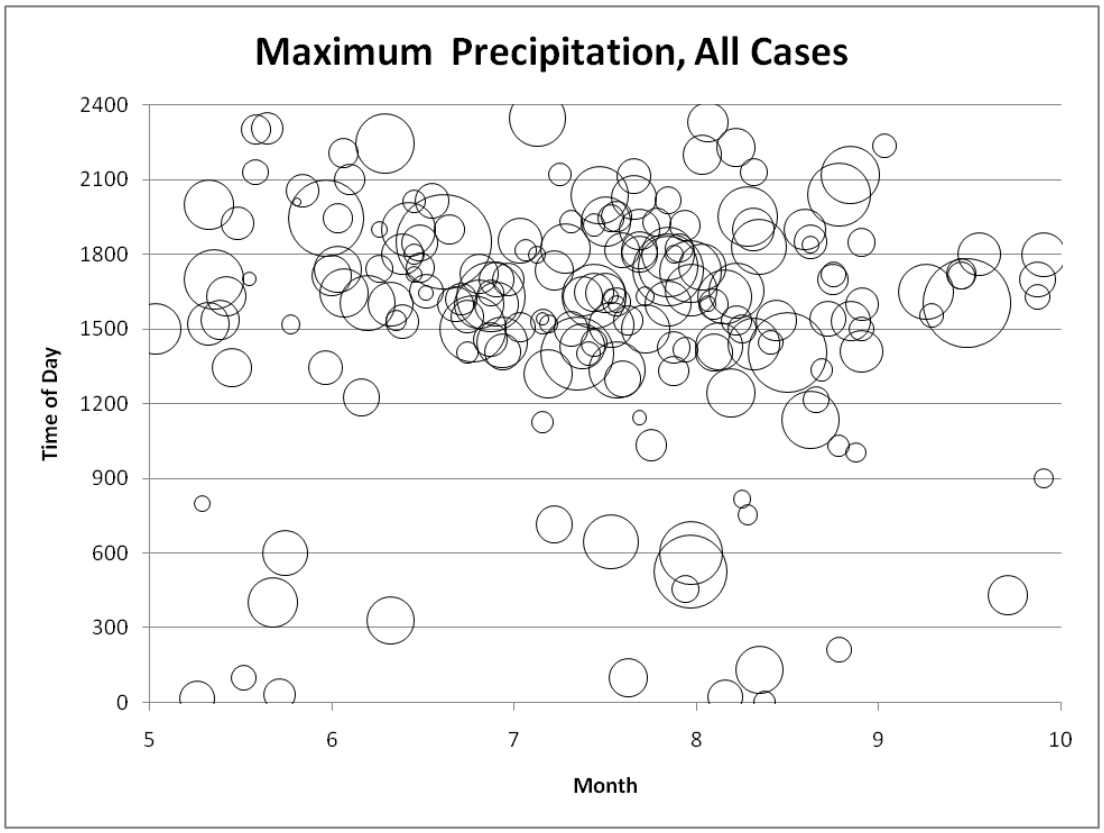

Figure 4.4 Maximum basin-averaged precipitation estimates for each case (circles) as a function of month (abscissa) and time of day (ordinate). The relative size of the circles indicates the magnitude of the precipitation. The time of day is the time cited in the flash flood report.

widest range of precipitation amounts, particularly from mid-May through August. These are the hours during which diurnally-driven convection is most intense (accounting for the heaviest precipitation estimates), and they are also the hours when even minor flooding is most likely to be detected and reported (which may account for the lightest precipitation estimates). Precipitation amounts tend to be moderate around midnight local time and show a slight increasing trend overnight until 6:00 am. This is most likely an artifact of the flash flood reporting process, which is dependent upon subjective reporting rather than objective detection via a stream gauge or other

automated device. Larger amounts of runoff, and thus larger amounts of precipitation, may be necessary to generate a flood that produces a nuisance significant enough to be reported in the overnight and early morning hours. In other words, a small creek that spills out of its banks onto adjacent backyards, other open space, or even onto a road would be less likely to be detected and reported as a nuisance when fewer people are out and about. It is unlikely, though, that there is a physical mechanism whereby precipitation amounts would necessarily increase overnight. In fact, once daylight breaks, the precipitation estimates associated with reported flash floods decrease significantly, generally less than 50 mm (1.97 inches) from approximately 7:30 am to 11:30 am. One possible explanation for this counter-intuitive dearth of high-precipitation events during the morning is that the high precipitation events are the result of one of two broad categories of storm types: relatively moderate duration (up to 6 hours) and high intensity events, such as the different types of linear and back-building events classified by Schumacher and Johnson (2006); and relatively long duration (12-24 hours) and moderate intensity events, such as those classified as LM and SYN events in this study. Neither of these storm types would be more likely to produce high precipitation in the morning than at later, potentially more favorable times of day, when both types of events would be forming or growing in strength from the de-stabilizing effects of solar heating. However, both of these classes of events would initiate or grow in intensity during the afternoon or early evening hours due to daytime heating and the resulting increase in instability, but the shorter-lived events would generate flooding much more rapidly than the longer-lived events producing more moderate precipitation rates. This hypothesis will be examined in the following section as the precipitation amounts are considered in conjunction with the storm type of each event.

4.3 Precipitation Properties of Flash Flood Basins as a Result of Event Types

Knowing whether each event type described in Chapter 3 tends to be associated with relatively larger or smaller precipitation totals can help forecasters to anticipate how severe the potential flood threat might be from a given storm system early in its development. Figure 4.5 displays boxplots of basin-averaged precipitation estimates for the basin in the vicinity of the flood report with the greatest estimated precipitation total; this basin was always in the vicinity of the flooded watershed, but not necessarily within the flooded watershed itself. Boxplots are displayed for each of the four broad groups of events: the *back-building* events; the events with *linearly* organized convection accompanied by a broader area of stratiform precipitation; the

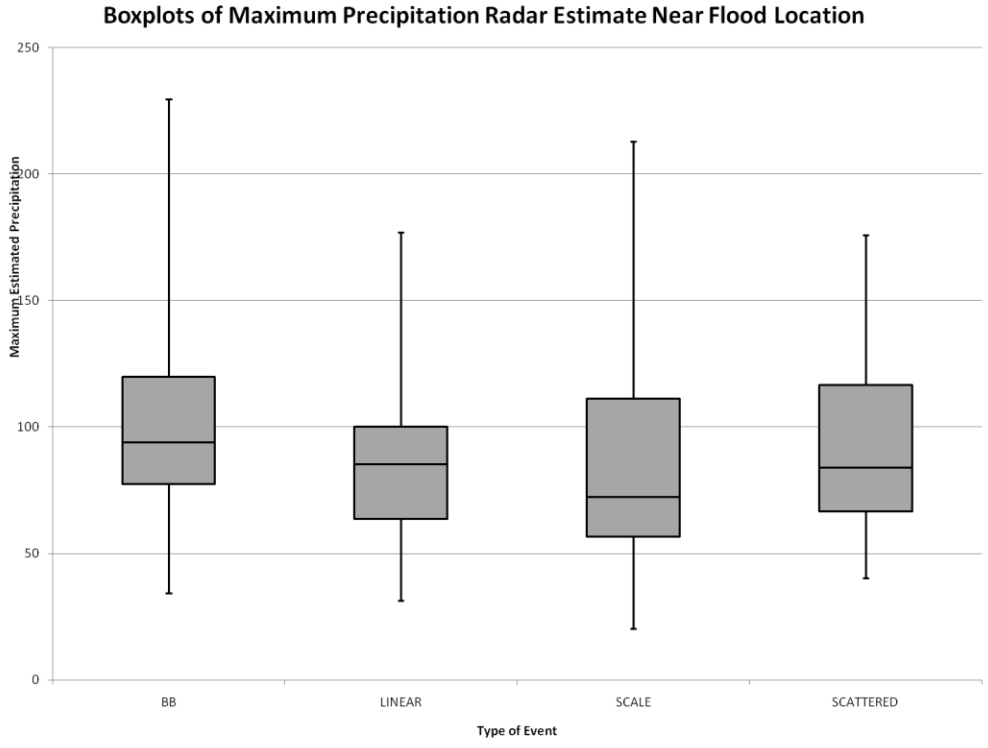

Figure 4.5 Boxplots of maximum basin-averaged precipitation estimates (mm) near the flood location for each of the four large groupings of event types.

events resulting from multiple, *scattered* features traversing the same area; and the events with a single, more disorganized feature identified by the *scale* of the feature. From the figure, it is evident that the centers of the distributions of these broad types of rainfall events do not differ appreciably, as indicated by the medians and the upper and lower quartiles. A two-tailed hypothesis test (Wilks, 1995) with the null hypothesis that the group with the largest mean – the back-building group – differs from the group with the smallest mean – the linear group – fails, as the null hypothesis cannot be rejected even at the fifty percent level. (The test statistic, *Z*, was .371.) The back-building events tend to produce somewhat higher median and quartile precipitation totals than the other types, and the scale events have both the lowest median and the largest inter-quartile range. That the scale events display the greatest variability comes as no surprise given that this group is comprised of events ranging from short-lived thunderstorms to broad synoptic scale storms. The key finding of this analysis is that all four broad types of flash flood events produce between 50 and 125 mm of precipitation for the majority of events examined in this study, and thus that no one group is likely to more commonly produce rainfall totals exceeding those of the other groups, given that flash flooding has occurred. This last qualification is important, as this study does not approach the question of how often these classes of precipitation organization occur on non-flash flood days and how much precipitation they produce when they don't cause a reported flood.

While comparing the precipitation distributions produced by each of the four broad categories of events provides some useful information about the precipitation totals associated with broad groups of events with robust sample sizes, looking at the precipitation distributions of the individual event types can better reveal whether any of these storm types is more prone to produce extreme or moderate precipitation. Figure 4.6 displays boxplots of maximum basin-averaged precipitation estimates for

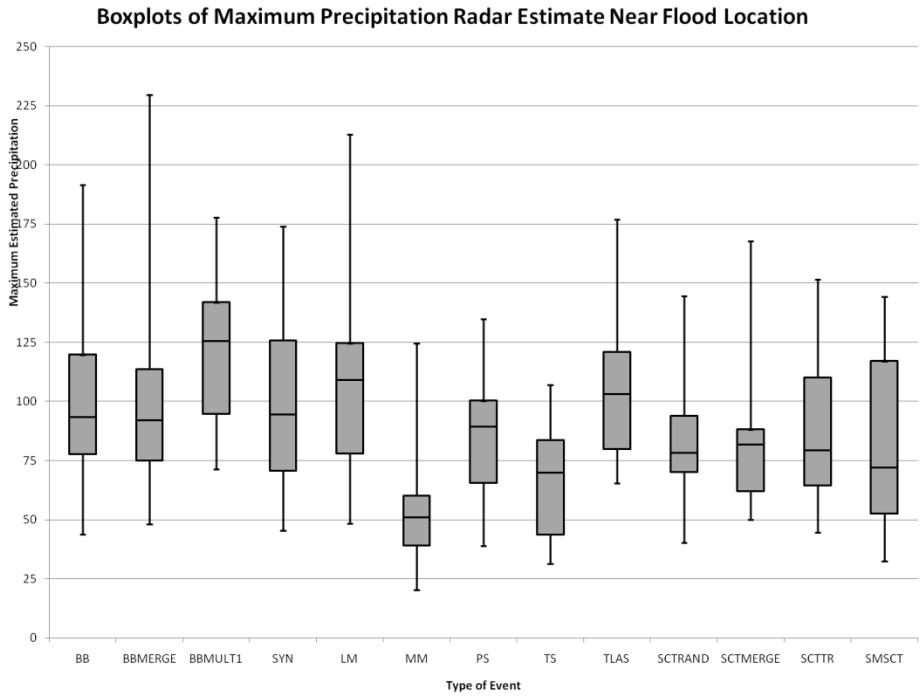

Figure 4.6 Boxplots of maximum basin-averaged precipitation estimates (mm) near the flood location for each category of events with at least five cases.

the basin in the vicinity of the flood report (though not necessarily within the flooded watershed) for each specific event type with at least five events. The first five boxplots on the left hand side of the figure, corresponding to the events of the back-building types and of the larger scalar events (synoptic and large mesoscale), are associated with relatively large median values, and these types account for all but one of the events exceeding 175 mm. These storm types are typically associated with long durations of moderate to heavy precipitation rates as a result of the sustained re-generation of convection, in the case of the back-building events, or as a result of the passage of large areas of persistent rainfall, in the case of the SYN and LM events.

The four boxplots in the center of the figure, corresponding to the smaller scalar (MM) events and the linear events, tend to have a narrower distribution of smaller precipitation totals. The one exception to this trend is the TLAS class of

events, which has a median precipitation total exceeding 100 mm and which produced the lone case aside from those in the above paragraph that exceeded 175 mm. Like the back-building and large scale events in the above paragraph, the TLAS type features a mechanism for sustained heavy rainfall rates: an elongated line of convection that trains over the same area. In stark contrast to all types of events described so far, the MM events produce tend to produce significantly less precipitation. The 75th percentile for the MM events is lower than the 25th percentile for all but two other event types. That the MM events produce notably lower precipitation totals reflects the appearance of this class of events on radar. The most disorganized of the single-feature events, they typically had no clear line of heavier convection (but may have a small core of heavier rainfall), and instead were usually nondescript moderate-sized areas of moderate precipitation rates moving at a moderate speed: a formula for relatively moderate precipitation totals. What is perhaps more remarkable is that these features, with their innocuous radar signatures, moderate precipitation rates and relatively low precipitation totals, were able to generate several flash flood reports. The TS cases displayed the narrowest range of precipitation totals and the smallest maximum precipitation total. All of the individual TS cases had similar structures on the radar, with a narrow band of intense convection trailed by a larger area of light to moderate precipitation, and they tended to move such that the convective line was roughly perpendicular to the direction of system motion. While, conceptually, a TS system could produce larger precipitation amounts if the orientation of the convective line were more closely parallel to the direction in which the system were traveling, an event of this type could more readily be classified as a TLAS system. As a result, the TS cases tended to feature relatively short periods of heavy rainfall, and as such, they produced similar, relatively small precipitation totals.

The final four boxplots on the right of Figure 4.6, representing the four categories of scattered cases, feature nearly identical medians (especially for the three "multiple" scattered categories – SCTRAND, SCTMERGE, and SCTTR) and very similar ranges of precipitation totals. Only two scattered cases of any type exceeded 150 mm, and only six cases exceeded 125 mm (three of them SCTSM, two SCTRAND, and one SCTMERGE), while at the lower end only six cases produced less than 50 mm of precipitation (again, three of which were SCTSM). Although the individual cases in the TS classes described above were similar in structure and duration, the scattered events were similar only in that the radar field was comprised of scattered features, often small in size; the features themselves may have been individual thunderstorms, squall lines, mesoscale features with both convective and stratiform signatures, or some combination of these. Despite the variety in appearances from case to case, there are plausible limits to the precipitation totals produced by the scattered types of events. First, it is likely that the lowest maximum precipitation totals would exceed those of other types of single-feature events such as the MM, SMISO, and TS events because, while those events included only one convective line or cell which may produce only a limited duration of heavy rainfall over a given location, a scattered event by definition includes at least two or three such periods of heavy rainfall as a consequence of the passage of multiple features (except for the SCTSM events). It is also plausible that during scattered events for which minor flooding resulted from relatively low precipitation totals, the forecasters may be less likely to contact local authorities to verify the minor flooding and, thus, no report was generated, as the apparent lack of organization in the convective features on the radar may appear to be an innocuous situation compared with, for example, a TS event producing the same rainfall total. At the other end of the scale, extremely high precipitation totals would conceivably be quite rare as a product of scattered events

owing to their disorganized nature. While the SCTMERGE events could, much like SYN and LM events, produce large rainfall totals as a consequence of their typically elongated areas of moderate to heavy rainfall rates, the cases with these large areas of rainfall tend to occur when one line is moving south-to-north, while another line advances relatively rapidly from west-to-east and sweeps the other line with it as a result of the merging of the two lines. This tends to produce shorter-duration rainfall at any one location than were only the south-to-north line in place, and this advective effect usually results in lower precipitation totals than for the SYN and LM types. Similarly, while it is very possible that individual cells (SCTRAND) or convective lines (SCTTR) could traverse the same area for a relatively long period of time, the gaps between the features would result in lower rainfall totals than a similar back-building (BB) or training (TLAS) mechanism producing near-constant high rainfall rates for the same duration.

While most scattered cases had both low precipitation totals and a relatively small spread among those totals for most cases, the precipitation distribution of SCTSM events (Figure 4.6) has a very large inter-quartile range compared with the overall range of SCTSM precipitation totals. Unlike most other storm types, which differed from case to case in their scale and in the direction and speed of their heaviest precipitation cores, the SCTSM cases were all relatively slow-moving thunderstorms no more than 25 km in length on the radar. As such, they were more likely to produce similar precipitation rates for similar durations (and not to produce extremely large or small rainfall totals), and thus to produce more similar precipitation totals than the other classes of events. The wide inter-quartile range of the SCTSM events suggests that the thunderstorms moved with a wide variety of speeds from one case to the next, but the relatively narrow range of precipitation totals suggested that there are rather

well-defined limits on this movement speed or on the lifetime of a near-stationary SCTSM storm.

The precipitation amounts produced by the different event types have visibly different distributions, as evidenced by the boxplots in Figure 4.6, but the relatively small sample sizes associated with these groups limit the extent to which these differences can be explained. The group with the largest mean precipitation estimate – the BBMULT1 group – and the group with the smallest mean precipitation estimate – the MM group – have sample sizes of 5 and 7, respectively. There was little overlap in the precipitation estimates generated by these two event types, as only the highest of the MM precipitation estimates exceeds the two lowest precipitation BBMULT1 cases; all other BBMULT1 cases produced more precipitation than all other MM cases. A two-tailed hypothesis test (Wilks, 1995) with the null hypothesis that the mean precipitation produced by the BBMULT1 group differs from the mean of the precipitation produced by the MM group fails, as the null hypothesis cannot be rejected at the ten percent level. (The test statistic, *Z*, was equal to 1.38) No other pairing of two event types produces a more favorable test statistic. So although there are plausible reasons that certain types of rainfall organization are more likely to produce more precipitation than others, and although some of the precipitation distributions presented in Figure 4.6 subjectively appear to be quite different from each other, these differences are not statistically significant due to the relatively small sample sizes and the relatively large spread of precipitation amounts associated with each storm type.

4.4 Observations of the Temporal Characteristics of Event Types

Earlier in this chapter, it was speculated that some storm types would tend to be more common during certain times of day; for example, it was hypothesized that the larger scalar events would be more likely than the other storm types to cause flash flooding in the overnight hours and through the morning because their large scale makes them more or less independent of the diurnal cycle. Figure 4.7 shows that, indeed, several of the flash flood events between midnight and noon local time were of

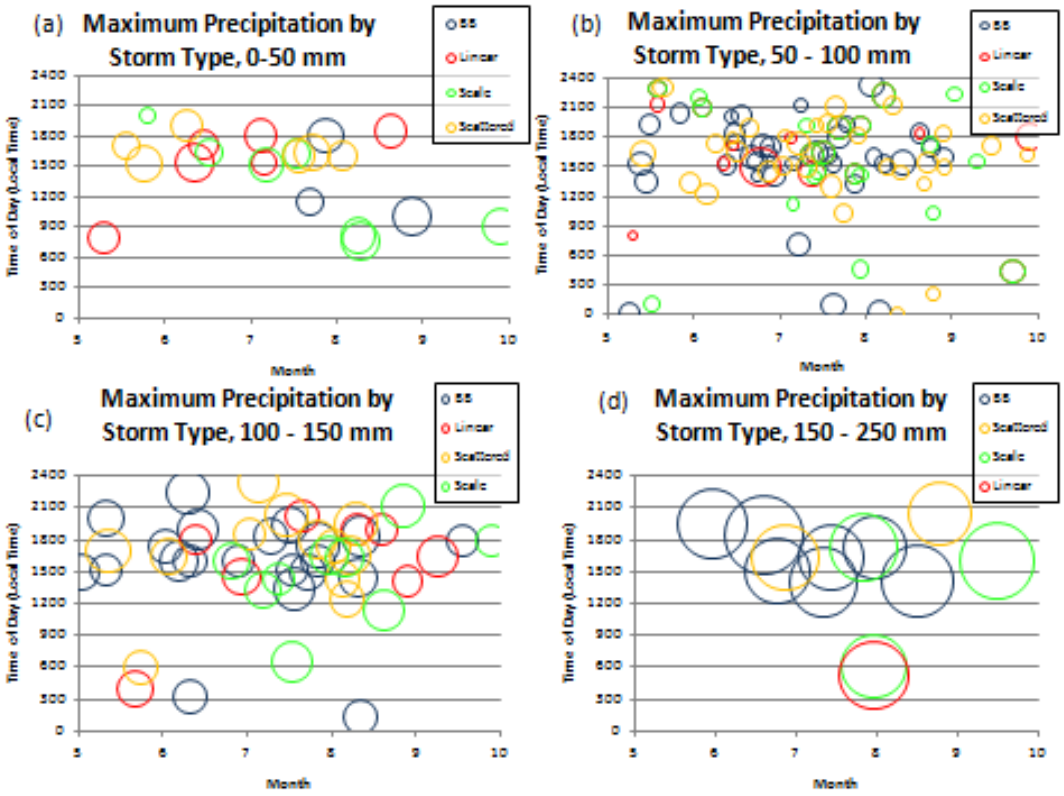

Figure 4.7 Basin-averaged precipitation estimates for the maximum basin in the vicinity of the flooded watershed (but not necessarily within the flooded watershed), as a function of month (abscissa) and time of day (ordinate). The size of the circles in each panel represents the relative amount of precipitation; however, the circle size is not proportional from one panel to the next. The color of the circles represents the general storm type of each event. Each panel represents an interval of precipitation amount.

the scalar variety, and Figure 4.8 confirms that these scalar events were mostly of the SYN and LM types, with two of the scalar events that produced relatively light amounts of precipitation were of the MM type. It is also apparent from Figure 4.7 that while the scalar events are most common overnight and through the morning, each of the other general storm types occurred at least twice, as well.

While there are some differences in which general event types occur during the overnight hours through the morning (Figure 4.7), all four event types display a

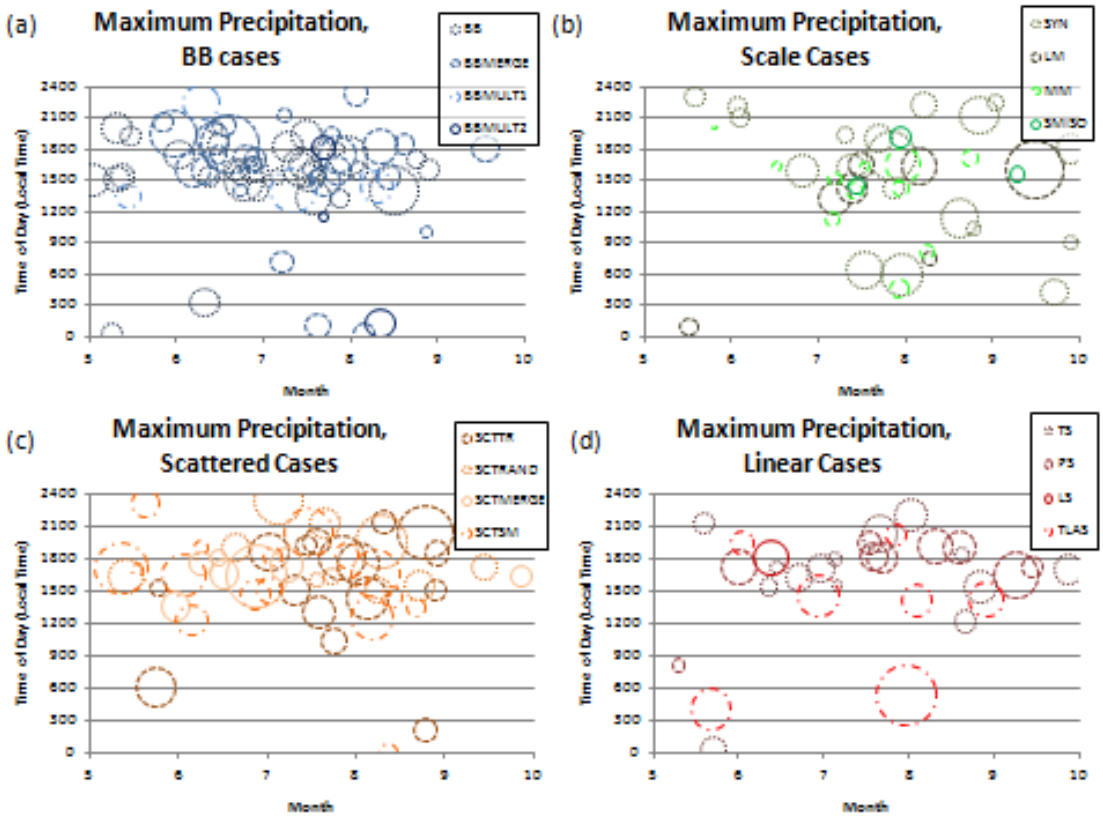

Figure 4.8 Basin-averaged precipitation estimates for the maximum basin in the vicinity of the flooded watershed (but not necessarily within the flooded watershed), as a function of month (abscissa) and time of day (ordinate). The size of the circles in each panel represents the relative amount of precipitation. The color of the circles represents the general storm type of each event. Each panel displays the sub-classes of one of the four general classes of storm type.

prominent peak in occurrence from noon until 9:00 in the evening local time for all precipitation ranges, and with this, all of the specific event types except the SYN type displayed the same tendency. In general, the scale class has the largest variety of timing, both in terms of their seasonal frequency and their diurnal frequency; most of this variety is attributable to the SYN events. While the SYN events tend to occur at a variety of times, the LM events producing the largest precipitation estimates are consistent in occurring between noon and 6:00 pm local time (Figure 4.8(b)).

In terms of the annual cycle, the scalar events are more common in September than any other event type. In September, the synoptic scale forcing is larger than in most of the summer (Bradley and Smith, 1994), but this forcing is also present in May, when soil moisture tends to be larger in much of the Northeast due to higher rainfall and recent snowmelt (and, therefore, the surface is more primed for flooding), yet the scale events are less common in May than the other three classes of events. It is possible that during late spring, these large scale events tend to produce main stem river flooding rather than more localized flash flooding, which tends to occur more often in response to early autumn large scale events. However, looking at the events that were classified as "Flood" events rather than "Flash Flood" events shows this not to be the case.

While the three panels of Figure 4.7 corresponding to the largest precipitation amounts show similar diurnal trends in the timing of flash flood producing precipitation throughout the warm season, there is a clear tendency for events with relatively low precipitation totals to occur earlier in the day as the warm season progresses. In May and June, most light precipitation events occur in late afternoon or early evening, but by August, more light precipitation flash flood events occur before noon than after noon. The correlation between the reported flash flood time and the time of year is was found to be -0.38, and the R^2 value indicated that the variance in

the time of year explained approximately 14% of the variance in the flash flood report time. There is no physical reason to suspect that this tendency is the result of some meteorological process or persistent changes in atmospheric conditions over the course of the warm season, as the other three precipitation ranges show no vestige of such a trend. It is, thus, likely an artifact of the small sample size of these "light precipitation" flash flood events. It is noteworthy that all of these events, which likely produced "nuisance flooding" rather than posing a serious threat to life and property, occurred approximately between dawn and dusk, when such minor flooding would be most likely to be detected and reported.

Chapter 2 noted a late July maximum in flash flood occurrence for the years 2003-2007 for the Northeast, while most other two-week periods had approximately the same number of flash flood event days. This late July maximum is visible in Figure 4.7 for the events producing 50 to 100 and 100 to 150 mm of precipitation, but this late July time period does not stand out in the frequency of light precipitation (<50 mm) or extreme precipitation (>150 mm) events. The late July peak is also prominent in all four storm types (Figure 4.8), so this peak is not a result of a specific atmospheric configuration that consistently forms and results in a particular storm type during this time period. It appears, though, that this two-week window seems to be the most favorable portion of the warm season for the concatenation of the ingredients for heavy rainfall and flash flooding – most significantly, moisture and a mechanism to lift that moisture (Doswell et al., 1996). Each year from 2003-2007 saw reports of at least six non-consecutive event days during the late July window, and no one year reported more than five consecutive event days. In other words, this late July maximum is not a statistical anomaly resulting from the freak occurrence of one or two abnormally wet years from the study period, but it seems, instead, to indicate a

consistently wet period from all five summers. However, as discussed in chapter two, it does not seem to be a persistent feature in the long-term climatology.

While all storm types (except SYN) tended to form in the afternoon hours, the back-building and scattered events tended to cluster during the afternoon to early evening hours from June through mid-August, centered on the time period from 3:00 pm to 6:00 pm local time (Figure 4.8). The back-building events tend to produce their largest rainfall totals during the mid-afternoon hours (Figure 4.7(d)), and as the day proceeds from the afternoon, into the evening, and eventually into the overnight and morning hours, the maximum rainfall totals from back-building events tend to decrease (Figure 4.7). The events in the scattered class were earlier hypothesized to be largely the consequence of diurnal convection, and as such, these events were expected to occur largely during the daylight hours and shortly after sunset. This tends to be mostly true, and the only two events to form in the wee hours of the night or early in the morning were of the SCTTR type (Figure 4.8(c)). Two other groups of events that could be expected to form as a result of daytime heating are the small scale events, SMISO and SCTSM. All of these events were found to occur between noon and midnight local time (Figure 4.8).

4.5 Observations of the Spatial Characteristics of Event Types

The locations of the events and the relationship, if any, between where flash flood producing storms occur and how much rainfall they produce could add another layer of information to inform the forecaster's decision-making process. Figure 4.9 displays maps containing the rainfall amount (size of symbols) for each specific type (color of symbols) of each general event type (shown on the four maps). It is evident that the back-building events (Fig. 4.9(a)) are much more evenly distributed across the

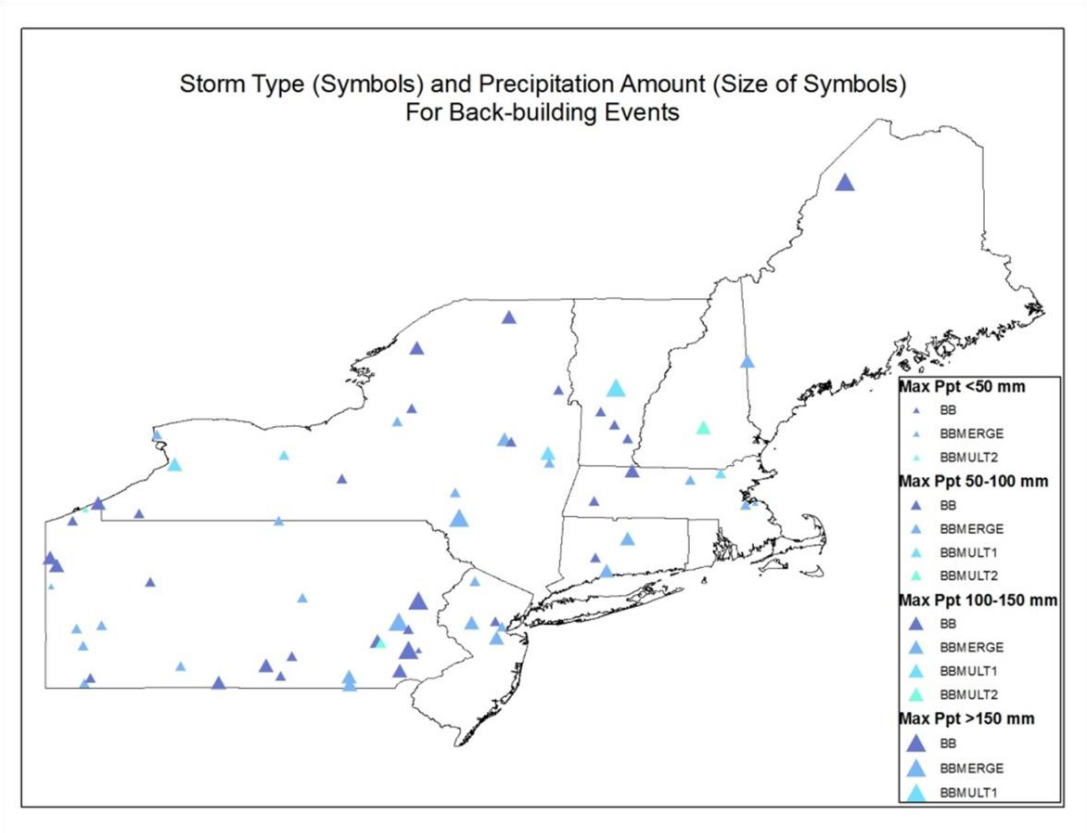

Figure 4.9(a) Map of back-building flash flood events by storm type. The size of the triangle indicates the precipitation amount, while its color represents the storm type.

Northeast than the other four general event types. This could suggest that the probability of a back-building event occurring in any two random locations in the Northeast is more similar than the probability of any other type of event occurring in the same two random locations in the Northeast, or it could simply suggest that back-building events tend to be either more easily recognized as a flash flood threat across the Northeast or more likely to cause a flash flood when a back-building event forms than any other storm type when that type of event forms. Most likely, it is a combination of all three of these hypotheses. In contrast to the relative spatial uniformity of the back-building events, the linear events are largely clustered in western Pennsylvania, with other linear events sprinkled throughout the rest of the

Northeast (Figure 4.9(b)). Many of these linear events in western Pennsylvania are of the TS and PS types, which are not very common elsewhere in the Northeast. Schumacher and Johnson (2006) found the TS type to be the second most common type of precipitation organization for extreme rainfall events in the region just to the west of Pennsylvania; this study's predominance of TS events in western Pennsylvania could be a reminder that meteorological phenomena do not follow arbitrary regional boundaries, and that western Pennsylvania could be part of a larger region that is more favorable for this type of event than the remainder of the Northeast. It could also be that because these events often produced low rainfall totals, they may have occurred in other regions and event types are also sprinkled throughout the rest of the Northeast.

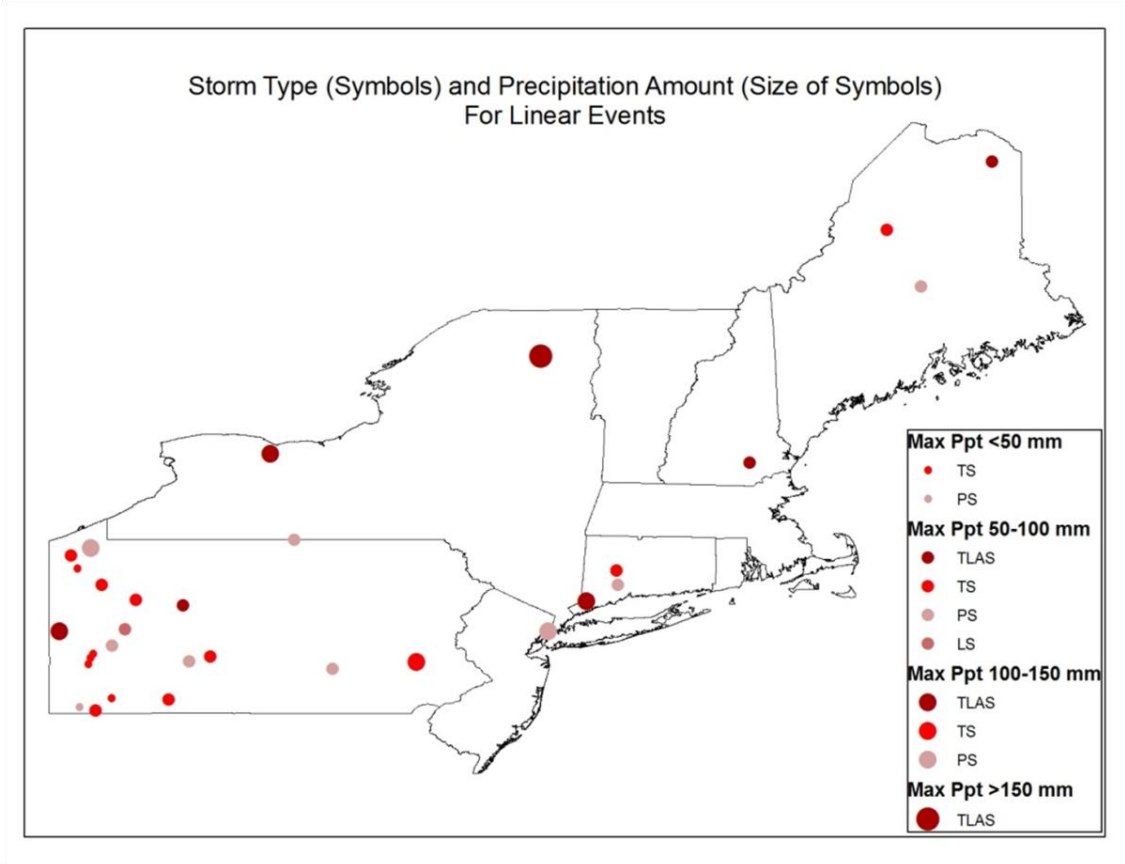

Figure 4.9(b) Map of linear flash flood events by storm type. The size of the circle indicates the precipitation amount, while its color represents the storm type.

Like the linear events, the sub-type of scalar events that was most common in western Pennsylvania, the MM type, was notably rarer in other portions of the Northeast (Fig. 4.9(c)). Six of the nine MM events, which were described earlier in this chapter as producing relatively low precipitation estimates and as being structurally nondescript, occurred in Western Pennsylvania and produced less than 50 mm of rainfall. Rather than having a meteorological or hydrological cause specific to this region, this concentration of low-precipitation events could be the result of more diligent verification by the Pittsburgh forecast office of the NWS. Most of the SYN and LM events occurred in western Pennsylvania and in the megalopolis stretching from the Philadelphia area to Boston. Among the scattered events (Fig. 4.9(d)), the SCTTR

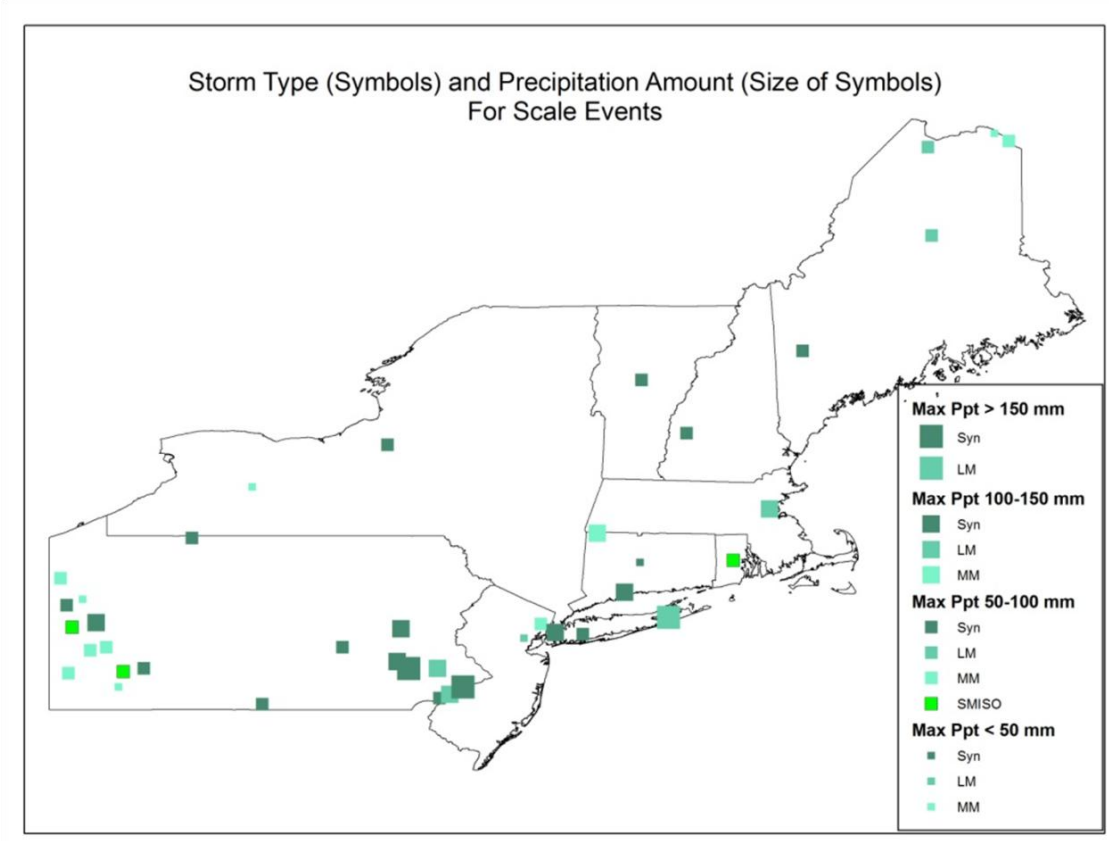

Figure 4.9(c) Map of scale flash flood events by storm type. The size of the square indicates the precipitation amount, while its color represents the storm type.

events stand out as occurring largely in western Pennsylvania and from eastern Pennsylvania through the New York metropolitan area, but they were scattered throughout the rest of the Northeast as well.

In addition to examining the spatial distribution of the events as a whole, it may be useful to look only at those producing both the greatest and the smallest precipitation totals. The events with the lowest estimated precipitation totals (<50 mm), shown in Figure 4.7(a) above and discussed briefly in the text, occurred mostly in western Pennsylvania, with other events scattered in New York, eastern Pennsylvania, and New Jersey (Figure 4.10). Only three flash flood events in New England received estimated precipitation totals less than 50 mm. These three New

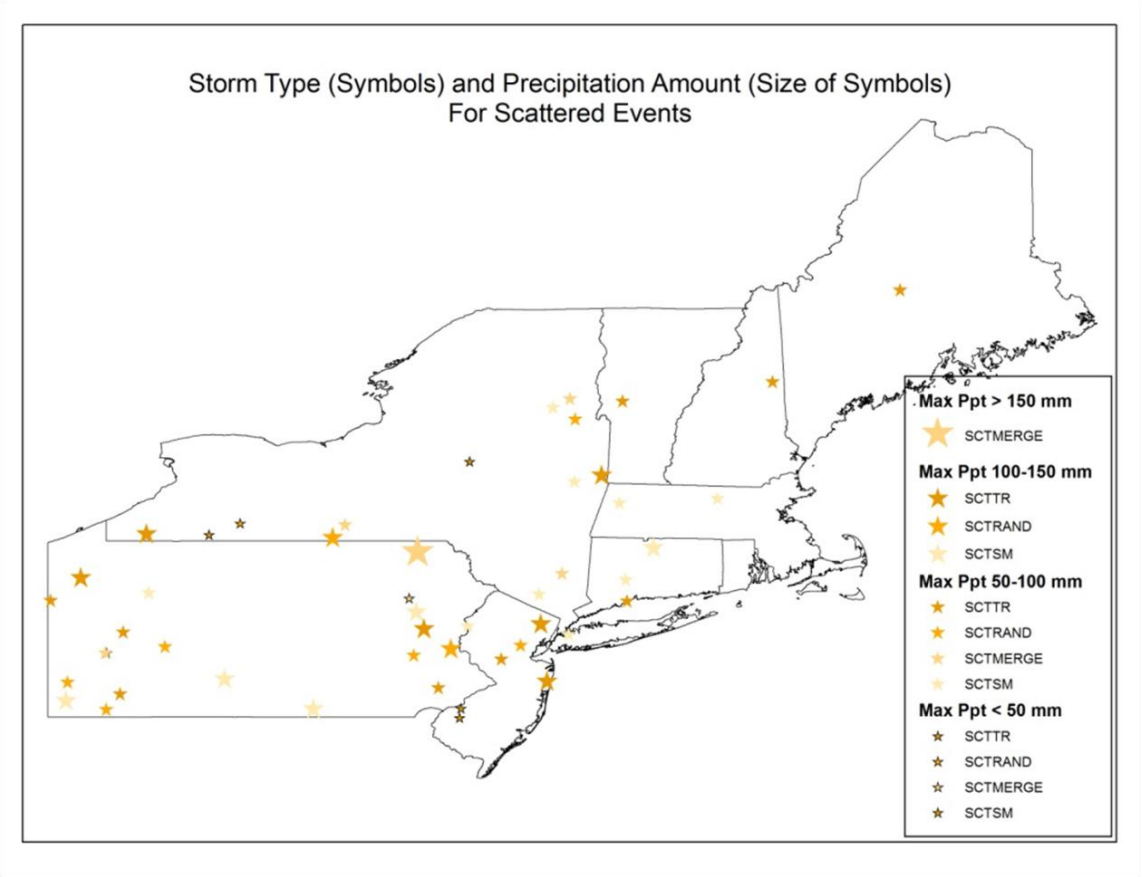

Figure 4.9(d) Map of scattered flash flood events by storm type. The size of the star indicates the precipitation amount, while its color represents the storm type.

England events occurred in the New Haven, CT and Boston, MA urban areas and in the downtown area of a small town in northern Maine. Most of these light precipitation events occurred in cities or towns, large or small, where there was a density of roads and buildings, and thus some likelihood for a somewhat swollen stream to impact roads, buildings, and other structures.

Much like the back-building cases in the map of all events shown in Figure 4.8(a), the scattered events tended to be the most evenly distributed among the locations receiving light precipitation totals. As Figure 4.7(a) shows, the light scattered events were also the most consistent in their timing, all occurring between 3:00 pm and 8:00 pm local time. It is not surprising that so many of these scattered

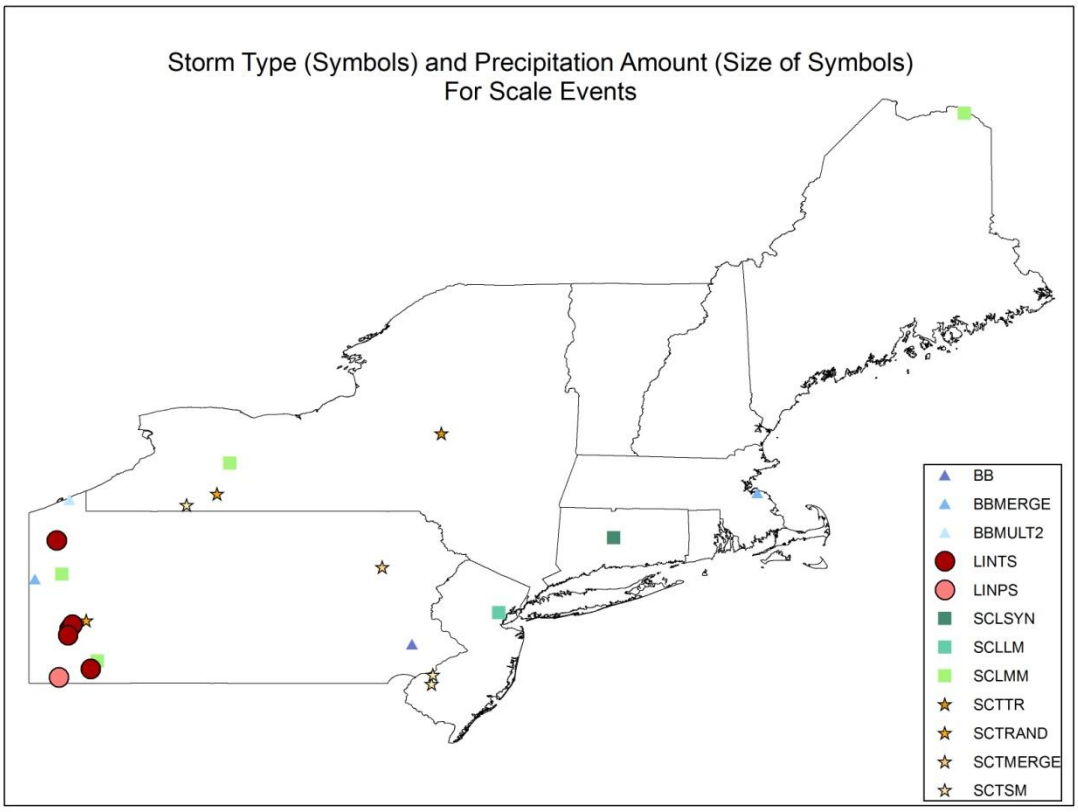

Figure 4.10 Map of flash flood events by type (shape and color) for events with maximum radar-estimated precipitation less than 50 mm.

events produce relatively lower precipitation totals, as the events do not necessarily have an internal mechanism for sustained moderate to heavy precipitation and are instead largely the result of intermittent moderate to heavy precipitation as the scattered features cross the flood's watershed. All of the linear events producing relatively little precipitation were located in western Pennsylvania. All but one of the linear events were of the TS type, and three of these events were closely clustered near Pittsburgh.

This chapter has, so far, discussed these event types purely in comparison with one another, and without a broader context. For the purposes of putting the flash flood events examined in this study in the context of the referred literature, Figure 4.11 displays a map of the events in this study with maximum radar-estimated precipitation meeting the spatially varying precipitation threshold used by Schumacher and Johnson (2006). More than half of these events are of the back-building type, as mentioned in the previous chapter. These back-building events are also the most evenly distributed spatially of all of the general event types, as each area that has at least one event has a back-building event, except for Long Island. In general, the map in Figure 4.11 is indicative of where events as a whole were most common – in eastern and western Pennsylvania and along New York/Pennsylvania border; and more scattered throughout upstate New York and New England. Unlike the light precipitation events, which tended to be in populated areas, the majority of high precipitation events tended to be in rural areas or smaller towns rather than in the downtowns of the big cities that comprise the megalopolis. The largest clusters of events are in northwestern Pennsylvania and in eastern Pennsylvania. These clusters of high precipitation events saw a variety of storm types, suggesting that the cause of this clustering is likely not due to these locations' tendency to favor a particular type of storm. Instead, these clusters may be due to a fortuitous combination of the location of the rain gauges in

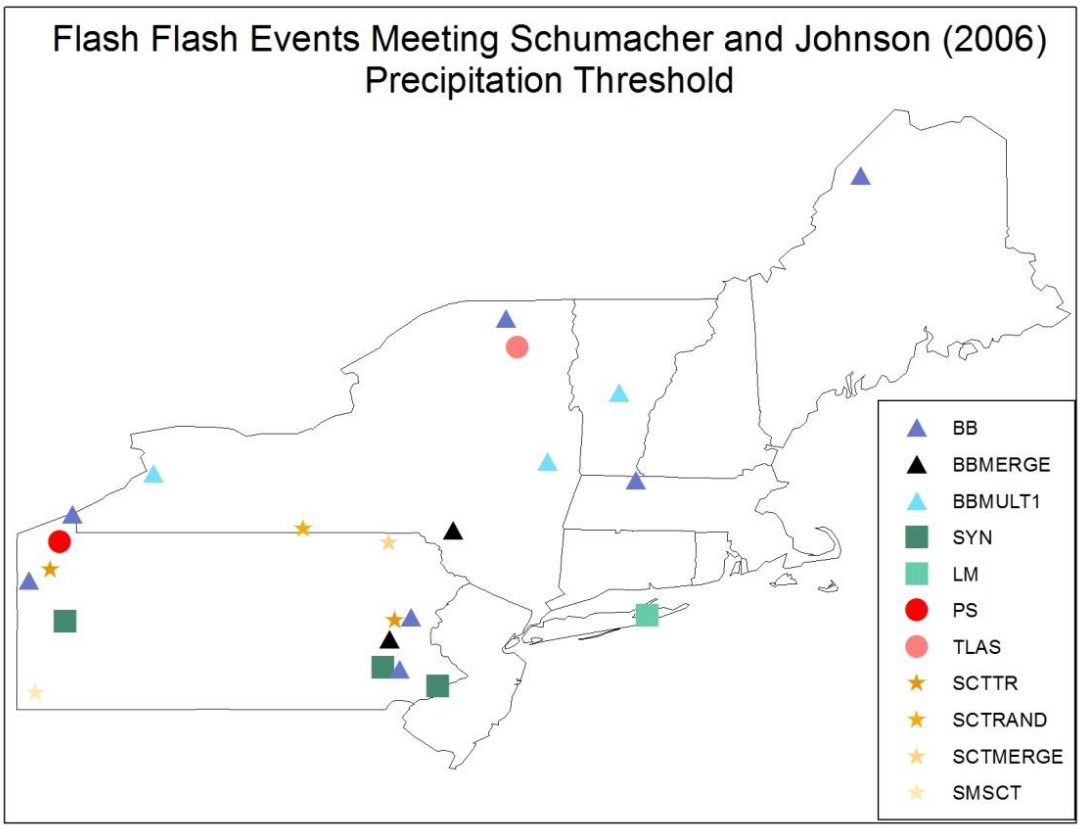

Figure 4.11 Events meeting the spatially varying precipitation threshold used by Schumacher and Johnson (2006).

these regions and the selection criteria used in this study; it is likely that on some of the high precipitation event days, there were many widespread flash flood reports, and these locations were selected because the nearby rain gauges reported the highest rainfall totals, even though other locations may have received more rainfall. It is also possible that the forecast offices in these locations more effectively located and recorded these flash flood events. In general, the events meeting Schumacher and Johnson's (2006) precipitation threshold form a less-than-representative sub-population of the events. While the back-building events taken alone appear to be a fair approximation of the spatial distribution of the events as a whole, the non-back-building events that meet Schumacher and Johnson's (2006) precipitation threshold

were only found in New York and Pennsylvania; this is clearly *not* indicative of the events as a whole. In this way, they are similar to Schumacher and Johnson's (2006) own sample of flash floods for the Northeast, which appeared to be at great odds with their samples of events for the other regions.

4.6 Summary

This chapter has examined the precipitation totals associated with the flash flood events in this study in terms of the categories of precipitation organization (defined in Chapter 3) as well as the spatial and temporal properties of the events. It has found that most rural events tend to be associated with small basin flooding, while suburban and urban flooding contains a mix of large, medium, and small basins. It is hypothesized that the more urban basins are able to concentrate runoff over a larger area more quickly due to increased impervious area and that these areas may potentially pose a greater local flood hazard from a given precipitation system due to the modification of stream channels.

The storm types producing the greatest precipitation totals tend to be those that conceptually should be the most favorable to form and sustain heavy rainfall: the back-building types, the larger scale types, and the TLAS type. The MM type was found to produce the least rainfall, and this is also not unexpected, as this type of event is frequently disorganized, with moderate rainfall rates. The other linear types of rainfall organization, and the scattered types of precipitation were generally found to produce moderate rainfall totals.

Except for the SYN event type, which was not associated with any particular time, all the event types tended to occur between noon and midnight local time. There was a tendency for overnight flash floods to increase in precipitation amount from

midnight to 6:00 am local time, but there was no preference for a certain event type of a certain location to explain this trend. There was also a peak in the frequency of flash flood events during the last two weeks of July, but no clear diurnal, spatial, or event type preference explained this tendency.

CHAPTER 5

METEOROLOGICAL CHARACTERISTICS OF FLASH FLOOD EVENTS

5.1 Methodology

To examine the environmental conditions associated with the 187 flash flood events in this study, re-analyzed data were downloaded from the National Centers for Environmental Prediction (NCEP) – the North American Regional Reanalysis (NARR). These data were downloaded for time periods from approximately nine hours before the reported beginning of flooding though three hours later than the reported beginning of the flooding. The NARR is available for time steps of three hours and utilizes a grid spacing of approximately 32.5 km by 32.5 km (NCEP, 2007) It contains the basic meteorological variables (geopotential height, sea level pressure, temperature, winds, and moisture) as well as a number of derived variables, such as convective indices.

From these data, composite maps were constructed for each of the storm types described in the previous chapters. First, the spatial data for each case were re-interpolated to a grid with the same grid spacing but a different location, such that the location of the flash flood in the original map was moved to the same arbitrarily assigned point, located in New York state, at 42° North, 74° West, using the National Center for Atmospheric Research (NCAR) Command Language (NCL; University Corporation for Atmospheric Research, 2010). After the maps for all cases were re-centered, composite maps were created to represent the mean atmospheric conditions for multiple events for the same storm type in a storm-relative sense. That is, all

composite maps to follow in this chapter re-located the reported flash flood location to the black dot on the maps at 42° North, 74° West. Composite maps were constructed for each specific event type by averaging the atmospheric variable in question over the re-centered maps for all cases in each event type, and individual maps of specific events or groups of events were created as needed. This chapter will discuss these composite and individual maps to shed light upon the atmospheric conditions associated with each type of event. The desired goal of this chapter is to develop a more complete understanding of the conditions under which each event type arises, so as to improve forecaster recognition and anticipation of potentially hazardous flash flood events.

5.2 Analysis of Scale Events

The composite maps of the scale events differed most significantly in their moisture fields. Figure 5.1 shows that at 850 hPa (and at other lower tropospheric levels not shown), the moisture field has a similar structure, and a similar amount of moisture is present upwind of the flood area, for all four scale event types. One might expect the SMISO events, in which thunderstorms form in isolation, to form in a much drier atmosphere than the LM events, for example, with their large, longer-lived swaths of rainfall. This composite, however, shows that on the average, the low-level moisture content for these two classes of events is similar. In the same vein, the SYN composite might be expected to be moister than any of the four scale event types, yet the MM composite has a greater pool of upwind low-level moisture than the SYN composite. However, when one looks at the moisture advection and takes into account the strength of the winds, then the LM and SYN composites look more favorable than the maps above them in Figure 5.1, as their stronger winds are advecting more

moisture into the eventual flood location than in the SMISO and MM composites.

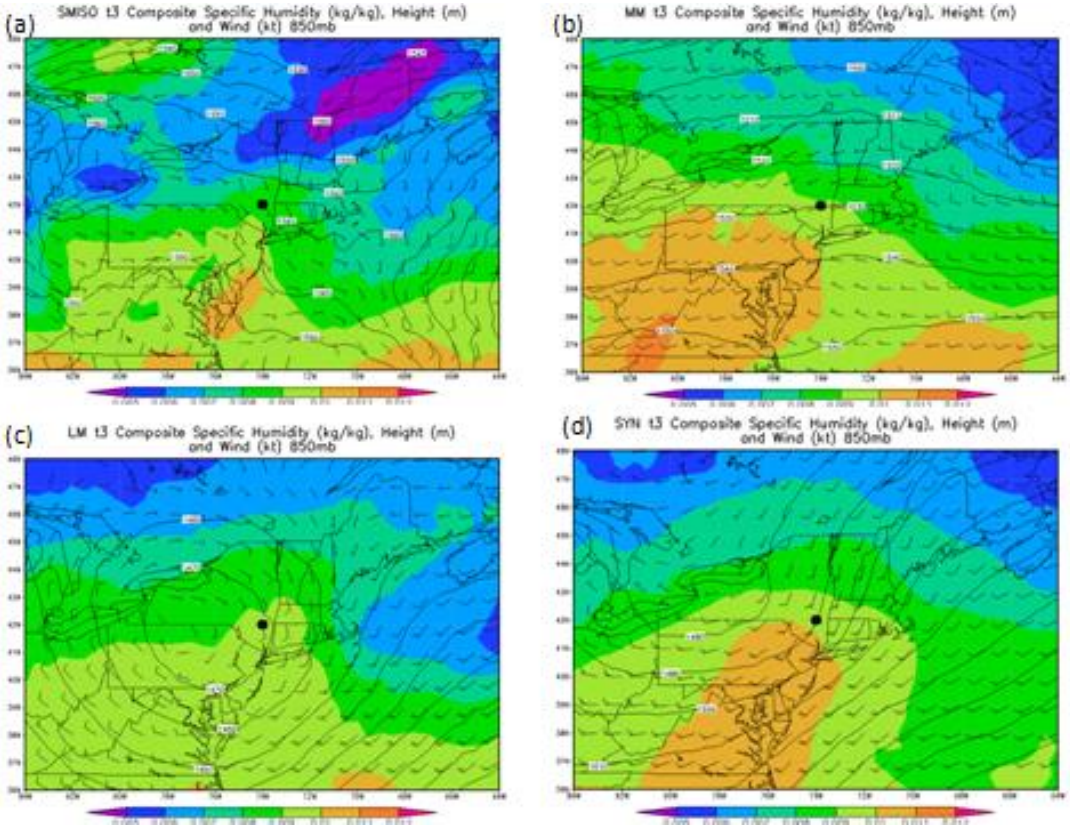

Figure 5.1 Composite specific humidity (shaded, kg/kg), geopotential height (contours, m), and wind (barbs, kt) at 850 hPa for the time period 3-6 hours before the flood report for (a) SMISO, (b) MM, (c) LM, and (d) SYN events.

The wavelengths of the lower tropospheric waves, evident in the height field, differ among the four event types. The SMISO composite does not display a clear wave pattern, but it does have an easterly wind flow from the Atlantic Ocean and a diffluent wind pattern (albeit with light winds of about 5 kt) in the vicinity of the flood area. A diffluent thickness pattern in the 1000 hPa to 500 hPa layer (and, because above the boundary layer the winds tend to parallel the height contours, diffluent winds in much of this layer) has been recognized as a potential contributing factor to some flash flood events (Funk, 1991), but they do not appear to be requisite for the

SMISO events, as this diffluent pattern was evident in only one of the three SMISO events. Two of the three individual SMISO events, both located in the vicinity of Pittsburgh, PA, featured an easterly flow of approximately 5 knots, while the third event, in Rhode Island, had a southwestly flow also of five knots. In Jessup and DeGaetano (2008), a group of flash flood events with easterly winds was noted to have affected the forecast area of the Binghamton, NY National Weather Service office. These flash flood events were believed to be the product of elevated thunderstorms, which feature a strongly baroclinic environment with strong lower- to midtropospheric wind shear and warm-air advection, no surface-based CAPE, and often occur in a hydrostatically stable environment (Colman 1990). Similarly, the SMISO composite displays a baroclinic zone, with a northwest-to-southeast oriented front at low levels (not shown), significant veering of the winds from easterly winds at 925 hPa (not shown) to northwesterly winds at 500 hPa (shown below in Figure 5.3), and a relatively low CAPE of less than 750 J/kg in the vicinity of the flood location (not shown).

The MM composite features a weak ridge directly over and to the north of the flood area at the time period from 3 to 6 hours prior to the flash flood report (Figure 5.1(b)). In the composite maps as well as in most of the maps of individual cases, this ridge forms and dissipates within a time span of approximately six hours; the ridge has often flattened out by the time the flash flooding is reported. Of the individual MM events, 8 of the 11 MM cases displayed this feature. There appears to be little to distinguish the three events that did not develop a short-lived weak ridge; all three events featured a convective line at least 25 km long with a continuous radar reflectivity of at least 55 dBz, but this type of organization was present in a few of the MM cases that did form the short-lived ridge as well. It appears that this ridge feature that appears in the composites often accompanies MM events, but it is not a requisite

feature for events of the MM type.

The SYN composite displays a negatively-tilted (northwest-to-southeast oriented) short-wave trough to the west of the flood location, and the flood location is just downwind of a low-level convergence zone. The winds directly over the flood area are 15 kt, but the wind speed just upwind of the flood area is 20 kt. In contrast to the SYN composite's short-wave trough, the LM composite displays a cut-off low that is located just to the west of the flood area. The mid-tropospheric winds over and near the flood area are relatively weak at only 10 kt. This, combined with an apparently homogeneous moisture field, means that the moisture advection for the LM composite is weaker than for the SYN composite. This may be evidence of why the LM features are associated with not necessarily less rainfall, but certainly with a much shorter lifetime of moderate to heavy rainfall and, perhaps, less total impact over the course of their lifetime than SYN events, which persist for a longer period of time. The SYN composite features a plume of moisture streaming toward the flood area from the south, which is efficiently lifted and condensed with the aid of a low-level convergence zone – a favorable set of conditions for sustained deep convection (Doswell et al., 1996). The LM composite, on the other hand, has some features in place for briefly sustained convection – relatively light winds which favor slow system movement and ample local moisture (Doswell et al., 1996) – but the LM composite doesn't have the advantage of an internal lifting mechanism as the SYN composite does with its convergence zone. At the same time, the LM composite signals a situation – a cutoff low surrounded by light winds and a lack of a nearby parent trough – which could persist for a period of perhaps up to several days, yet the convection related to the LM event day forms and decays in less than 24 hours. Only two of the seven LM events occur in temporal isolation; that is, most of the LM event days are preceded or succeeded by at least one flash flood event day with another storm type.

So, the LM events do tend to be associated with "active" periods, but the LM event day is only one phase of these active periods.

But do the individual event days of SYN and LM events look distinctly different from each other? And do they resemble the composites? Ironically, the closed lows from the individual cases for the LM events tended to be closed within a larger parent trough – closed lows rather than pure cut-off lows (much like the tilted trough of the SYN composite). On the other hand, the cutoff lows for the SYN events were often cut off within an otherwise zonal flow, with no larger parent trough in close proximity (or much like the LM composite). Furthermore, in the LM events, the troughs in the vicinity of the flood location often appeared to be like large limbs, while the troughs in the vicinity of the SYN events appeared more like small protrusions or "knobs" off of the large limbs or directly off of the primary lows in the large-scale flow. In other words, the majority of the individual cases looked very much like the opposite large-scale composite scenario (Figure 5.2). Five of the seven LM cases featured a closed low which was not far removed from a nearby "limb trough" (see Figure 5.2(a)); in the LM composite, the cutoff low was preserved, while the attached trough was lost, likely as a consequence of the different tilt orientations of the troughs. The SYN events, in addition to the type just mentioned, also featured isolated, drifting cutoff lows and protruding knobs from larger troughs (see Figures 5.2(b) and (c), respectively), smaller features which were smoothed over in the compositing process. As a result of the compositing process, the most common feature of the individual LM and SYN cases – a cutoff low and a negatively tilted trough, respectively – remained, while the other, less prominent features were lost and did not appear in the composite.

While the moisture composites at low levels displayed little difference among the scale event types, a moisture composite for the middle troposphere (500 hPa), however, tells a much different story (Figure 5.3). Here, the moisture decreases with

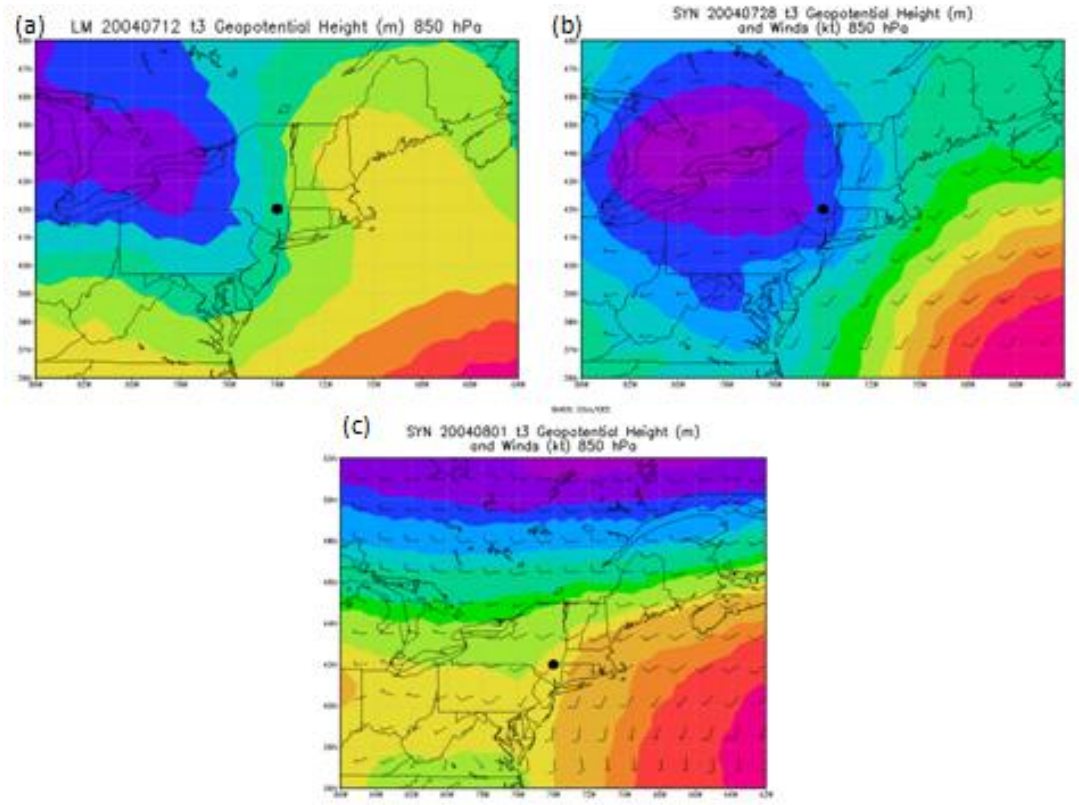

Figure 5.2 Sample cases to illustrate variations of troughs and lows in SYN and LM events. (a) A "long limb" low event. A large trough (negatively-tilted in this case) extends from a closed low toward the flood area. In some cases, a second closed low was close to the flood location. (b) A sample cut-off low event. The low is surrounded by relatively weak winds and sits far from a parent trough. (c) A sample "protruding knob" event. A small bump on a long-wave trough sits just upwind of the flood area, shaded in light green.

decreasing scale length, from the SYN composite down to the SMISO composite. The SMISO composite displays weak "dry air" advection, with weak winds moving from drier air west of the trough axis into somewhat moister air east of the trough axis. The moistest air remains farther to the east, where southerly winds transport moist air towards the north – moisture that has likely already made its way north from the

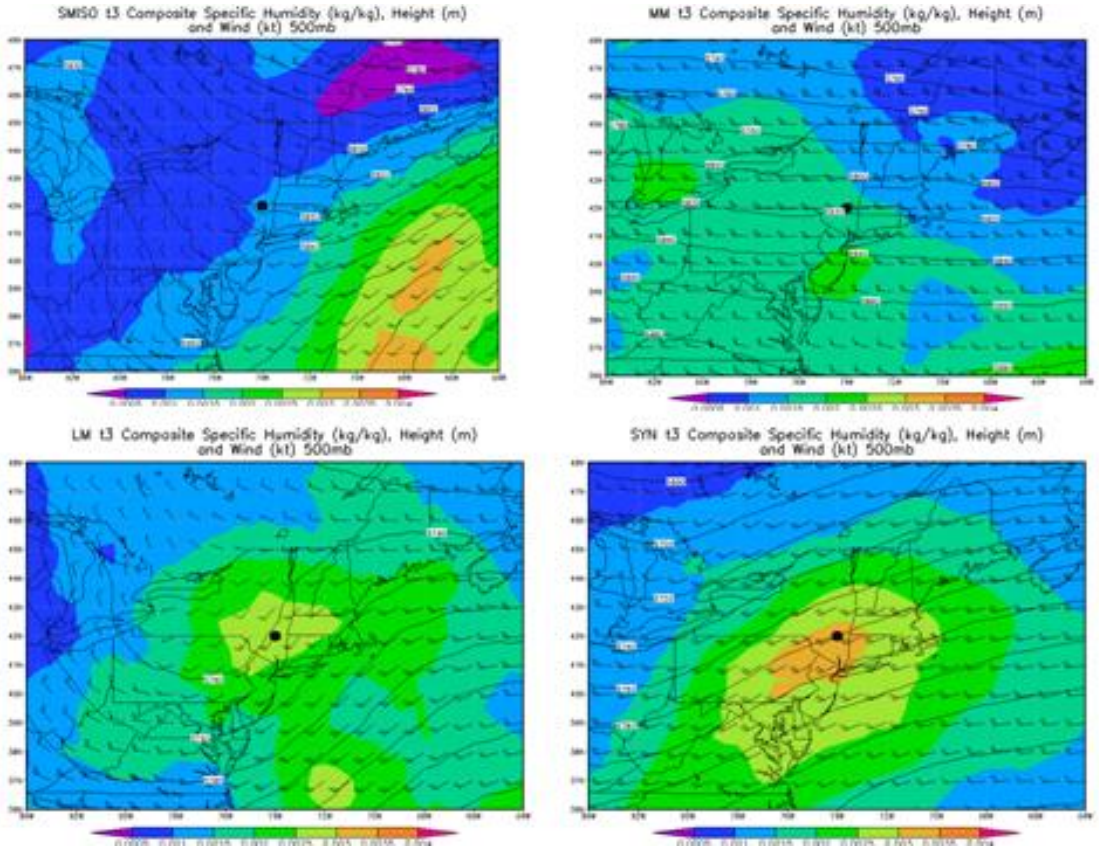

Figure 5.3 Composite specific humidity (shaded, kg/kg), geopotential height (contours, m), and wind (barbs, kt) at 500 hPa for the time period 3-6 hours before the flood report for (a) SMISO, (b) MM, (c) LM, and (d) SYN events.

tropics. This moisture does not appear to interact with the inland SMISO thunderstorms. The MM composite at mid-levels is non-descript, with relatively moderate zonal winds (25 kt) and little evidence of mid-tropospheric waves. The air being transported to the flood area has approximately the same moisture content as the air near the flood location. Overall, there is little of significance to distinguish the SMISO and MM events at mid-levels, as much of their development appears to take place in the lower troposphere.

Unlike the smaller scale event composites, both the SYN and the LM

composite have a local maximum of moisture centered on or very close to the flood location. With strong winds coinciding with this moisture maximum, the moisture advection is favorable for the composites of these two large scale event types. As in the 850 hPa maps above, the biggest difference between these two types is again in their wave structure: the SYN composite features a long wave, while the LM composite displays a short wave. For both composites, the flood location coincides with the inflection point of the wave at the time three to six hours before the flash flooding is reported. The individual cases, however, show variability from the idealized scenarios portrayed by the two composite maps. Of the seven LM cases, three were short waves, three were closed lows, and one was a long wave. Each of these was located to the west of the flood location, so it is clear that the shortwave and closed low cases helped to generate the short wave pattern with a trough to the west of the flood location in the composite. The 19 SYN cases consisted of ten long waves, two short waves, two closed lows, and five cases in which a long wave contained embedded short waves. For two of these latter cases, the trough was located to the east of the flood location; for the other 17 SYN cases, the trough or closed low was centered to the west of the flood location. The long-wave and long-wave/short-wave cases varied from short wavelength, high amplitude cases to long wavelength, weak amplitude configurations, and so in the composite, a moderate wave in between these extremes is apparent.

To gain greater insight into why some of these events produced extreme precipitation while others generated only more pedestrian amounts, the remainder of this section will examine the differences between "high precipitation" (>100 mm) and "low precipitation" (< 100 mm) composites for the SYN and LM event types. (The MM group provided only one high precipitation case and the SMISO group provided none, so they have been eliminated from this analysis.) Figure 5.4 displays the

moisture, geopotential height, and wind at two levels (500 Pa on top and 850 hPa on bottom) for the "high" (left) and "low" (right) precipitation amounts. At 500 hPa (Figure 5.4(a) and (b)), the composites are nearly the same, with 30 kt winds in the vicinity of the flood location, as well as a local moisture maximum, and a long wave in the height field. However, the flood location is west of the inflection point in the high precipitation composite, but the flood location lies to the east of the inflection point in the low precipitation composite. The differences between the two scenarios are more pronounced at 850 hPa. There is a broader, moister low-level upwind

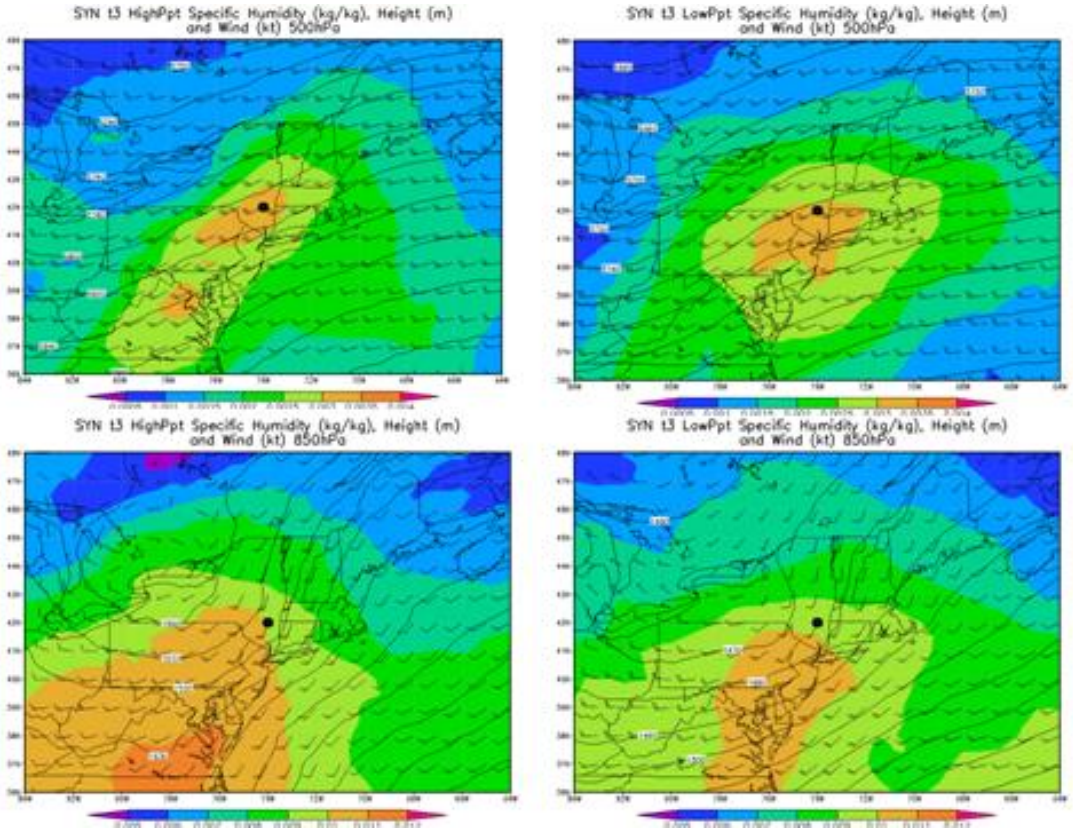

Figure 5.4 SYN composites of moisture (kg/kg), geopotential height (m), and winds (kt) at 500 hPa (top) and 850 hPa (bottom) for events with "high" (>= 100 mm, left) and "low" (<100 mm, right) precipitation estimates at the time corresponding to 3-6 hours before the report of flash flooding.

moisture supply for the high precipitation composite. The flood location in the high precipitation composite is also located in the core of fastest winds to maximize the advection of moisture into the flood area, while this core (and, presumably the most favorable moisture advection) is located to the east of the flood location in the low precipitation composite. There is also a more pronounced negatively tilted short wave trough in the high precipitation composite than in the low precipitation composite. Overall, some slight differences in the low-level composites distinguish the aggregated higher precipitation events from the aggregated lower precipitation events, and these differences suggest either higher or lower precipitation, according to what one might expect from the dynamical consequences.

Figure 5.5 displays the same fields for the LM composites. Unlike in the SYN high/low precipitation comparison, here the moisture fields differ appreciably between the high and low precipitation composites. The moisture maximum for the high precipitation composite is centered on the flood area, while the moisture maximum is farther downwind (and therefore less favorable for advecting moisture into the flood area) in the low precipitation composite. The high precipitation composite has a shallower, positively tilted trough at 500 hPa than the low precipitation composite. As a result of this tilt, the winds over the flood location are stronger, but with less lateral wind shear in the high precipitation composite, particularly toward the southeast, as compared with the low precipitation composite. At 850 hPa, there is a significant difference in upwind moisture, with the high precipitation composite more favorable for the development and sustenance of heavy rainfall. At 850 hPa, the high precipitation composite has a negatively tilted trough, and furthermore, at 850 hPa, this negatively tilted trough contains a closed low – much like a melding of the overall LM composite (Figure 5.1(c)) with the overall SYN composite (Figure 5.1(d)). The

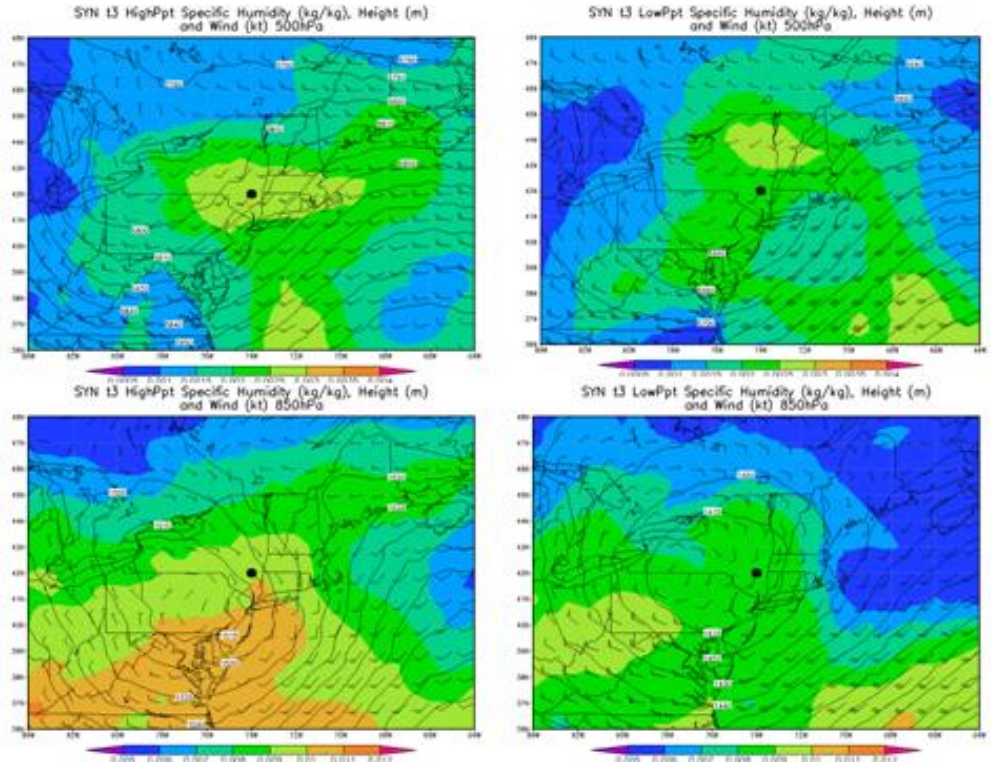

Figure 5.5 LM composites of moisture (kg/kg), geopotential height (m), and winds (kt) at 500 hPa (top) and 850 hPa (bottom) for events with "high" (>= 100 mm, left) and "low" (<100 mm, right) precipitation estimates at the time corresponding to 3-6 hours before the report of flash flooding.

low precipitation composite at 850 hPa, meanwhile, has a symmetrical cut-off low surrounded by a positively-tilted trough. Much like at 500 hPa, this creates more lateral wind shear to the southeast of the flood location, which may help to reduce the amount of moisture being transported into the flood area. The negative tilt of the closed low in the high precipitation case also helps to generate more veering between 850 hPa and 500 hPa than in the low precipitation case. This veering can contribute to warm air advection in the lower troposphere, which, through the process of frontogenesis, can combine with the westerly "steering" winds aloft to generate an extended region of heavy precipitation along an amplifying low-level boundary

(Davis, 2001). In short, the high precipitation LM composites display several mechanisms for sustained convection, while these mechanisms are not present in the low precipitation LM composites, nor are they present to the same extent in the SYN high or low precipitation composites. Perhaps the prevalence of these features in the "high" precipitation composite explains why four of the seven LM cases exceeded 100 mm of estimated precipitation, while only six of the 19 SYN cases exceeded this threshold.

5.3 Analysis of Linear Events

The linear events are archetypes of precipitation organization that have been identified in the literature. This section seeks, first, to describe the atmospheric conditions accompanying each of these types of events and, second, to determine if these conditions are in any way different from what has been described for these types of events in the literature.

Figure 5.6 displays composites of moisture, geopotential height, and winds at four levels for the trailing stratiform (TS) events. The events are dominated aloft (300 and 500 hPa) by a long-wave trough to the west and a long-wave ridge to the east. The flood area sits just to the northeast of the inflection point of this wave. The inflection point intersects the location of greatest moisture content at 300 hPa and 500 hPa, just upwind of the flood area. At lower levels, the flow in the vicinity of and upwind of the flood area is uniformly southwesterly, with a broad plume of moisture from southwest to northeast. This creates a favorable situation for moisture advection into the flood area. At 925 hPa, there is an indication of a weak short-wave trough axis near the flood location, and accompanying this narrow trough axis is a local

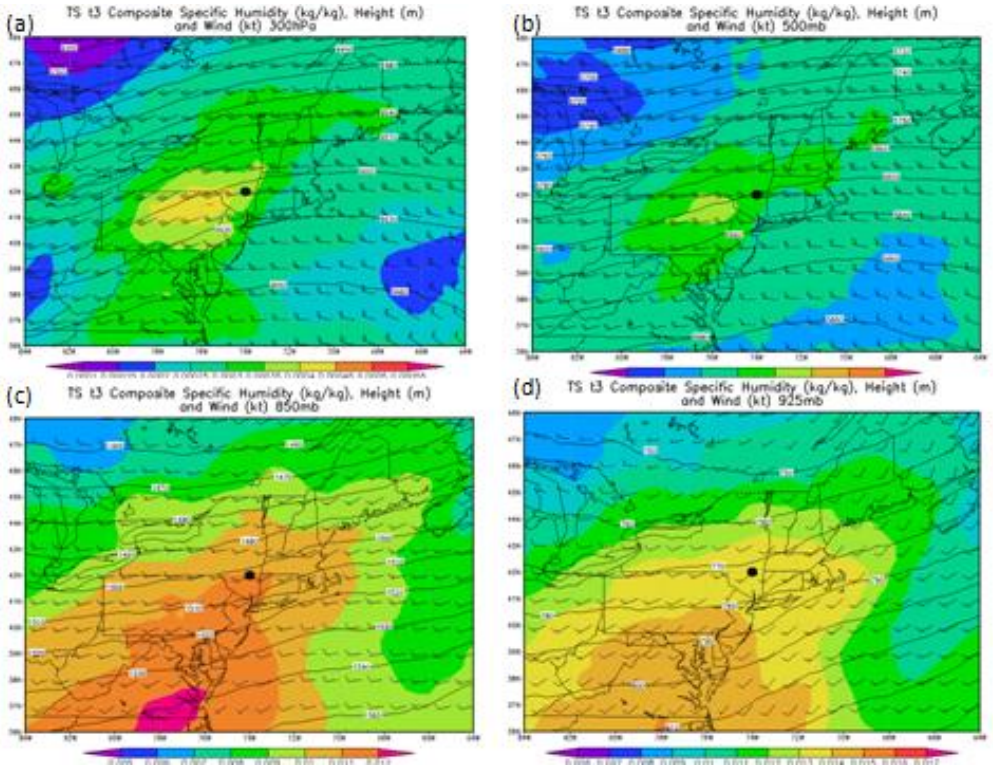

Figure 5.6 Composites of moisture (shaded, kg/kg), geopotential height (contours, m), and winds (barbs, kt) at 4 levels ((a): 300 hPa, (b) 500 hPa, (c) 850 hPa, and (d) 925 hPa) for TS events.

maximum in winds of 15 kt. Though too weak to qualify and as a low-level jet, this local wind maximum increases the flow of moisture into the flood area. A bit higher, the moisture at 850 hPa near and to the south of the flood area is among the most ample moisture for any event type at this level, and the winds in a relatively small area centered on the flood location are, as at 925 hPa, a bit faster (20 kt) than the surrounding wind field. This deep layer of moisture with positive moisture advection through 300 hPa, with both low level and upper level dynamical support, make the TS composite scenario a very favorable one for heavy precipitation.

What separates the most extreme TS events (with an estimated precipitation total greater than 100 mm) from events with more moderate precipitation amounts

(less than 100 mm)? Figures 5.7(a) and 5.7(b) compare the mean mid-level (700 hPa) moisture for high precipitation and low precipitation cases. While the low-precipitation cases have more mid-level moisture than the high-precipitation cases, this high moisture-content air is located southwest of the flood location and is being advected by westerly winds to the south of the flood location; in short, in low

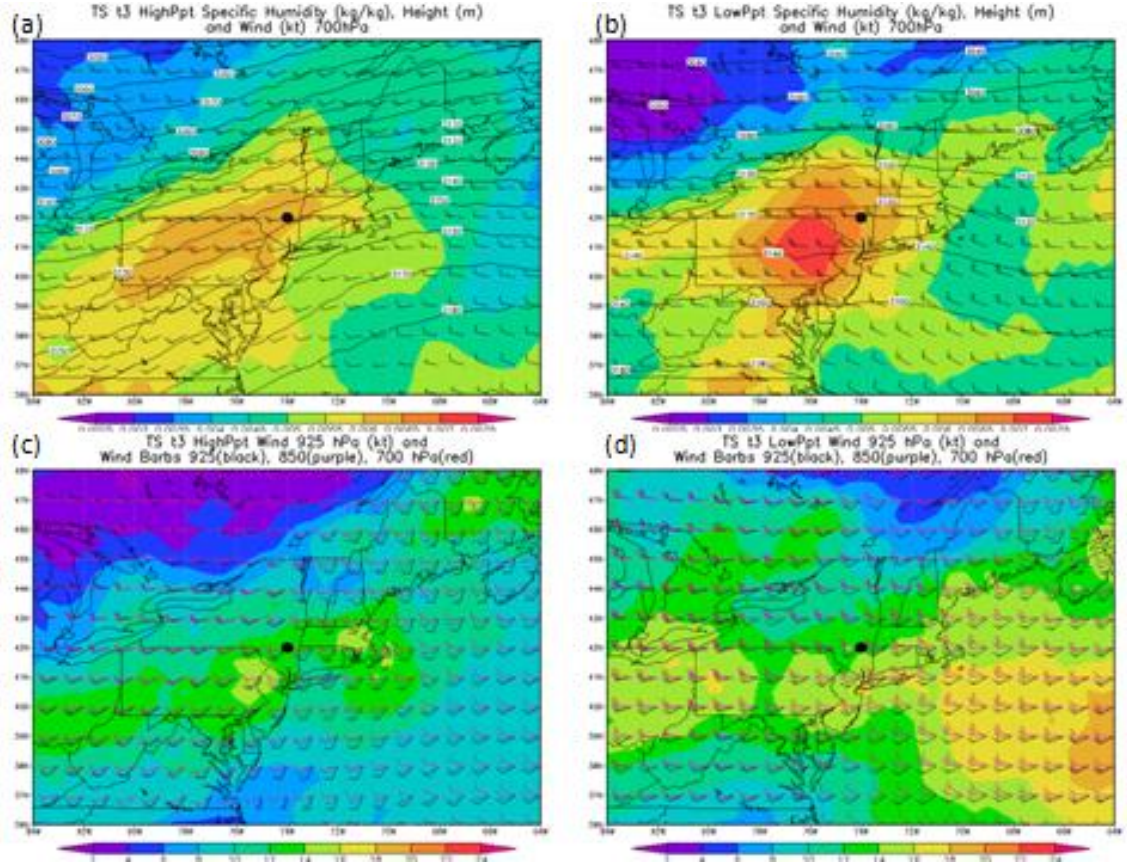

Figure 5.7 High precipitation (a) and low precipitation (b) specific humidity (shaded, kg/kg), geopotential height (contours, m), and winds (barbs, kt) at 700 hPa; high precipitation (c) and low precipitation (d) wind speed (shaded, kt) at 925 hPa and wind vectors (barbs, kt) at three levels: 925 hPa (black barbs), 850 hPa (dark purple barbs), and 700 hPa (dark red barbs), for TS events.

precipitation events, the flood location is not co-located with the strongest moisture advection, while it is in the high precipitation events. The height field hints at a weak

short-wave ridge just downwind of the flood location and looks nothing like the trough-to-ridge wave segment that was apparent in the 500 hPa composite discussed above. While short-wave ridges aloft can be associated with heavy precipitation (Davis, 2001), this is more common in the middle-to-upper troposphere (500 hPa to 200 hPa), and this may explain why, despite a favorable 700 hPa moisture field, this composite is representative of cases that resulted in more moderate precipitation totals. Meanwhile, the high precipitation 700 hPa composite (Figure 5.7(a)) features a trough-to-ridge wave segment very similar to the overall TS composites at 500 hPa and 700 hPa. The southwesterly winds created by this trough-to-ridge structure parallel the swath of relatively high moisture content that is being advected toward the flood area, and these winds are traveling through the region in which quasigeostrophic theory (Holton 2004) suggests that ascent aided by vorticity advection is most likely, creating a more ideal scenario for sustained heavy rainfall than in the lower precipitation composite.

Figure 5.7 contrasts the low level wind speed (925 hPa) and low level shear (from 925 hPa to 700 hPa) for high precipitation (c) and low precipitation (d) events. In the high precipitation composite, there is a small area of amplified 925 hPa winds just to the southwest – just upwind – of the flood area. Though this area is not strong enough to constitute a low-level jet, it provides enhanced low-level warm, moist air to the flood area. The composite shows nearly uniform wind direction with height to the west of the flood area, but in the vicinity of the flood area, there is significant veering, with most of this veering in the layer from 850 hPa to 700 hPa. East and southeast of the flood area, the veering is more balanced between veering from 925 hPa to 850 hPa and from 850 hPa to 700 hPa. It appears that the "sweet spot" where the flooding arises is related to this area of minimal low-level shear that allows for a thicker layer (up to 850 hPa) of low-level moisture ingestion, with veering at mid levels to orient

the direction of the MCS's travel approximately from west-to-east, so that this TS system ingests moisture on its southern flank as it travels approximately west-to-east. The low precipitation low-level wind composite has similar structure to the high precipitation composite, but here the 925 hPa wind has a much broader area of relatively high winds that stretches from west to east and passes south of the flood area; as such, it is not the most conducive to bringing warm, moist air into the flood area. The vertical wind shear in the 925 hPa to 850 hPa layer is approximately equal to the vertical wind shear in the 850 hPa to 700 hPa layer, so the low-level moisture transport from the south is apparently not quite as strong, and the preference for low-level moisture transport seen in the high precipitation composite does not appear here. There is also a much more pronounced northerly component of the wind throughout the 925 hPa to 700 hPa layer to the east and southeast of the flood area. Overall, while the low precipitation low-level shear composite is conducive to significant rainfall, it is not as favorable for heavy precipitation rates as the high precipitation low-level shear composite.

In the TLAS composite (Figure 5.8), the flood area sits upwind of a weaker long wave ridge at 300 hPa (Figure 5.8(a)) as compared to the higher amplitude wave in the 300 hPa composite for the TS events above. Here, the flood area is much closer to the ridge axis than in the TS composite, creating less favorable conditions for the uplift of warm, moist air from below. Although the upper-level dynamics are less favorable in the TLAS 300 hPa composite than in the TS 300 hPa composite, the moisture is more favorable, even at upper levels. Because the TLAS event type had the highest precipitation values of the linear event types, it makes sense that its composite had the deepest layer of moisture directly over and upwind of the flood area. This area of moisture extends down to 500 hPa (Figure 5.8(b)), where a broad area of fairly high mid-level moisture is centered just west of the flood area. The

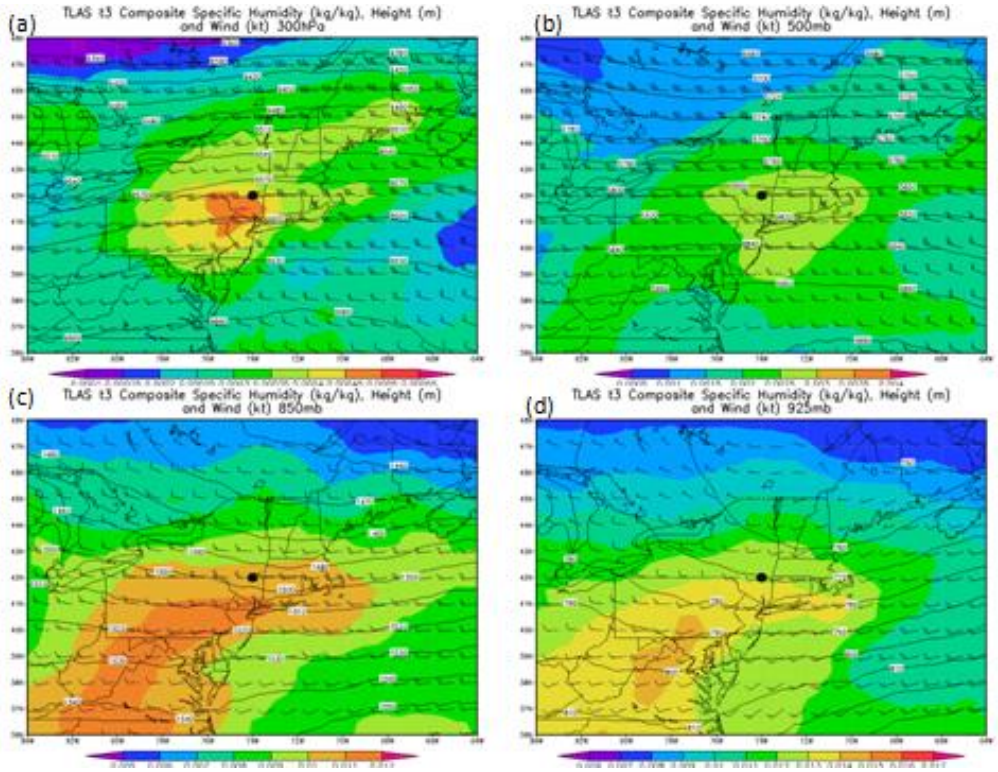

Figure 5.8 Composites of moisture (shaded, kg/kg), geopotential height (contours, m), and winds (barbs, kt) at 4 levels ((a): 300 hPa, (b) 500 hPa, (c) 850 hPa, and (d) 925 hPa) for TLAS events.

winds at this level are zonal. At 850 hPa, like at 300 hPa, the flood area is situated just upwind of a long-wave trough. There is ample moisture in the TLAS composite, but it is not quite as moist as in the TS 850 hPa composite; the moisture advection is also not as favorable as in the TS composite. The low-level (850 hPa) winds are stronger (20 kt) than in the TS composite, but the winds do not meet the low-level jet (LLJ) criterion from Schumacher and Johnson (2005) of 30 kt. The low-level moisture field is elongated in the direction of the low-level winds, from west to east, but it is centered south of the flood area. At 925 hPa, the TLAS flood area is situated in a positively tilted (southwest-to-northeast) trough with an ample supply of moisture in the flood area with positive (though not ideal) moisture advection. The winds are

more moderate than at 850 hPa, at 10 kt, and they are westerly upwind of the flood area, much like at 850 hPa and 500 hPa. Overall, the TLAS composite looks less ideal to produce flash flooding than the TS composite, with weaker dynamics and somewhat less favorable moisture advection, but TLAS events produced the greatest mean precipitation estimate of the linear events. These composite figures do not agree with the composites presented in Schumacher and Johnson (2005) to describe TLAS events, as their composites featured a southerly low-level jet with mid- and upper-level winds from the west, much like the scenario described above in the TS composites.

Can the difference between high precipitation and low precipitation TLAS flash flood events explain some of the perceived shortcomings of the overall composite above? The 700 hPa moisture field (shaded in Figure 5.9(a) and Figure 5.9(b)) has a much broader area of low-level moisture for the high precipitation composite as compared to the low precipitation composite. The prevailing winds for the TLAS case were previously described to be westerly to south-westerly at most levels. Here, it is obvious that to the west of the flood area, winds throughout the 925 hPa to 700 hPa layer are vertically stacked in the westerly direction, and at 925 hPa (shaded in Figure 5.9(c)) there is a broad area of stronger (16-18 kt) low-level westerly winds for the high precipitation composite. This is evidence not necessarily of a low-level jet (at least not according to Schumacher and Johnson's (2005) definition of 30 kt), but it is evidence of a broad area of unidirectional flow to transport warm, moist air toward the flood area. In close proximity to the flood area – over and just upwind and downwind – the winds at 925 hPa are southwesterly, with veering above this level such that the winds at 850 hPa and 700 hPa are westerly and aligned with the moisture field at these levels. This could help to transport warm, moist air near the surface toward the flood area. Farther to the east, the 700 hPa winds veer even further,

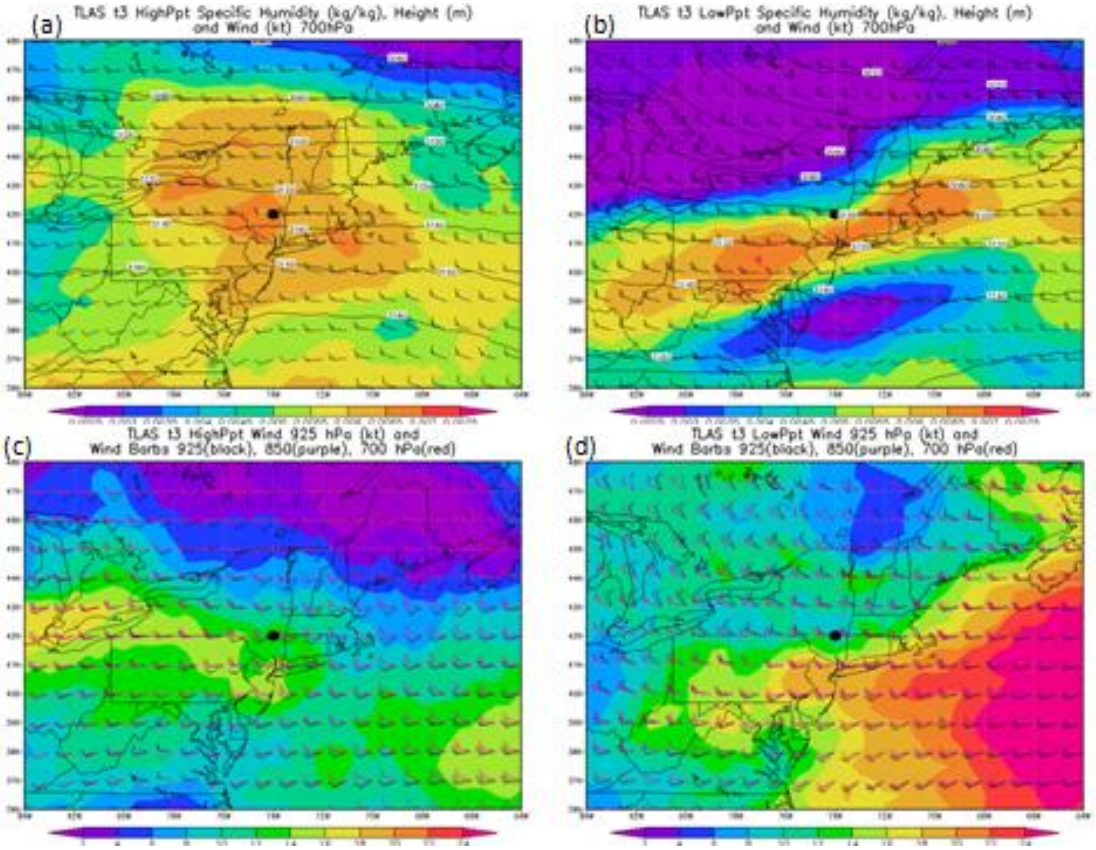

Figure 5.9 High precipitation (a) and low precipitation (b) specific humidity (shaded, kg/kg), geopotential height (contours, m), and winds (barbs, kt) at 700 hPa; high precipitation (c) and low precipitation (d) wind speed (shaded, kt) at 925 hPa and wind vectors (barbs, kt) at three levels: 925 hPa (black barbs), 850 hPa (dark purple barbs), and 700 hPa (dark red barbs), for TLAS events.

so that they have a northerly component, which makes this area less conducive to heavy precipitation by reducing the input of warm, moist air. So, much like in the TS composite, there appears to be a relatively narrow area with a favorable low-level wind structure for the generation and sustenance of heavy rainfall in the TLAS high precipitation composite.

In the TLAS low precipitation composite (Figure 5.9(d)), instead of the

vertically uniform low- and mid-level winds upwind of the flood area that were found in the high precipitation composite, there is pronounced backing with height upwind of the flood area. This backing makes conditions less favorable for heavy precipitation because the greatest moisture is most often found to the south, so the northwesterly lower-level winds associated as found in the low precipitation composite would tend to advect drier air towards the flood area rather than moister air. Over the flood area, there is weak backing from 925 hPa to 850 hPa and a uniform westerly wind from 850 hPa to 700 hPa. Downwind of the flood area, the winds veer only slightly, much less than in the high precipitation composite. The maximum 925 hPa wind speeds at the longitude of the flood area and upwind are to the south of the flood area, a less than ideal configuration for the advection of warm, moist air into the flood area. Overall, while the high precipitation composite offers some evidence as being a favorable set-up for heavy precipitation and flash flooding, the low precipitation composite appears to be relatively unfavorable, and it helps to explain why the composites for the TLAS events as a whole appeared less than favorable for flash-flood producing rainfall.

At 300 hPa, the PS composite (Figure 5.10) places the flood area downwind of a weak upper level long wave ridge and upwind of a weak upper level trough. This is the type of scenario that Davis (2001) has cited as one in which flash flooding is possible, even though the synoptic situation appears fairly benign. The flood area is slightly more moist than the surrounding area, but not as moist as in the TS and TLAS composites. Overall, the dynamics and the upper level moisture are not as conducive to heavy rain as the TS and TLAS composites. The long-wave trough is better-defined at 500 hPa, and it is located just downwind of the flood area. In association with the

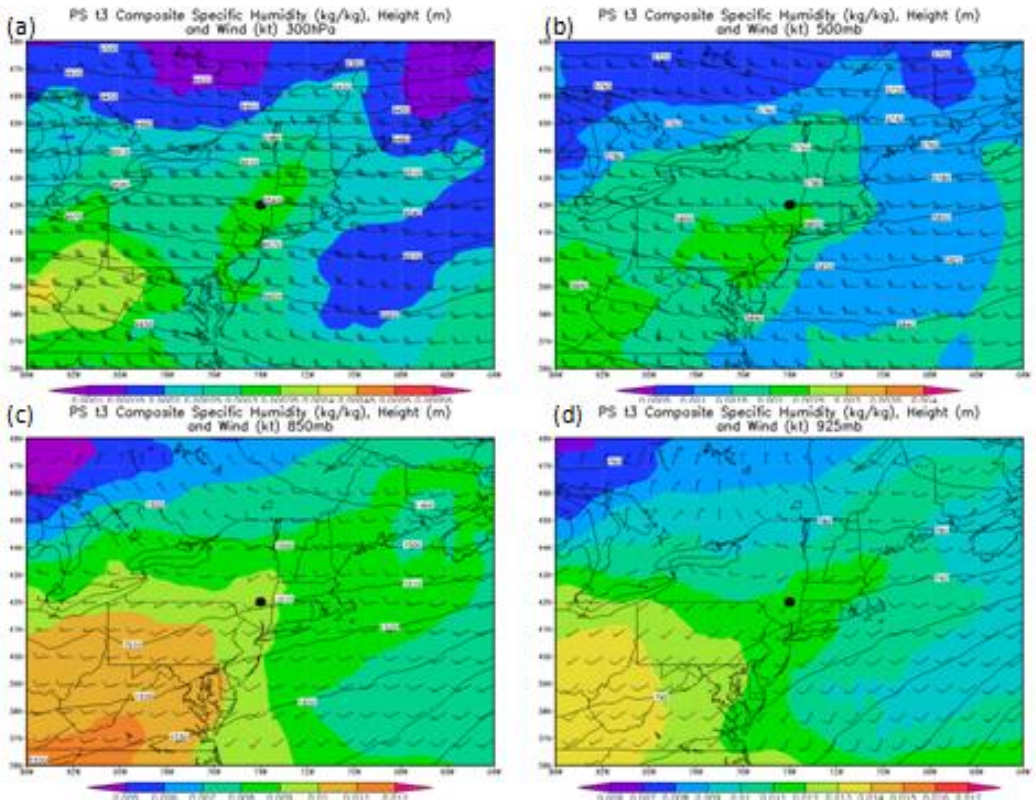

Figure 5.10 Composites of moisture (shaded, kg/kg), geopotential height (contours, m), and winds (barbs, kt) at 4 levels ((a): 300 hPa, (b) 500 hPa, (c) 850 hPa, and (d) 925 hPa) for PS events.

weak trough, the winds are westerly at approximately 25 kt. There is relatively little moisture at mid-levels as compared to the other linear composites. Moving down to 850 hPa, the moisture field becomes more conducive to producing heavy precipitation, with moisture levels more similar to those of the other linear event types, and with southwesterly winds which will advect the warm, moist air that lies to the southwest toward the flood area. The winds are light, as there is a confluence zone to the north of the flood area. This description fits the 925 hPa composite as well. It appears that the PS events are identified by their weak low level winds – and, hence, slow system motion – and a limiting of the moisture in the lower troposphere.

What distinguishes the average high precipitation PS event from the average low precipitation PS event? One would suspect that more moisture would be present in the middle to upper levels in the high precipitation composite, and this is indeed the case. At 700 hPa, there is up to 25% more moisture present upwind in the high precipitation composite as compared to the low precipitation composite (Figure 5.11(a) and Figure 5.11(b)). There is also a narrow band of moisture that is greater than the surrounding environmental moisture content for the high precipitation

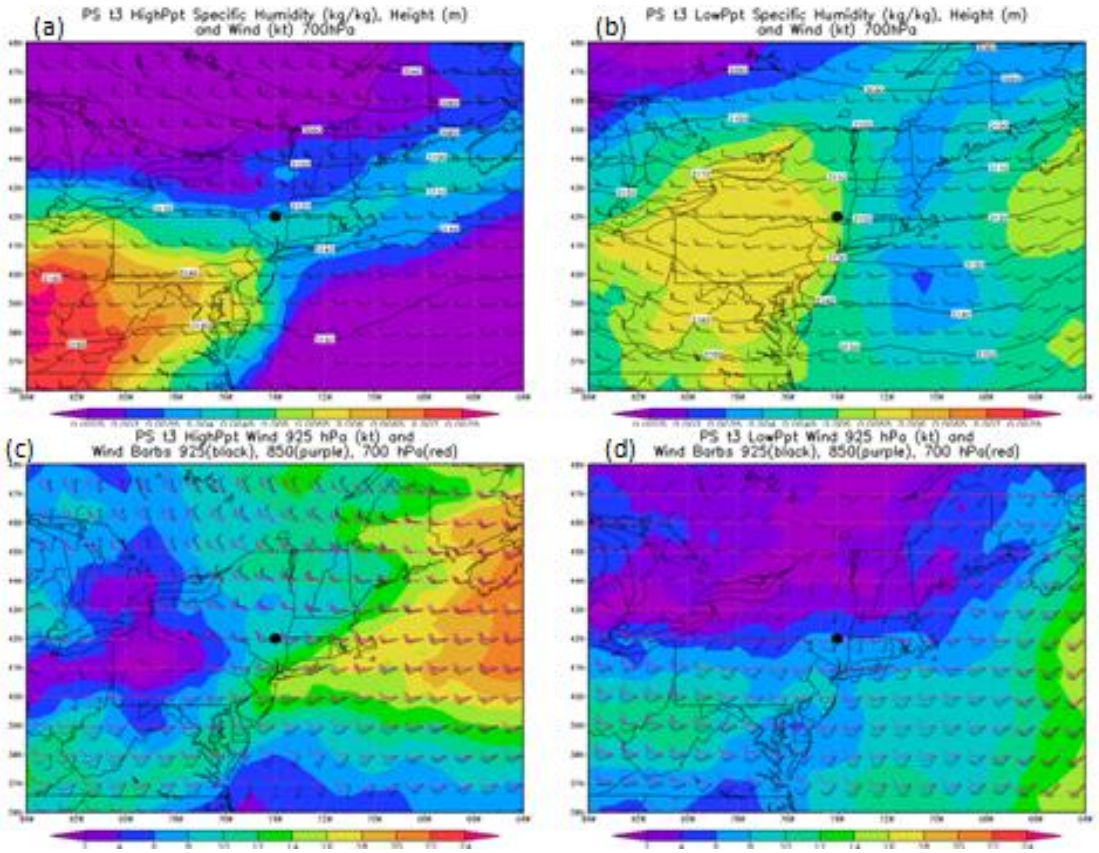

Figure 5.11 High precipitation (a) and low precipitation (b) specific humidity (shaded, kg/kg), geopotential height (contours, m), and winds (barbs, kt) at 700 hPa; high precipitation (c) and low precipitation (d) wind speed (shaded, kt) at 925 hPa and wind vectors (barbs, kt) at three levels: 925 hPa (black barbs), 850 hPa (dark purple barbs), and 700 hPa (dark red barbs), for PS events.

composite – a band that could correspond with the mean orientation of the convective line in these PS events. The winds back significantly with height – especially from the 850 hPa level to the 700 hPa level – in the northwest corner the high precipitation composite (Figure 5.11(c)). Approaching the flood area in a straight line from the northwest corner of the composite, the backing shifts in the vicinity of Lake Ontario (in the composite, but not necessarily at this location in individual cases) to be approximately balanced between the 925 hPa to 850 hPa layer and the 850 hPa level to 700 hPa layer. In the vicinity of the flood area, the flow is nearly unidirectional, with weak veering over the flood area. This unidirectional flow is indicative of the structure and movement of the PS systems – long, narrow swaths of rainfall that often have a significant component of motion parallel to the orientation of the line. Parker and Johnson (2000) found that PS events, indeed, tended to have a strong line-parallel wind component, especially in the middle to upper troposphere. Moving away from the flood area in the downwind direction, especially to the south and south-southeast of the flood location, the veering becomes more pronounced. The PS wind shear low precipitation composite (Figure 5.11(d)) is also notable for its relatively light winds (<4 kt) to the west of the flood location and relatively strong winds (<15 kt) to the east of the flood location at 925 hPa. Is it significant that an area of unidirectional flow with height occurred over the flood area for the high precipitation composite? It does seem to be a marker for the high precipitation events, as such an area is not present in the low precipitation composite (Figure 5.11(d)), although it is hinted in the 925 hPa and 850 hPa composites in Figure 5.10(c) and Figure 5.10(d). The wind profile for the low precipitation composite shows veering winds across the majority of the composite. Whereas the high precipitation composite displayed vertically uniform winds over the flood area, here the flood area is subject to veering winds from south-southeasterly winds of 5 kt at 925 hPa to west-southwesterly winds of 15 kt at 700

hPa. The vertical speed shear in the vicinity of the flood area is the largest of any location on the composite. In contrast, the low-level winds are light and variable to the northwest of the flood area, while to the southeast, significant veering from southwesterly at 925 hPa to westerly at 700 hPa dominates while the speed remains at approximately 10 kt. Thus, in the low precipitation composite, it appears that the large low-level vertical speed shear and lateral shear from upwind to downwind is most significant, while in the high precipitation composite, winds are uniformly from westerly to west-southwesterly over the flood area in the lower troposphere.

5.4 Analysis of Back-building Events

Back-building events have been described in the literature, but without further dividing these events into sub-classes based on the passage of other features before, during, or after the lifetime of the back-building storm. Schumacher and Johnson (2005) found back-building events to be associated with a tongue of high equivalent potential temperature air and a lower level jet, both at 850 hPa, which also coincided with the area of heaviest precipitation. This chapter seeks to explore (1) how well this paradigm of the environmental conditions during back-building events matches the mean conditions observed for the back-building types of events in this study and (2) how these different categories of back-building events compare to each other.

For the BB events (Figure 5.12), the flow is largely zonal at upper levels, with weak indications of a trough to the west and a ridge to the east of the flood area at 300 hPa. There is a slight elevation of moisture amounts in the vicinity of the flood area at 500 hPa, but there is otherwise no indication in the middle to upper level moisture field that flash flooding would be likely. In the lower troposphere, there is a more ample supply of moisture and positive moisture advection (however, this is still less

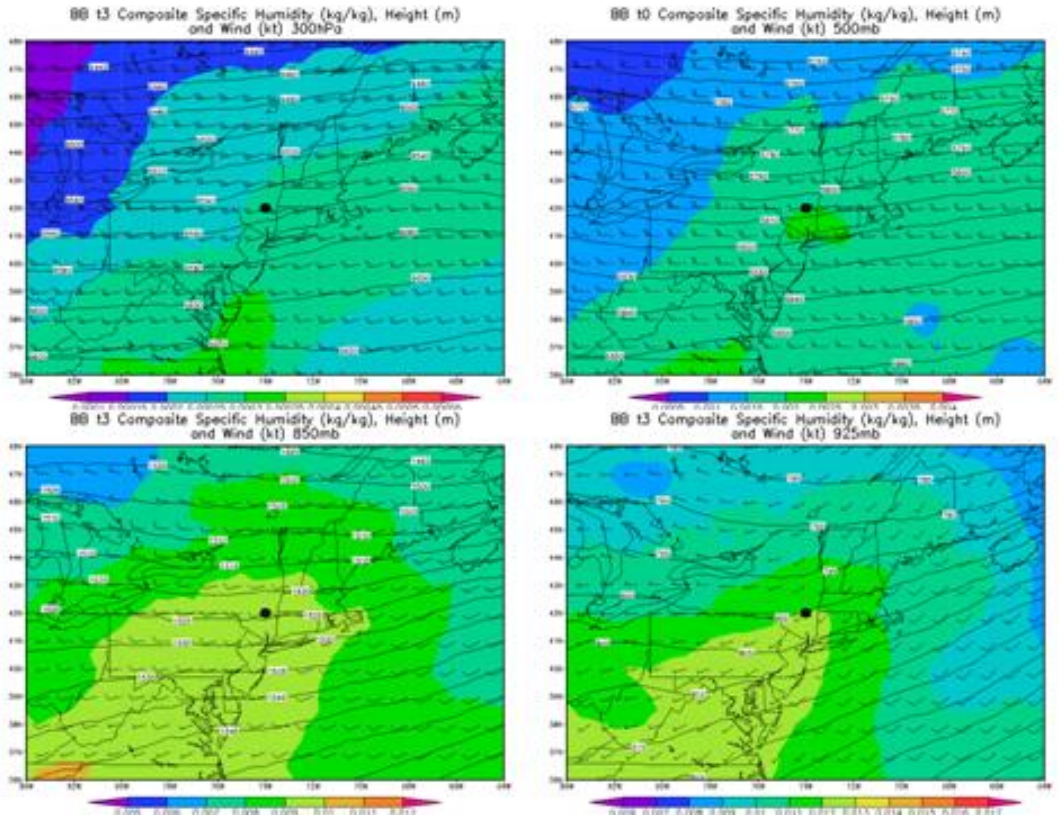

Figure 5.12 Composites of moisture (shaded, kg/kg), geopotential height (contours, m), and winds (barbs, kt) at 4 levels ((a): 300 hPa, (b) 500 hPa, (c) 850 hPa, and (d) 925 hPa) for BB events.

than the moisture amounts for most other storm types at these levels). The relatively lower moisture totals may be a consequence of the large number of BB cases (31) as compared to the typically much smaller number of cases (7-13) of most other event types. It may also be possible that because the re-generation of storm cells occurs on the storm scale as a result of rear-flank storm outflow, the concentration of moisture in many BB events is a more local phenomenon not reflected in these composite maps. At lower levels, the winds are southwesterly to westerly and fairly light (about 5 kt at 925 hPa and about 10 kt at 850 hPa). Schumacher and Johnson (2005) had found that BB events were often associated with a southerly low-level jet of approximately 30 kt

at 850 hPa. Such a feature is not at all evident in these composites, but it may still occasionally occur in individual cases in the Northeast. The difference is likely in the scale of the BB events – the cases in the Northeast typically appeared to be narrower in width and shorter in length (up to an order of magnitude difference) than the cases that Schumacher and Johnson (2005) studied. There is a weak trough just upwind of the flood area at 925 hPa.

Much like the BB cases, the middle and upper level moisture content is low for the BBMERGE composites (Figure 5.13). Winds are west-southwesterly at both 300 hPa and 500 hPa, with a weak trough to the west and a weak ridge to the east. At

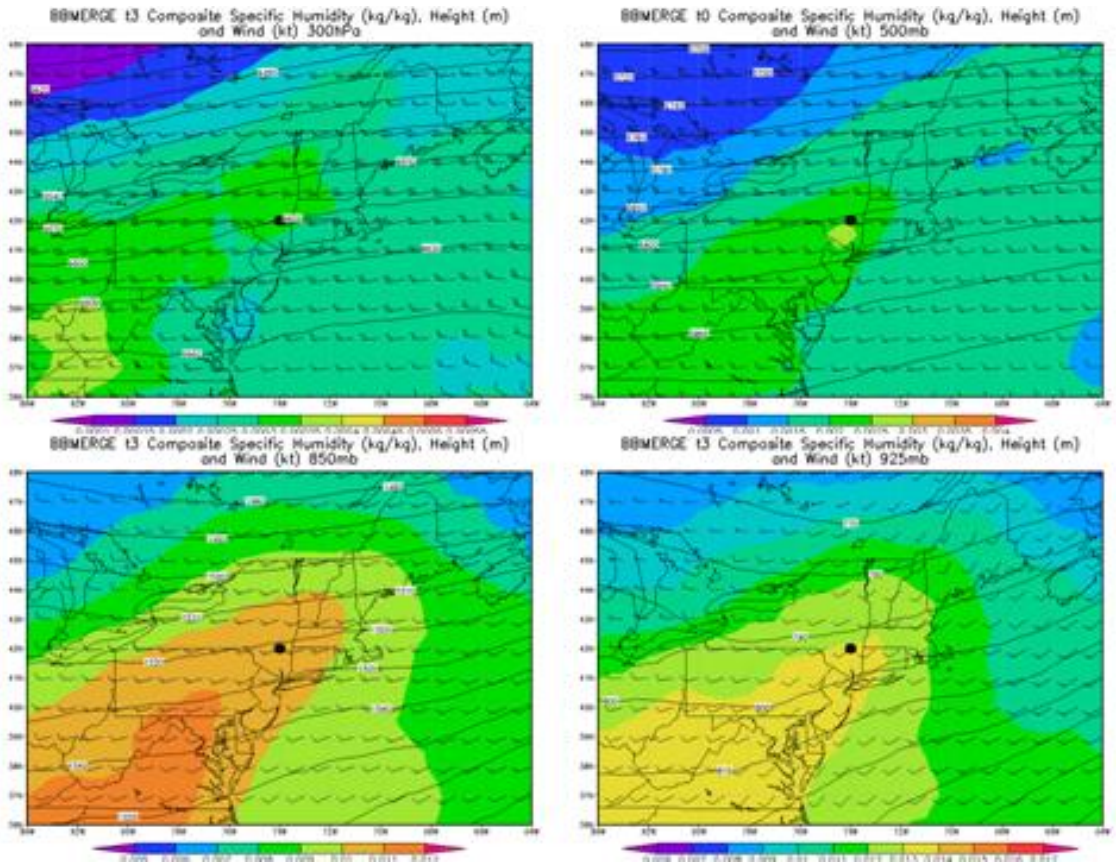

Figure 5.13 Composites of moisture (shaded, kg/kg), geopotential height (contours, m), and winds (barbs, kt) at 4 levels ((a): 300 hPa, (b) 500 hPa, (c) 850 hPa, and (d) 925 hPa) for BBMERGE events.

lower levels, there is considerably more moisture than in the BB composites, especially at 850 hPa. Moisture advection is more favorable than in the BB composites as well, due to stronger winds to transport this greater moisture toward the flood area. At 925 hPa, there is a shortwave trough to the west of the flood area; this trough is likely associated with the convective line that passes through the flood area and ends the persistent precipitation associated with the back-building convection. This trough appears to be a shallow feature, as it is weakly (if at all) evident at 850 hPa.

Unlike in the composites for most event types, in the BBMULT1 composite (Figure 5.14), the moisture anomalies tend to be greatest in the upper troposphere (300

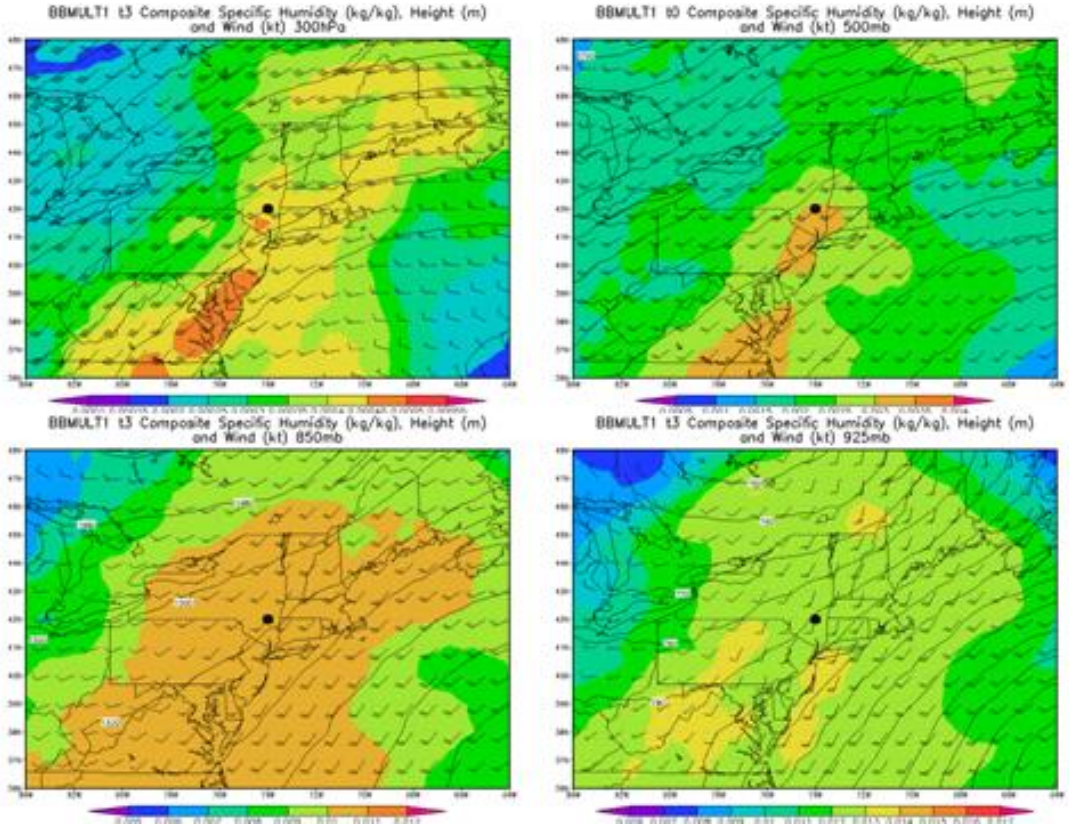

Figure 5.14 Composites of moisture (shaded, kg/kg), geopotential height (contours, m), and winds (barbs, kt) at 4 levels ((a): 300 hPa, (b) 500 hPa, (c) 850 hPa, and (d) 925 hPa) for BBMULT1 events.

(300 hPa), indicating a deep layer of ample moisture. This moisture is advected toward the flood area by strong (40 kt) winds moving from an amplified trough toward a ridge located over Nova Scotia and Newfoundland. The flood area is downwind of the inflection point between the trough and the ridge. At 500 hPa, these relatively strong composite winds and anomalously high moisture are still apparent, but not quite as favorable for heavy precipitation as at 300 hPa. At lower levels, a large, broad area of moisture is present upwind of, in the vicinity of, and downwind of the flood area. What is it that makes the flood area the favored location for the formation of heavy precipitation? It appears that the flood area is in an area of lateral shear, with faster winds to the north and east, and lighter winds to the south and west. The flood location is in the boundary between these two regions. Furthermore, at 850 hPa, the flood area is in a small area of relatively lighter winds (15 kt) surrounded by relatively stronger winds (20 kt) to create a small convergence zone. Unlike in the BBMERGE low-level composite, there is no short-wave trough or other small scale feature to indicate the presence of the convective line that will eventually traverse the area.

The BBMULT2 composite (Figure 5.15) features ample moisture in the upper troposphere at 300 hPa, but the moisture maximum is located to the east and southeast of the flood area and, thus, is not being advected into the region. However, there is still above average moisture over the flood area and this region is also located in the right entrance region of the jet, which is associated with upper level divergence and rising air, making it a favorable location for the formation and sustenance of heavy precipitation. This trend of the greatest moisture being located to the east of the flood area and the flood area's location in an area of favorable dynamics continues into the lower troposphere. The greatest moisture at 500 hPa, 850 hPa, and 925 hPa remains to the east of the flood area, and the most favorable dynamics in the composite lie in the confluent zone near the flood location at both 850 hPa and 925 hPa. There is

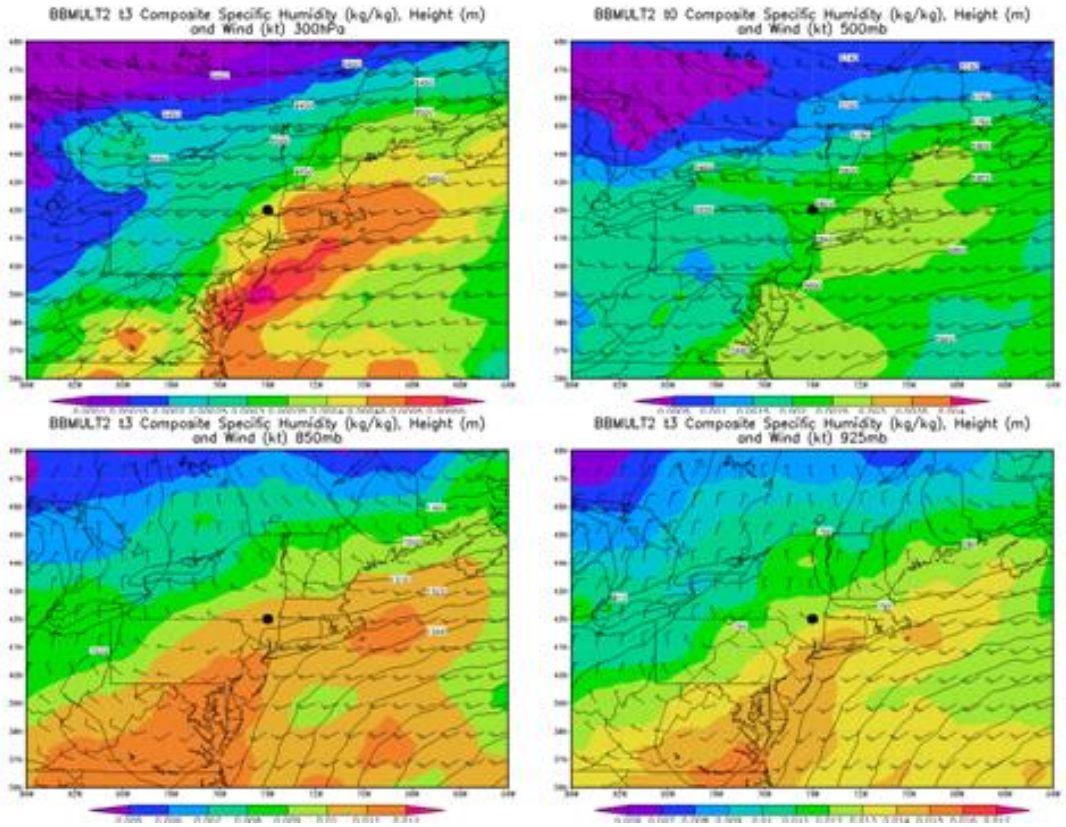

Figure 5.15 Composites of moisture (shaded, kg/kg), geopotential height (contours, m), and winds (barbs, kt) at 4 levels ((a): 300 hPa, (b) 500 hPa, (c) 850 hPa, and (d) 925 hPa) for BBMULT2 events.

significant vertical wind shear, especially in the middle to upper troposphere, with 60 kt winds at 300 hPa, 25 kt winds at 500 hPa, and winds of only 5 kt at 850 and 925 hPa. This is also the only event type to display backing - counterclockwise turning of the wind - with height through the depth of the troposphere, as the wind direction shifts from northwesterly at 925 hPa to southwesterly at 300 hPa. The light surface winds and moderate mid-level winds may correspond with slow storm motion and may help to create an environment that favors the formation and development of back-building cells, despite the unfavorable backing profile.

The high precipitation BB cases (Figure 5.16(a)) have much more moisture

upwind of the flood location than the low precipitation BB cases. Both the high and low precipitation BB cases have a local moisture maximum just south of the flood area. The flood area is co-located with a ridge axis at 700 hPa in the high precipitation cases, while in the low precipitation cases, the flood area is just downwind of a trough axis. Lower level winds are quite light (<8 kt) over a large area for both the high and low precipitation BB cases. Both high and low precipitation composites display minimal veering over and upwind of the flood area, with little speed shear (approximately 5 kt of shear in low precipitation events and approximately 10 kt of

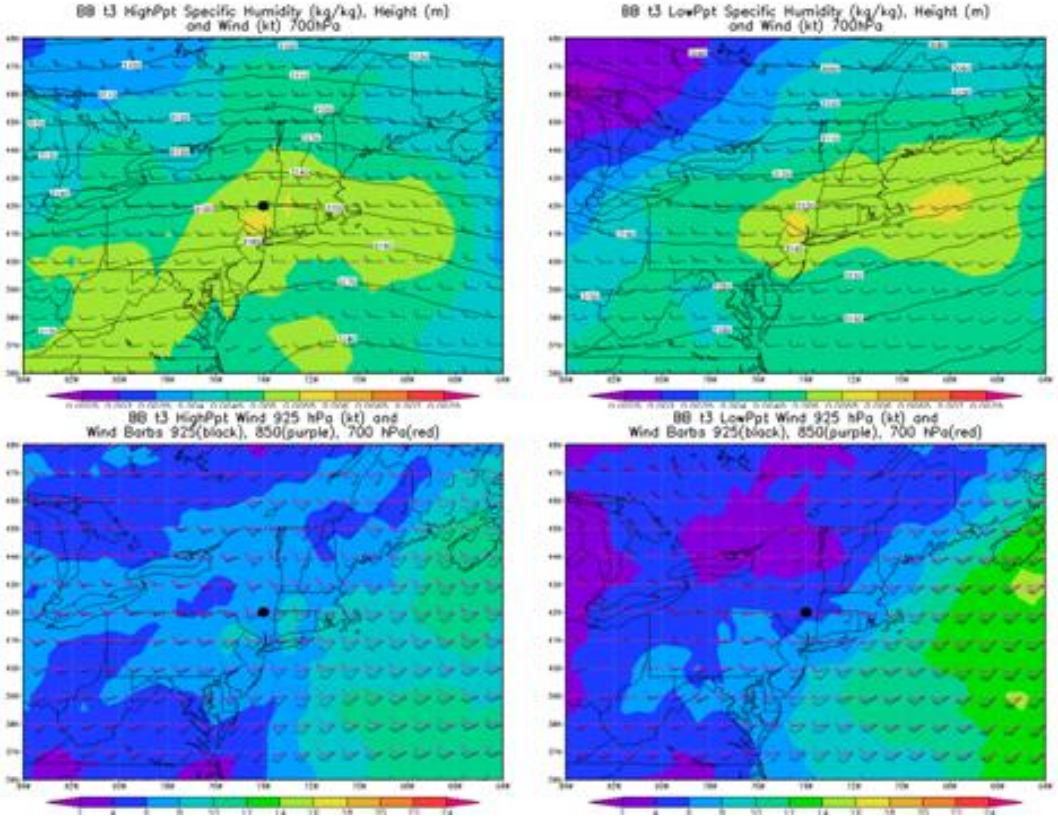

Figure 5.16 High precipitation (a) and low precipitation (b) specific humidity (shaded, kg/kg), geopotential height (contours, m), and winds (barbs, kt) at 700 hPa; high precipitation (c) and low precipitation (d) wind speed (shaded, kt) at 925 hPa and wind vectors (barbs, kt) at three levels: 925 hPa (black barbs), 850 hPa (dark purple barbs), and 700 hPa (dark red barbs), for BB events.

shear in high precipitation events). It is perhaps a bit surprising that the winds are somewhat faster in the high precipitation events than in low precipitation events, as one might expect slower cell movement and, hence, slower environmental winds for events producing larger precipitation totals. However, in a backwards-propagating system, these fast winds are negated, as described below.

Corfidi et al. (1996) developed a technique for predicting the net movement of mesoscale convective systems. They defined cloud layer movement as the mean of the velocity vectors at 850 hPa, 700 hPa, 500 hPa, and 300 hPa. This vector represents the mean flow of the cloud layer, and it approximates the motion of established individual cells. After determining this mean cloud layer vector, a vector representing the inflowing low level jet was found. This inflow vector was determined to be best represented by the 850 hPa wind. When subtracted from the mean cloud layer, the low level jet (or 850 hPa wind) represents the net system propagation as a result of newly formed cells. For a back-building event, one would expect a very small resulting mesoscale-beta element (MBE) vector, as the propagation vector tends to be in the opposite direction of the mean cloud layer vector. Overall, it was found in this instance that there was very little difference in this MBE vector between the high and low precipitation cases, as the winds at 300 hPa and 500 hPa were similar in magnitude and direction. It appears that the most significant difference between BB events producing high precipitation totals and those producing more moderate precipitation totals (but still producing flash floods) is in the waveform in the vicinity of the flood area – high precipitation BB cases were found near a ridge (from 850 hPa to 300 hPa), while low precipitation BB cases were found near a trough (from 925 hPa, where the trough is positively tilted, to 300 hPa).

The high precipitation BBMERGE cases are located in an area of high

moisture at 700 hPa with favorable moisture advection (Figure 5.17(a)), while the low precipitation BBMERGE cases are located in an area of somewhat less moisture with similarly favorable moisture advection (Figure 5.17(b)). The two classes of events feature similar wind speeds, with the high precipitation BBMERGE events having a more southwesterly direction at 700 hPa owing to a short-wave trough located upwind of the flood area, while the low precipitation events had a more zonal flow in the absence of such a feature. This short-wave trough for the high precipitation events is likely indicative of the convective line that eventually intersected the back-building

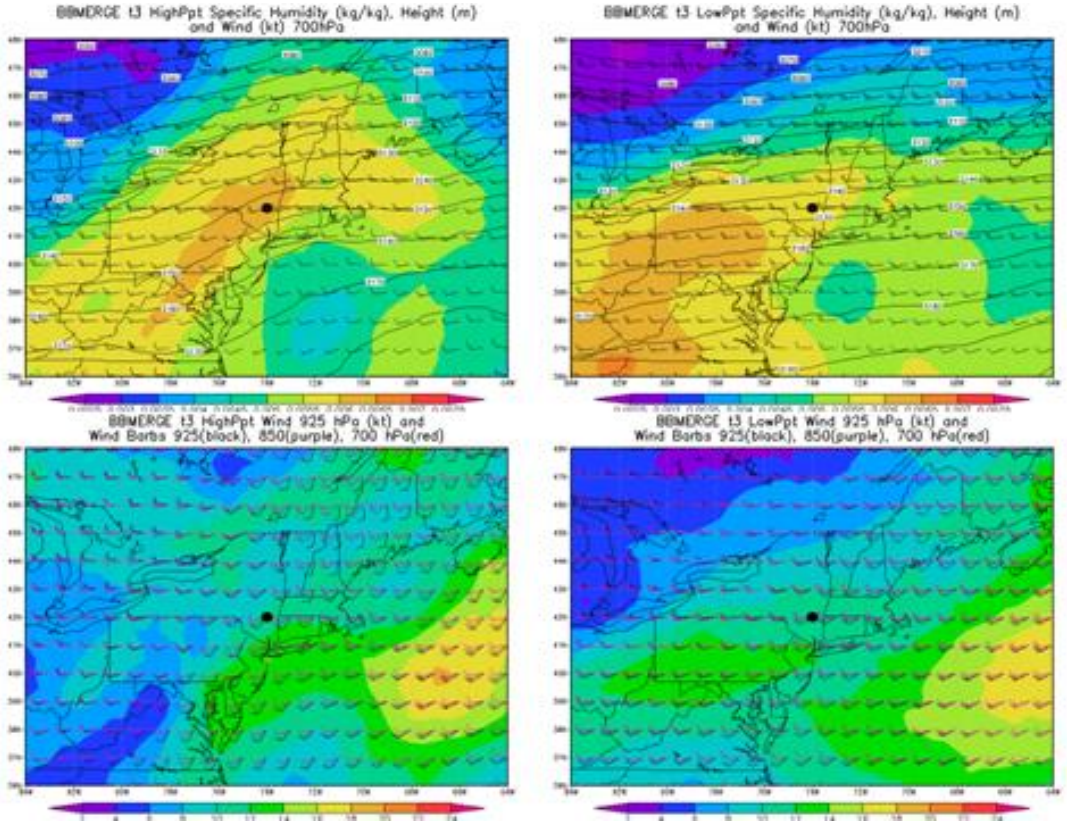

Figure 5.17 High precipitation (a) and low precipitation (b) specific humidity (shaded, kg/kg), geopotential height (contours, m), and winds (barbs, kt) at 700 hPa; high precipitation (c) and low precipitation (d) wind speed (shaded, kt) at 925 hPa and wind vectors (barbs, kt) at three levels: 925 hPa (black barbs), 850 hPa (dark purple barbs), and 700 hPa (dark red barbs), for BBMERGE events.

feature in the flood area. It is not surprising that such a feature is evident on the high precipitation composite, but it is a bit surprising that such a feature is altogether absent from the low precipitation composite, as one would expect some evidence of the merging convective line, which tended to be visible on radar well in advance of its merging with the back-building convection. Of course, the linear composites above in section 5.3 often offered little indication of the convective line, so perhaps this expectation for some indicator of the convective line in the environment is unfounded. In terms of the wind fields, the lower tropospheric trough for the high precipitation events leads to greater veering in the lower tropospheric winds from 925 hPa to 700 hPa, while the winds are more unidirectional with height for the low precipitation BBMERGE events. This is indicative of the lower-level trough that is present in the high precipitation composite, but not in the low precipitation composite.

For the high and low precipitation BBMULT1 cases (Figure 5.18), the height and wind fields at 700 hPa are similar, with a trough to the west and a ridge to the east. The center of the low to the northwest of the flood area and the center of the Bermuda high to the southeast of the flood area are approximately equidistant in the high precipitation composite. On the low precipitation composite, on the other hand, there is little indication of the low to the northwest, as this composite appears to be dominated by the Bermuda high. The moisture fields at 700 hPa, furthermore, are very different. There is ample moisture centered on the flood area with favorable advection in the high precipitation composite (Figure 5.18(a)), while the greatest moisture in the low precipitation composite is located far to the south in comparison. This low- to mid-level moisture difference appears to be the most significant difference between the high and low precipitation composites. The wind shear composites (Figures 5.18(c) and (d)) show a similar amount of wind shear over the flood area between 925 hPa and 700 hPa, but in the low precipitation composite, all of

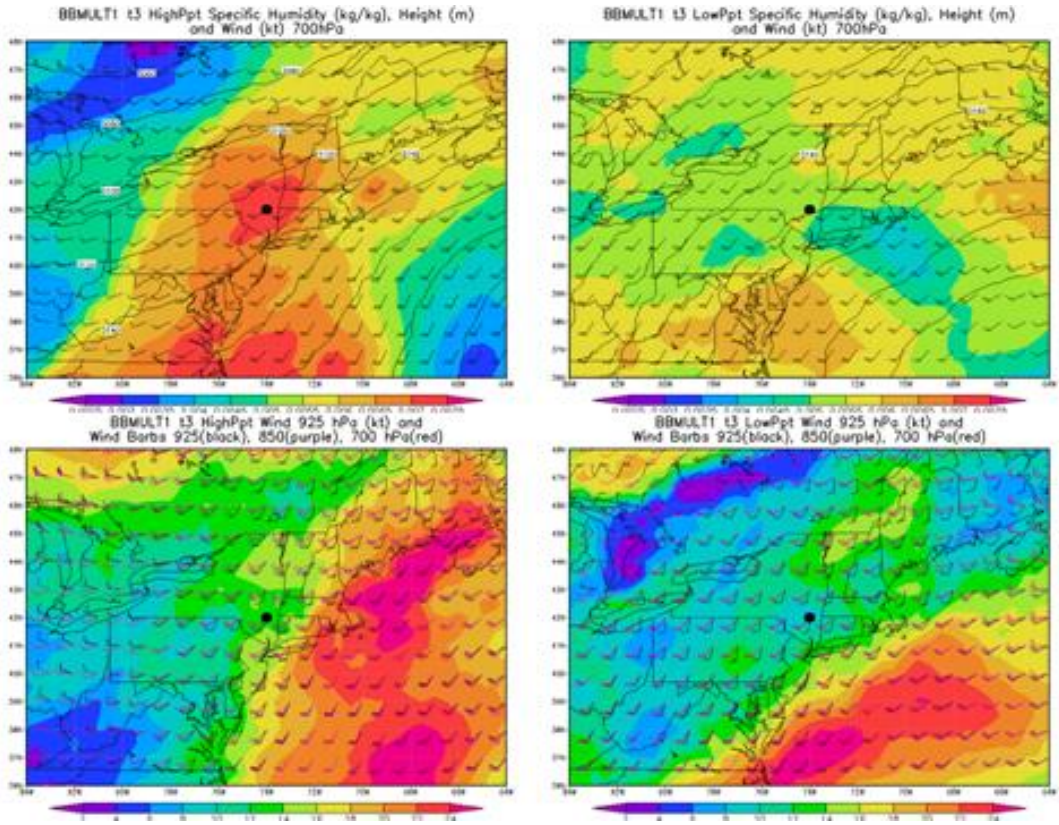

Figure 5.18 High precipitation (a) and low precipitation (b) specific humidity (shaded, kg/kg), geopotential height (contours, m), and winds (barbs, kt) at 700 hPa; high precipitation (c) and low precipitation (d) wind speed (shaded, kt) at 925 hPa and wind vectors (barbs, kt) at three levels: 925 hPa (black barbs), 850 hPa (dark purple barbs), and 700 hPa (dark red barbs), for BBMULT1 events.

this wind shear occurs between 925 hPa and 850 hPa, while in the high precipitation composite, this wind shear is evenly divided between the 925 hPa to 850 hPa layer and the 850 hPa to 700 hPa layer.

One question yet to be fully addressed in this section is how the back-building events differ from similar events that have been discussed in the literature. Figure 5.19, from Schumacher and Johnson (2005), shows a south-to-north cross-section of equivalent potential temperature (solid contours), relative humidity (dashed contours),

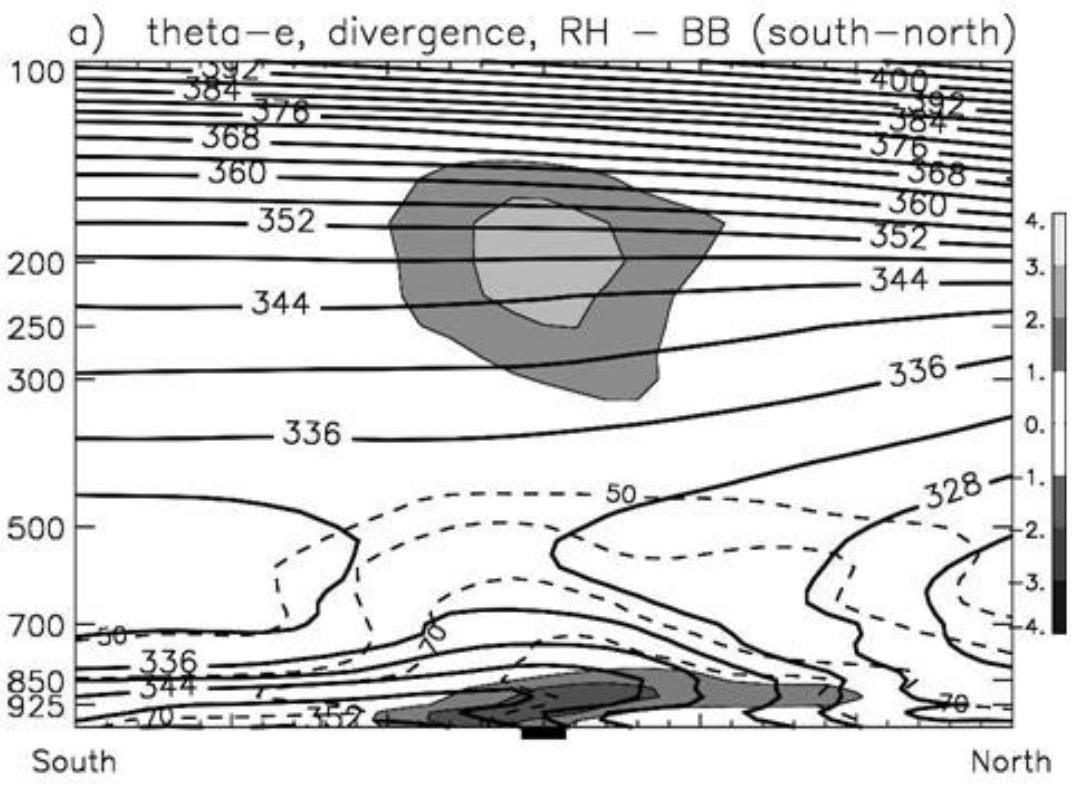

Figure 5.19 Equivalent potential temperature (solid contours), relative humidity (dashed contours), and divergence (shaded) for back-building events across the central United States. From Schumacher and Johnson (2005). The black square represents the area receiving the heaviest precipitation.

and divergence (shaded) for the BB events in their study. The cross section shows a large area of upper level divergence above the area receiving heavy precipitation. There is an inversion of the equivalent potential temperature and a tilted surface in the equivalent potential temperature field from south to north over the area of heaviest precipitation. Co-located with this region is an area of low-level convergence, with an upward tilt from south to north of its own. The relative humidity field is at its maximum directly above the high precipitation area. Overall, this figure represents an ideal scenario for sustained heavy precipitation, with ample low level moisture, a low level supply of additional moisture via the plume of equivalent potential temperature,

and dynamical support via mass continuity (upper level divergence and lower level convergence).

A similar figure is displayed for the BB and BBMERGE events in the current study (Figure 5.20), from 1000 hPa to 700 hPa. In the BB composite, at both the time three to six hours before flooding was reported (Figure 5.20(a)) and at the time from three hours before up until the time that flooding was reported (Figure 5.20(c)), there was convergence to the south of the flood area, coincident with a dome of higher equivalent potential temperature air. There was also a maximum in the relative humidity field overhead, extending from approximately 925 hPa up to approximately

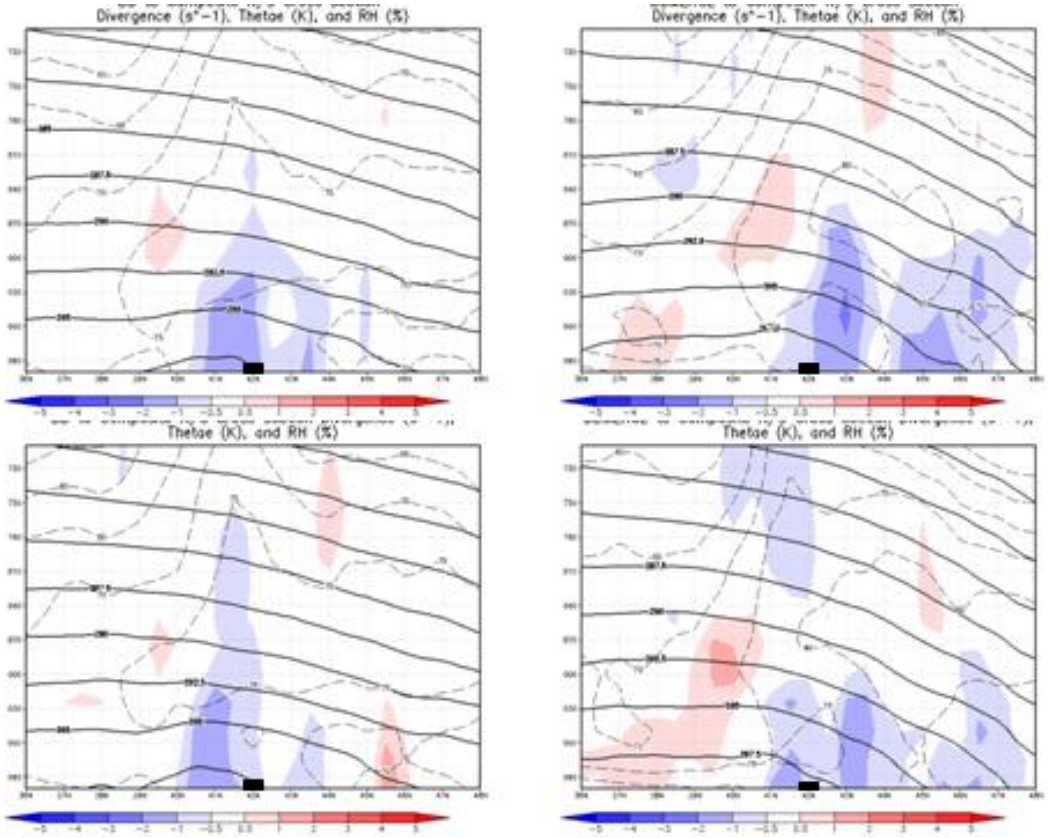

Figure 5.20 Equivalent potential temperature (solid contours, K), relative humidity (dashed contours, %), and divergence (shaded, $\times 10^5$ s^{-1}) for BB (left) and BBMERGE (right) at the time from 3-6 hours before the event (top) and 0-3 hours before the event (bottom) events across the northeastern United States, 2003-2007.

750 hPa. While there is not a true inversion of equivalent potential temperature, and there is likewise not a slope to the convergence, this is a similar configuration of these fields as in the Schumacher and Johnson (2005) figure. Like the BB composites, the BBMERGE composites show many of these features. During the time period from six to three hours before the flooding was reported (Figure 5.20(b)), the convergence is centered to the north of the flood area. By the time period three hours later, from three hours before and up until the flood report time (Figure 5.20(d)), the convergence is centered to the south of the flood area, as in the BB composite. Much like in the BB composite, there is a near-surface intrusion of air with a relatively high equivalent potential temperature from the south to just north of the flood area, and there is a region of high relative humidity air (≥75%) from approximately 925 hPa to 750 hPa over the flood area. Both cross sections, when extended to 250 hPa (not shown), display upper level divergence. The area of upper level divergence for the BBMERGE events is larger and approximately twice as strong in the BBMERGE cross section as in the BB cross section. Although there are some differences in the details, both the BB and BBMERGE cross sections display similar features to those recognized in these types of events in the literature. The biggest difference between the back-building events in this study and those reported by Schumacher and Johnson (2005) is the lack of a low-level jet in the events in this study.

5.5 Analysis of Scattered Events

Unlike the previous groups of event types, the scattered events comprised a completely new set of types of convection that can produce heavy precipitation that leads to flash flooding. Except for the SCTMERGE events, which consist of the

merging of two broad areas of precipitation, the relative disorganization of these types of events as it appears on radar suggests that the environmental conditions may imply little more than a tendency for these events to occur in the warm sector of an extratropical cyclone. One would further expect the wind fields to reflect the relative motion of the individual storm cells and MCSs in the SCTTR and SCTRAND event composites. This section seeks to examine composite maps of the scattered events to determine their environmental properties.

The SCTTR composites display mean conditions of what one would typically expect for the warm sector of an extratropical cyclone (Fig. 5.21). At middle to upper levels, the flood area is located near the inflection point between a long-wave trough

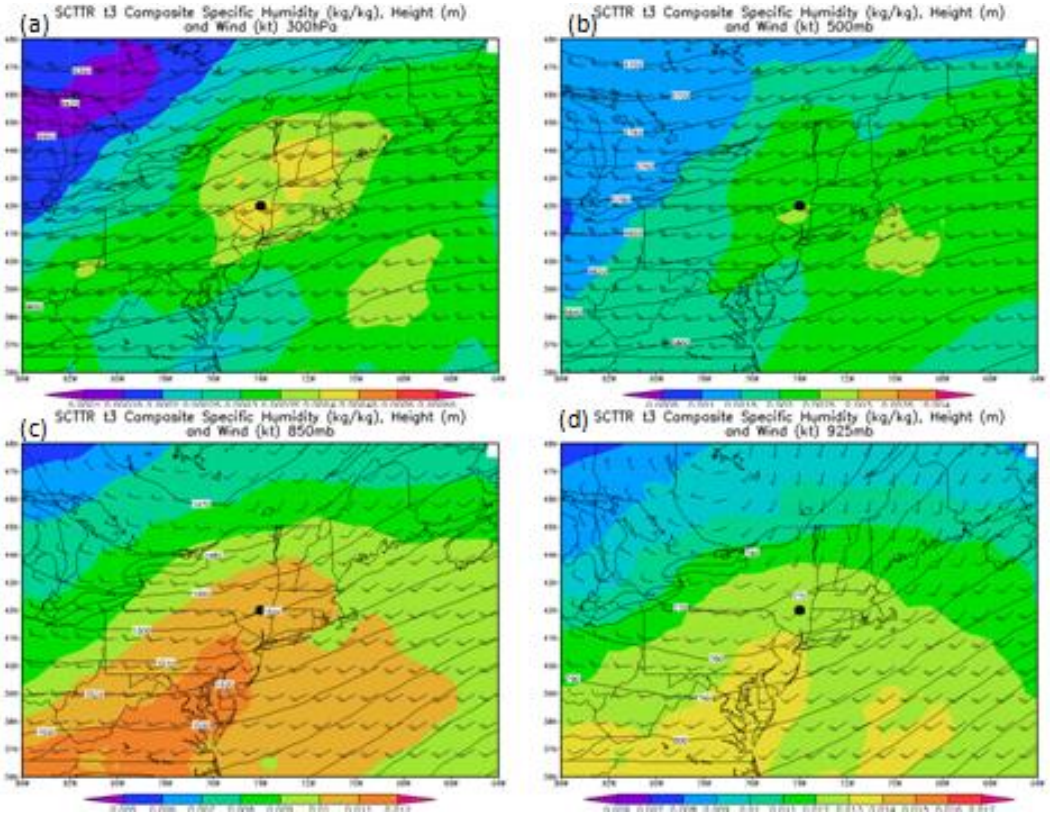

Figure 5.21 Composites of moisture (shaded, kg/kg), geopotential height (contours, m), and winds (barbs, kt) at 4 levels ((a): 300 hPa, (b) 500 hPa, (c) 850 hPa, and (d) 925 hPa) for SCTTR events.

to the west and a long-wave ridge to the east. This has been previously described to be dynamically favorable for uplift. The flood area is in a relatively large local moisture maximum at 300 hPa. In the 500 hPa composite, the only signal to represent where the flood occurred is a very small, and very weak, moisture maximum near the flood area; the isoheights are stretching in a long wave from west-southwest to north-northeast. At 850 hPa, however, the moisture field is much more favorable for the formation of flash-flood producing precipitation, with a broad area of high moisture content stretching from the southwest corner of the composite toward the flood area. Accompanied by moderate southwesterly winds of approximately 20 kt, this is the level at which the moisture profile was most favorable for heavy precipitation. At 925 hPa, a moist tongue extends from south to north toward the flood area. There appears to be low-level convergence toward the flood area, as the winds to the south are approximately 15 kt, while over the flood area the winds are 10 kt. Farther to the north, the winds slow further to about 5 kt. This low-level speed convergence, coupled with the upper-level divergence provided by the large wave aloft, provides a favorable dynamic environment for the development and sustenance of heavy precipitation.

Figure 5.22 shows the difference between the high precipitation and low precipitation SCTTR events. It is clear that while the low precipitation events have ample moisture at 700 hPa, there is an even greater low-level moisture supply for the high precipitation events. In both the high precipitation and low precipitation composites, the flood area sits between a trough to the west and a ridge to the east at 700 hPa, but this pattern is amplified in the high precipitation composite, resulting in somewhat greater wind speeds. There is little low-level directional wind shear in both composites, and almost no wind shift within the 850 hPa to 700 hPa layer. There are subtle differences between the composites: the high precipitation composite features

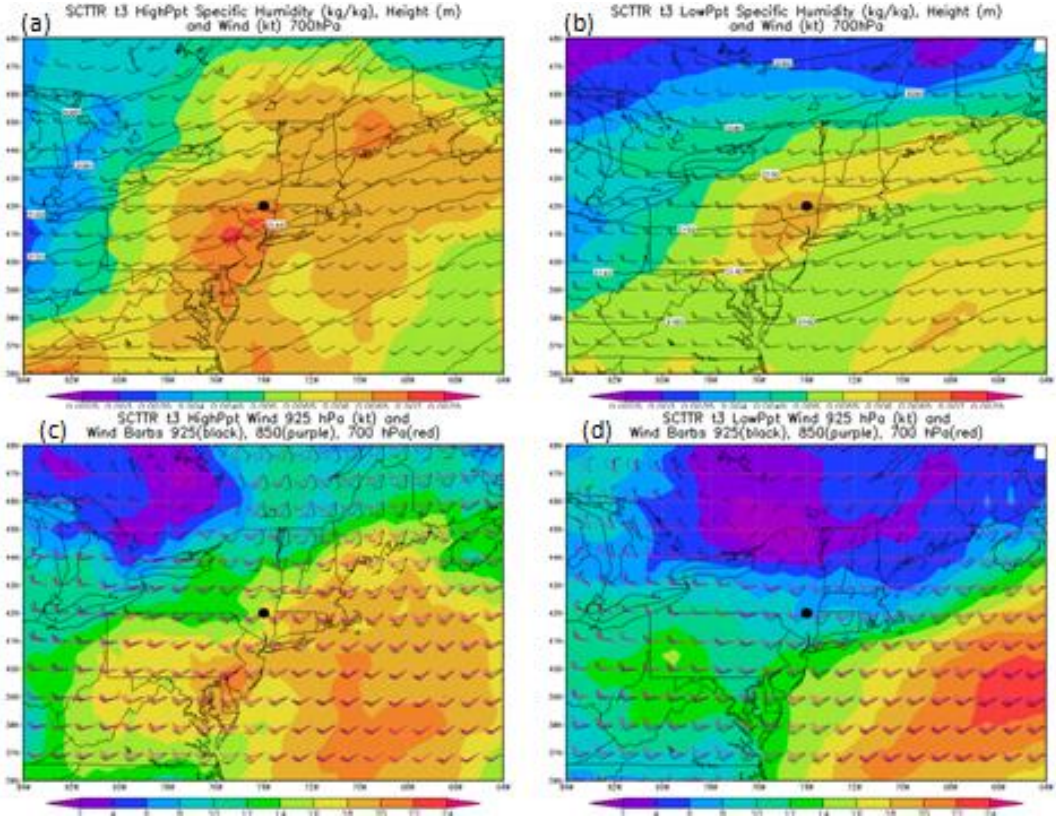

Figure 5.22 High precipitation (a) and low precipitation (b) specific humidity (shaded, kg/kg), geopotential height (contours, m), and winds (barbs, kt) at 700 hPa; high precipitation (c) and low precipitation (d) wind speed (shaded, kt) at 925 hPa and wind vectors (barbs, kt) at three levels: 925 hPa (black barbs), 850 hPa (dark purple barbs), and 700 hPa (dark red barbs), for SCTTR events.

southwesterly winds across the majority of the composite, while the winds in the low precipitation composite are westerly to the west of the flood area. Furthermore, the high precipitation composite features little speed shear in addition to little directional shear in the vicinity and upwind of the flood area, with wind speeds consistently between 15 and 20 kt. The low precipitation composite, in comparison, features 5 kt winds over the flood location at 925 hPa and 20 kt winds at 700 hPa; this trend is not consistent across the composite, however, as the low-level winds tend to be 15 to 20 kt

across the majority of the domain. The seemingly out-of-place light winds near the flood location seems to be a marker of SCTTR events which can cause flash floods, but not necessarily the most devastating floods of this type.

In contrast to the SCTTR events, the SCTRAND events were typically events with slow-moving storm cells, seemingly drifting in random directions. One might expect to see little dynamic influence present in these events along with light winds and lateral directional wind shear. Figure 5.23 shows that flood area is located just downwind of a short-wave trough at 300 hPa, making it favorable for the lifting of moisture at lower levels. There is a slight moisture maximum over the flood area, but the 300 hPa level is drier than in the SCTTR composite. As expected, the winds are

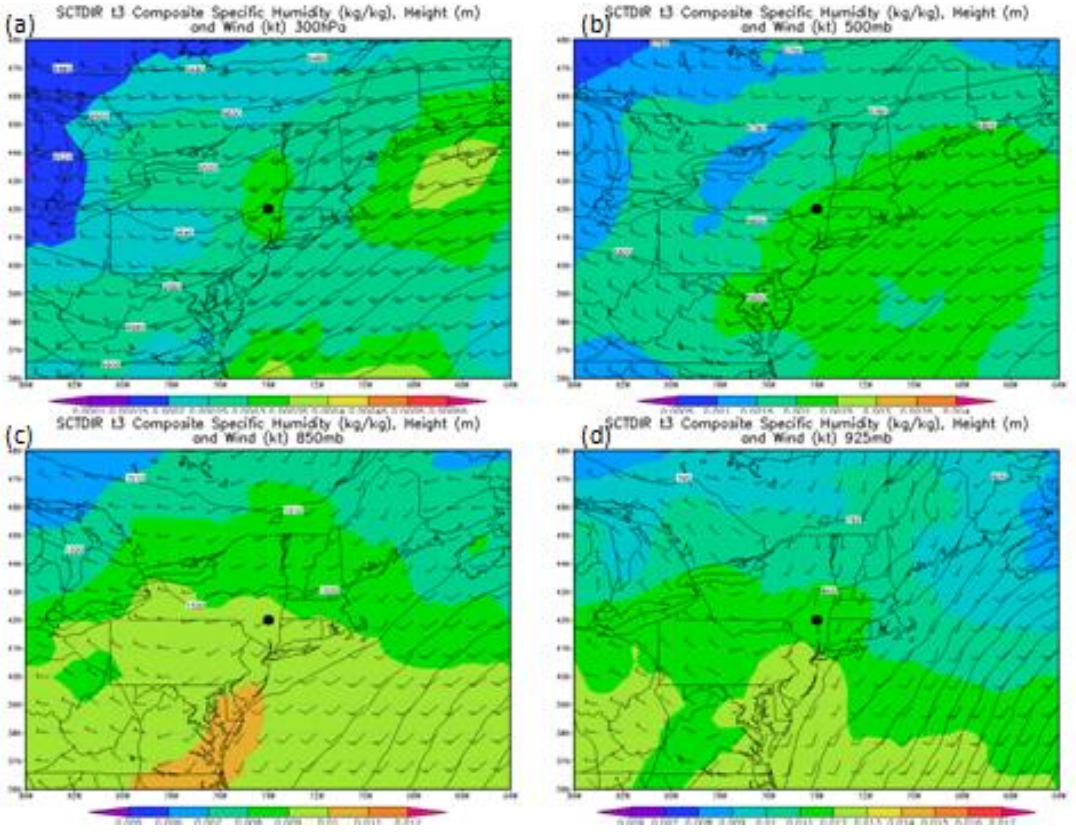

Figure 5.23 Composites of moisture (shaded, kg/kg), geopotential height (contours, m), and winds (barbs, kt) at 4 levels ((a): 300 hPa, (b) 500 hPa, (c) 850 hPa, and (d) 925 hPa) for SCTRAND events.

light, especially to the west and northwest of the flood area, where the winds only reach 20 kt. Directly over the flood area, the winds are approximately 25 kt, while to the east and southeast, the winds increase up to about 35 kt. These winds, relatively light for the 300 hPa level, are indicative of the winds at lower levels, as well. At 500 hPa, 850 hPa, and 925 hPa, the winds remain light, and the moisture remains relatively low. A weak short-wave trough is apparent in all four composites, but the dynamical effects of these short-wave troughs are weak as a consequence of the light winds. As one might expect, these events that feature small convective cells moving in seemingly random directions feature moderate levels of moisture and little in the lower, middle, or upper troposphere to direct their motion. Although the wind direction shifts in conjunction with the short wave trough, there is no clearly delineated wind shift line, suggesting that the seemingly random directions of the individual storm cells may be directed by the short wave trough. The short wave trough at 925 hPa, in particular, offers a very rapid change in the direction of these light near-surface winds over a short distance that might make nearby cells appear to be moving randomly.

Figure 5.24 shows that for both the high precipitation and low precipitation composites of the SCTRAND events, the area of most ample low- to mid-level moisture is not directly upwind of the flood area. In the paragraph above, it was shown that the moisture throughout most of the troposphere was lacking compared to the composite maps of the other event types; this displacement of the maximum moisture away from the flood area may be an indication as to why, especially in the low precipitation composite, where the moisture maximum at 700 hPa is well off-shore. The dynamics also appear to play a role in differentiating between high precipitation and low precipitation events, as the low precipitation events feature zonal flow to the north and northwest of the flood location, while in this region of the high

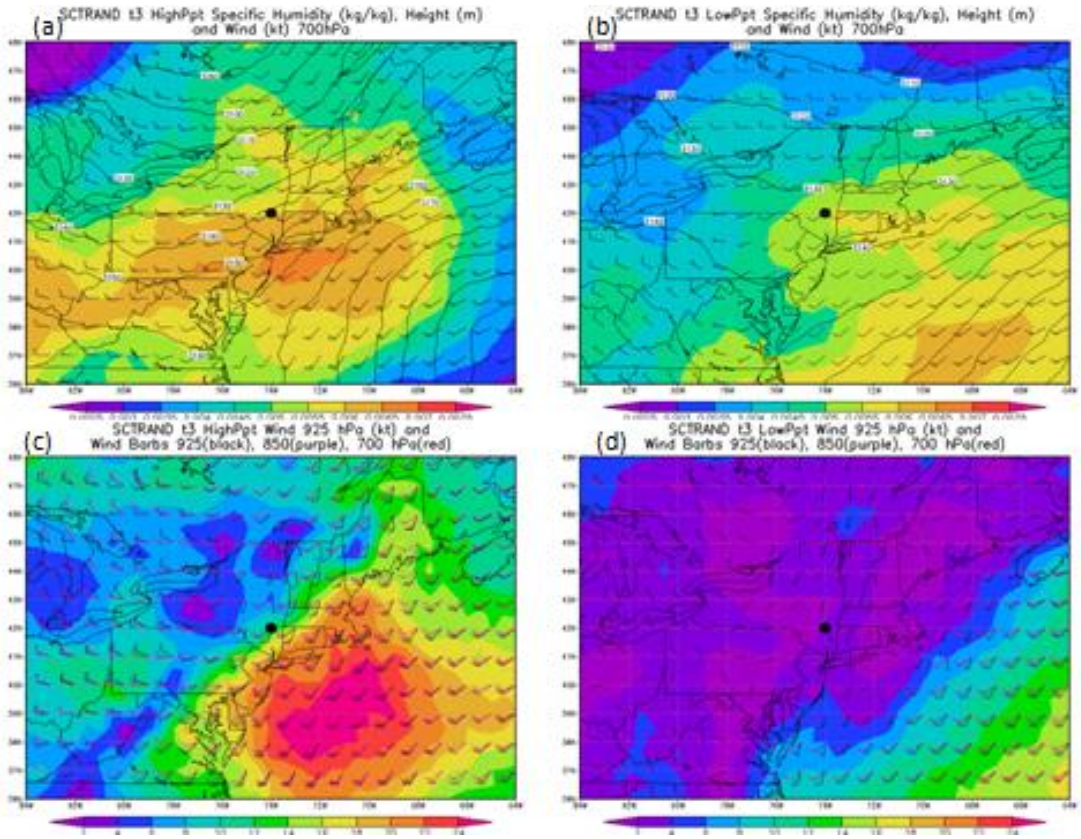

Figure 5.24 High precipitation (a) and low precipitation (b) specific humidity (shaded, kg/kg), geopotential height (contours, m), and winds (barbs, kt) at 700 hPa; high precipitation (c) and low precipitation (d) wind speed (shaded, kt) at 925 hPa and wind vectors (barbs, kt) at three levels: 925 hPa (black barbs), 850 hPa (dark purple barbs), and 700 hPa (dark red barbs), for SCTRAND events.

precipitation composite, a trough dominates. This trough causes a faster southwesterly flow at 700 hPa of about 15 kt over the flood area (with winds of approximately 20 kt nearby), as opposed to the approximately 10 kt winds at 700 hPa in the low precipitation composite. With such strong low- to mid-level dynamics, one might wonder why the convective storms were observed to move randomly. The high precipitation wind shear composite (Figure 5.24(c)) appears to have the answer. Here, the winds at 925 hPa are southerly to southwesterly, as opposed to the stronger west-

southwesterly winds near and upwind of the flood area. To explain the differential motion of different convective storms, one might suppose that some storms are rooted in the boundary layer with the more southerly winds, while others are rooted above the boundary layer, where the winds are more westerly. A similar hypothesis would explain the low precipitation events, with their light and variable winds at 925 hPa and stronger southwesterly to westerly winds aloft. Why are the events with stronger winds also the events that produce higher rainfall totals? This is undetermined, but perhaps it is because of the winds themselves, which may help to generate more intense convection, including greater rainfall rates, larger storms, longer-lived storms, or some combination of these. Even though high precipitation storms may move faster than low precipitation storms, they may produce more precipitation in a shorter time – which may also lead to more intense flash flooding via more intense runoff in response to the faster rainfall rates.

One might expect that much like the SCTRAND composites (Figure 5.23 above), the SCTSM composites (Figure 5.25) would feature a relatively benign synoptic and mesoscale environment. It turns out, though, that in the 300 hPa composite, the flood area lies near the axis of a positively-tilted (southwest-to-northwest) short-wave trough. It is a weak trough, as the winds are light over the flood area at only 15 knots. The composite also has an extremely low moisture content at 300 hPa compared to all of the other event types. Accompanying the very large southwest-to-northeast moisture gradient is a large gradient in wind speed to greater than 50 kt not far to the east of the flood area. The flood location lies in the narrow band of low winds and tight moisture gradient, just to the east of the trough axis. In sharp contrast to this amplified picture in the upper troposphere, at middle and lower levels the environment in much calmer, with winds ranging from 10 to 15 kt and veering with height from the south-southwest (925 hPa) to the southwest (850 hPa), to

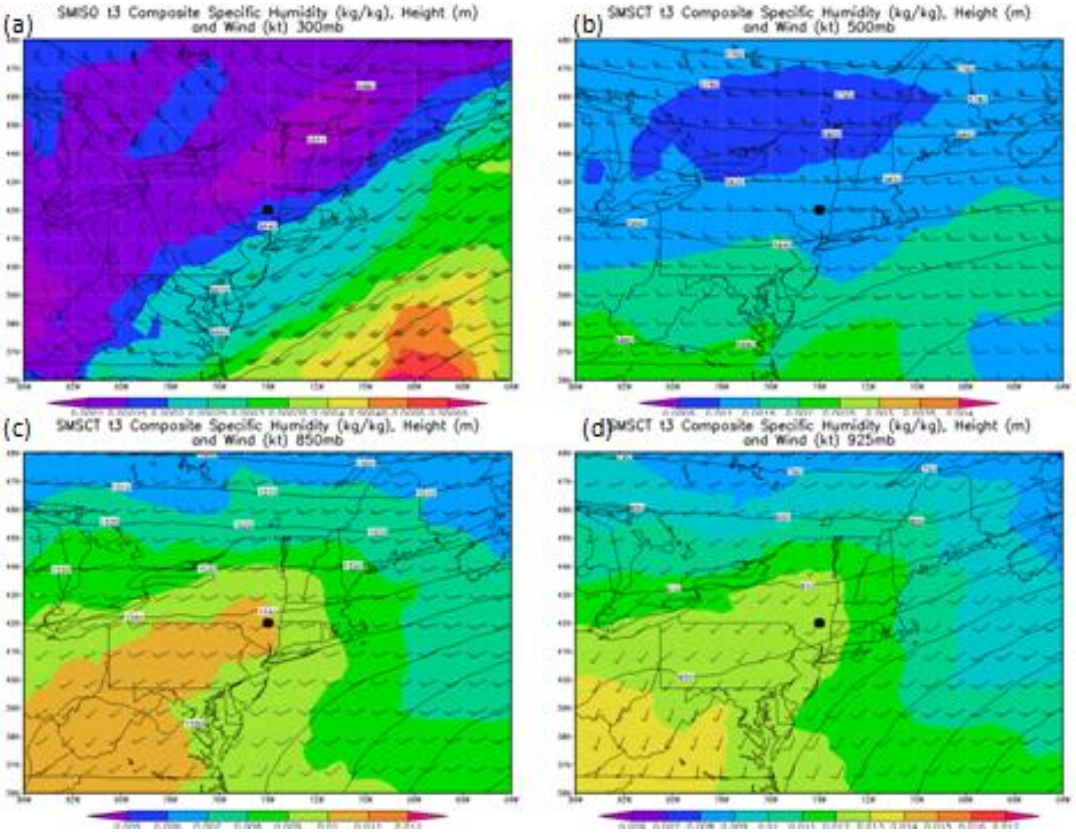

Figure 5.25 Composites of moisture (shaded, kg/kg), geopotential height (contours, m), and winds (barbs, kt) at 4 levels ((a): 300 hPa, (b) 500 hPa, (c) 850 hPa, and (d) 925 hPa) for SCTSM events.

the west (500 hPa). The moisture content is still quite low at 500 hPa, but becomes more favorable than in the SCTRAND composite at lower levels (850 hPa and 925 hPa). Unlike the warm sector scenario in the SCTTR composite, the SCTSM composite seems to reflect a typical, benign summer day across the Northeast, and other than the positively tilted trough aloft and the weak confluent zone in the lower troposphere, there is little in the composites to pinpoint the flood location.

Without a large scale dynamical feature present in the overall composite, what is it that makes some SCTSM events more extreme than others? The high precipitation and low precipitation SCTSM composites (Figure 5.26) suggest that

wind speed and low- to mid-level moisture supply separate the more intense scattered thunderstorms from the less intense ones. The high precipitation composite boasts a greater moisture supply, which can be tracked back through Pennsylvania, Ohio, West Virginia, and southward through western Virginia, Kentucky and Tennessee. Such a trajectory would seem to favor locations in the southern and eastern portions of the study area, especially in Pennsylvania. Indeed, three of the four high precipitation SMSCT events were in western Pennsylvania. Regardless of whether the location is

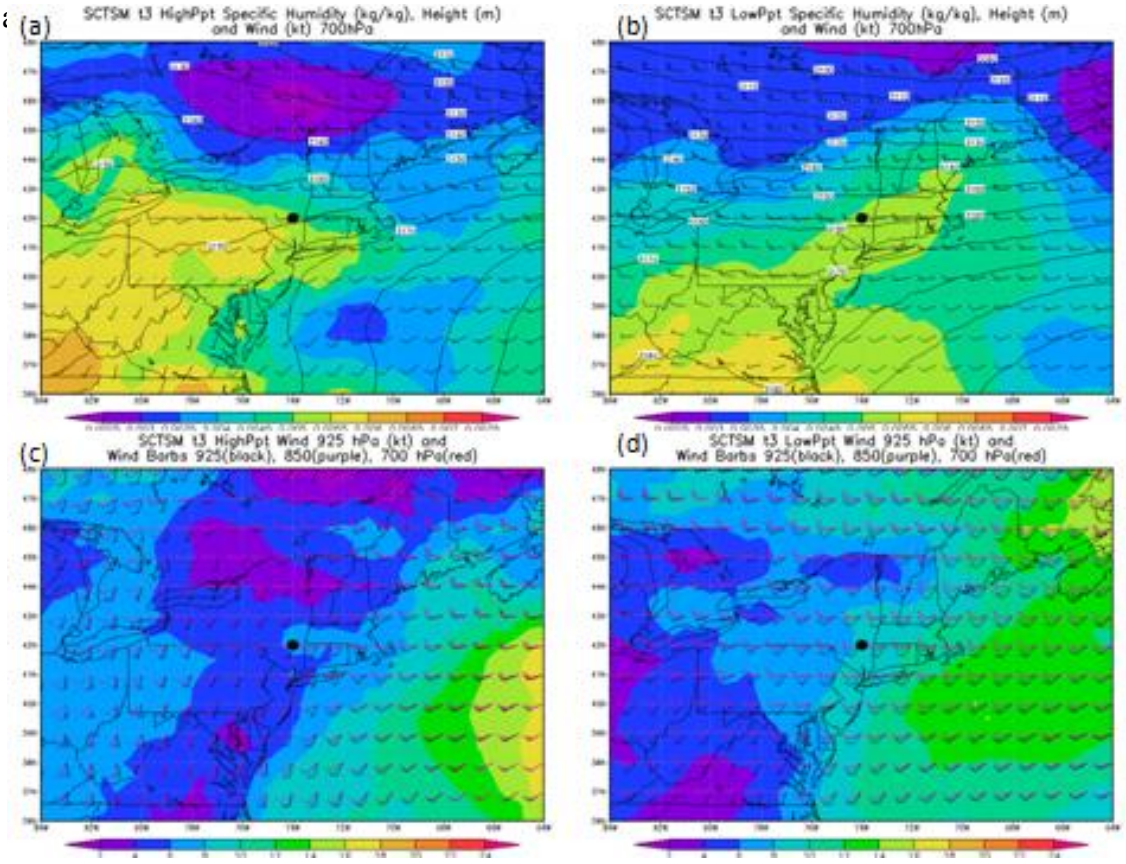

Figure 5.26 High precipitation (a) and low precipitation (b) specific humidity (shaded, kg/kg), geopotential height (contours, m), and winds (barbs, kt) at 700 hPa; high precipitation (c) and low precipitation (d) wind speed (shaded, kt) at 925 hPa and wind vectors (barbs, kt) at three levels: 925 hPa (black barbs), 850 hPa (dark purple barbs), and 700 hPa (dark red barbs), for SCTSM events.

more closely related to the cause or the effect, a stark contrast to this moisture-laden trajectory is present for the composite of the low precipitation cases, with westerly winds and negative moisture advection toward the flood area. Likewise, the wind speeds near and upwind of the flood area for the high precipitation composite are of those for the low precipitation composite (20 kt). These slower wind speeds for the high precipitation SMSCT events facilitate slower storm movement and thus prolong the duration of rainfall over each basin that the storm traverses, increasing the basin-average rainfall and, thus, the likelihood of flooding. The wind shear composites (Figure 5.26(c) and Figure 5.26(d)) show more veering, especially in the 850 hPa to 700 hPa layer, for the high precipitation composite as compared to the low precipitation composite, while the shear is approximately equal in the 925 hPa to 850 hPa layer and the 850 hPa to 700 hPa layer in the vicinity of the flood area. The high precipitation composite's thicker layer of the lower troposphere with unidirectional winds may help the high precipitation convective storms to ingest a more plentiful supply of moisture through greater depth with the wind profile of the high precipitation composites, deriving lower level (surface to 850 hPa) moisture from the south and mid-level (700 hPa) moisture from the southwest via the circuitous path described above.

In contrast to the very benign conditions that prevailed for the SCTSM events, the 300 hPa and 500 hPa composites for the SCTMERGE events feature a deep trough coupled with an amplified ridge, with the area of highest moisture located near the inflection point, just upwind of the flood area (Fig. 5.27). The 500 hPa features are shifted slightly to the east of the features at 300 hPa. The broad, high amplitude couplet of long-wave trough and ridge through the middle and upper troposphere is indicative of one of the broad swaths of rain that eventually merges with another to form a single, coherent feature. The amplified wave in the 300 hPa composite is

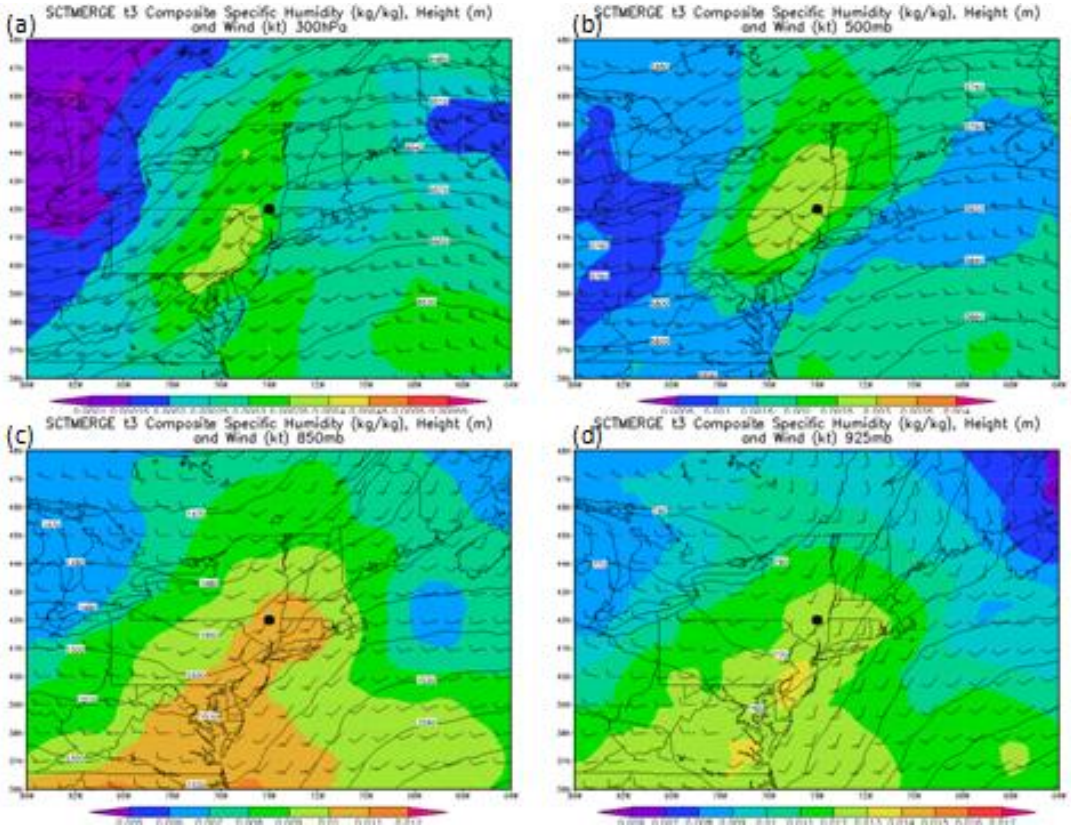

Figure 5.27 Composites of moisture (shaded, kg/kg), geopotential height (contours, m), and winds (barbs, kt) at 4 levels ((a): 300 hPa, (b) 500 hPa, (c) 850 hPa, and (d) 925 hPa) for SCTMERGE events.

reminiscent of the large amplitude waves that were present in the SYN and LM scale composites, much as the broad swaths of rain present for the LM and SYN events. What seems to separate these SCTMERGE events from the SYN and LM composites discussed above in section 5.2 is the lower levels, especially at 925 hPa, in the SCTMERGE composite (Figure 5.27(d)). The 925 hPa moisture is much less than in the SYN and LM composites. At lower levels, there is also a negatively-tilted (northwest-to-southeast) trough centered just to the west of the flood area. Though such features appeared in the LM and SYN composites, the high amplitude of this feature down to low levels in the SCTMERGE composite sets this scenario apart.

Indeed, by looking at the 925 hPa composite (and, to a lesser extent, the 850 hPa composite), one can visualize the prototypical SCTMERGE event. To the south of the flood location, the winds are southerly (southwesterly in the 850 hPa composite); one can visualize a broad swath of rain in this area being advected from south to north (or southwest to northeast if the steering level is 850 hPa) toward the flood area. To the west of the flood location, the winds are westerly; one can visualize a broad swath of rain in this area being advected from west to east toward the flood area, where it would merge with the other swath of rain from the south. The merged precipitation entity would then proceed toward the north (following the 925 hPa wind field) or, as it is more often observed to do, proceed toward the northeast (following the 850 hPa wind field).

5.6 Summary

For the scale events, the mid-level moisture was found to be significant at separating the event types by scale from large (relatively high moisture) to small (relatively low moisture), but low-level moisture was not effective at separating these event types. Like the moisture aloft, the wavelength was found to separate between the four scales of the events, with no waves but, rather, a diffluent pattern present for SMISO events; a long wavelength ridge present for MM events; a cutoff low or short wave present for LM events; and a long wavelength present in the SYN composite map. Although all four types of the scale events displayed features that were favorable for the formation and sustenance of heavy rainfall, the LM high precipitation events displayed the best combination of lower tropospheric and upper tropospheric dynamical elements which typify a textbook example of a flash-flood producing heavy rain event.

Among the linear events, the event type found to be associated with the lowest precipitation totals was found to occur when the atmospheric conditions were the most favorable for heavy rainfall, according to the theory presented in the literature. The trailing stratiform composites revealed ample moisture, with the flood area just downwind of the intersection between the maximum in mid-level moisture and the inflection point between long-wave trough to west and long-wave ridge to east. In contrast, the TLAS events, found to generate the highest precipitation totals of the linear event types, had less favorable composite figures than the TS composites. They were also found not to match the composite for TLAS events presented by Schumacher and Johnson (2005), as they were missing a southerly (or any) low level jet. This may be partly due to the variety of orientations observed for the training lines of convection in the northeastern events in this study. The PS events were found to resemble the TLAS events more than the TS events, in that they featured weaker dynamics, less moisture at all levels, and slower wind speeds at low levels than in the TS and TLAS composites. Like the PS events reported in Parker and Johnson (2000), they were found to have winds, especially at middle to upper levels, that were parallel to the orientation of the convection line; however, these winds were weaker than in Parker and Johnson's study.

The back-building composites in this study were generally found to have similar properties to the back-building events presented in Schumacher and Johnson (2005), but their composites of back-building events featured a southerly low-level jet into the area of heaviest precipitation, while a low-level jet was not apparent in the composites of back-building events in this study. The BB and BBMERGE events were found to have relatively low moisture throughout the troposphere – though a later cross-section found the relative humidity to be greater than 75% for much of the lower troposphere in the vicinity of the flood location. The BBMERGE events were further

found to display a shortwave trough at 925 hPa, which was found to be present for the high precipitation BBMERGE events but not for the low precipitation BBMERGE events; this trough is thought to indicate the approximate position of the merging convective line. In contrast, the BBMULT composites, likely because of their much smaller sample sizes, showed noteworthy dynamical features. The BBMULT1 events found the flood area situated in a convergence zone indicated by the wind speed at 850 hPa, while the BBMULT2 events featured a confluent zone near flood area at 850 hPa and 925 hPa. This composite displayed significant vertical speed shear, from a jet of about 60 kt at 300 hPa to light winds of approximately 5 kt near the surface; it was also the only event type to display backing through the depth of the troposphere.

As one would expect, because the scattered event types were described based upon the relative motion of the individual features, the event types tended to be distinguished by their wind field. The SCTTR events appear to typically form in the warm sector of an extratropical cyclone, as evidenced by the height fields. The SCTRAND events appear to be often dominated by a deep short wave trough from the upper troposphere to lower troposphere that provides differential winds over a relatively short distance that may lead to seemingly random motion; furthermore, the differential motion may also result from whether storms are rooted in or above the boundary layer, as there was significant veering of the winds between 925 hPa and 850 hPa. The SCTMERGE events reflected their motion, as well. Aloft, these events were dominated by a deep trough and an amplified ridge, while at lower levels, a shortwave trough with south-to-north flow on the east side of the trough and westerly flow to the west created the requisite conditions for the two broad areas of precipitation that will merge. Finally, the SCTSM events occurred under generally benign conditions with no dynamical features except a weak positively tilted trough at 300 hPa.

CHAPTER 6

CONCLUSION

This study has examined the appearance on radar and the environmental conditions associated with 187 flash flood events in the northeastern United States. Events were selected from the *Storm Data* online publication for the states of Pennsylvania, New York, New Jersey, Connecticut, Rhode Island, Massachusetts, Vermont, New Hampshire, and Maine. The radar data for these events were used to determine the organization of the precipitation for each event, and then further used to estimate the precipitation totals for each event. North American Regional Reanalysis data were used to determine the environmental conditions associated with each type of event. These pieces of information were used to attempt to answer several questions about flash flooding in the northeastern United States. This chapter will endeavor to answer these questions to the extent that the evidence collected in this study allows.

1. Are the predominant patterns of organization of flash-flood-producing precipitation different in the northeastern U.S. than in the central U.S.?

It appears that, although there has been found to be a high frequency of back-building events in both regions, there are significant differences in which non-back-building storm types most frequently affect each region. In the central U.S., there appears to be a much higher percentage of linear mesoscale events, while in the northeastern U.S., there appears to be a higher percentage of both long duration, large scale events and short duration, relatively disorganized mesoscale events Perhaps most significantly, those mesoscale events with a well-defined convective line and

accompanying stratiform precipitation (linear events) that have been a focus of the literature (e.g. Houze et al. (1990) and Schumacher and Johnson (2006)) were the least common of the four groups of events in the Northeast that were examined in this study.

2. Do those events whose radar signatures have been identified in the literature share similar environmental characteristics in the Northeast?

Yes, both the Northeast events in this study and the events that occur largely in other parts of the country that have been examined in other studies are similar in that considerable amounts of moisture (or high equivalent potential temperature) are in place, that an environment favorable for the advection of this moisture (or equivalent potential temperature) is in place, and that dynamical features such as upper-level divergence, lower-level convergence, or other mechanisms are in place to lift and condense the warm, moist input air. Other features associated with individual storm types were also found to be associated with these types of events in the Northeast; for example, the PS composite, like the example provided by Parker and Johnson (2000), also displays the line-parallel flow. The biggest difference between the composites of storm types that have been described in the literature and the same storm types in this study is the lack of a low level jet (previously defined to be 30 kt) in the composite maps for the TLAS and BB events in this study. This does not necessarily mean that this feature was always missing in individual cases or even in the composite maps, but this feature was washed out of the composites to appear to be weaker than in Schumacher and Johnson's (2005) paper.

3. Are there new classifications of flash flood events that haven't been identified for other regions, and, if so, do the new classifications of events have distinctive environmental characteristics as compared to the environmental characteristics of the types already identified in the literature?

Yes, there are new classifications of event types. These "new" types of events include several of the scale event types – large mesoscale (LM), medium mesoscale (MM), and small mesoscale isolated (SMISO), as well as all of the scattered event types – scattered training (SCTTR), scattered and moving in "random" directions (SCTRAND), scattered, merging features (SCTMERGE), and single, small mesoscale scattered (SCTSM) events. Additionally, while back-building events have been described in the literature and formally explained by Schumacher and Johnson (2005), this study has recognized three new types of back-building events, in addition to the back-building events that occur in isolation: merging back-building events (BBMERGE), back-building events that precede the passage of a convective line or other mesoscale feature (BBMULT1), and back-building events that follow the passage of a convective line or other mesoscale feature (BBMULT2).

Although this study has added many new types of convective organization to previous classification schemes, this is not to say that these features were not recognized. Instead, they were perhaps not considered to be as much of a flash flood threat in other regions as they seem to be in the Northeast. They may still cause flash flooding in other portions of the country, but either the frequency of their causing flash flooding or the precipitation amounts associated with these types of events did not meet the threshold criteria of the studies in other areas. Selection criteria may also be important – other studies may have either sought to exclusively identify mesoscale features, limiting the events to those exceeding a certain size or using rain gauge data

and selecting a minimum rainfall threshold that may not be exceeded very often by the smaller scale or more disorganized features discussed in this study.

Are the environments of these new event types distinct from those that had been previously recognized? The short answer is no. The composites of these new event types come in a variety of scenarios that have been previously described in the literature. For example, while the LM composites are distinct from the SYN composites, the individual cases show variety that suggests that these general trends should not be expected on a case-to-case basis. However, the general location of flash flooding relative to the middle to upper tropospheric waveform is similar for not just the LM and SYN cases but also for other cases with a trough to the west and a ridge to the east, suggesting a preferred location for flooding. This can be very useful to the forecaster: a preferred location near and just downwind of the inflection point between the upwind trough and the downwind ridge is the most likely area for flash flood-producing rainfall to occur.

While event types such as SCTMERGE and SCTRAND may not have been discussed in the literature, both are situations of which a forecaster is likely aware and has seen at least several times while on duty. The SCTMERGE events can easily be diagnosed early in their lifetime based on the large areas of precipitation and their relative movement as a scenario that is likely to produce a flash flood hazard. In contrast, the SCTRAND events present the opposite problem. The precipitation is widely scattered, and it can be difficult to forecast which areas have the greatest potential for flooding. In this regard, this scenario presents a recognize-and-react exercise, and real-time monitoring of precipitation becomes important. The danger in recognizing these events as a flash flood threat is that there may be a tendency to over-react and produce false alarms. This represents a broader split between the event types; some, such as the larger scale events (SYN and LM) and other events with large

areas of moderate to heavy rainfall (TLAS and SCTMERGE), leave little doubt that widespread flooding is likely to occur, but the pressing issue is to anticipate where the flooding will be most severe. (This is also true of the tropical events that were excluded from this study.) For the other events, such as the smaller scale events, most of the linear events, and the scattered events, the difficulty is in recognizing, first, whether a flood threat is likely, and second, where flooding is most likely to arise. Further work is needed to determine how often event days with this type of precipitation organization occur without producing observed flooding, a key component to addressing this problem.

4. How do events producing heavy or extreme precipitation compare to events of the same type that produce more moderate amounts of precipitation?

Generally, the composites for the heavier precipitation events displayed some combination of more favorable moisture content, more favorable moisture advection, or more favorable dynamics for the lifting of this moist air – the main "ingredients" for flash flooding cited by Doswell et al. (1996). However, one must use caution when using composites, as they may not reflect the variety in the individual cases, and they may not recognize the unique properties of the storm type. Examples of the latter include differences in low level wind shear, which in some cases was more unidirectional in the high precipitation composite than in the low precipitation composite. This scenario made the conditions for flash flooding seemingly more favorable because it coincided with the lower-level moisture and, therefore, improved the advection of low-level moisture toward the flood area. In other cases, though, the winds were unidirectional in the 925 hPa to 850 hPa layer, with significant veering from 850 hPa to 700 hPa. This scenario also made the conditions for flash flooding

seemingly more favorable because it placed the low-level inflow on the flank of the mid-level steering wind, creating the potential for an elongated area of precipitation with a persistent input of moisture below.

Furthermore, some of the event types that produced relatively less precipitation (such as the TS type) produced composites that appeared more favorable for the production of heavy rainfall than other event types that, in reality, produced larger estimated rainfall totals. Always, it is important for forecasters to monitor the precipitation itself (the radar) and not just the weather conditions (hourly observations and model forecast output) to remain alert to a potential flood threat.

In summary, this dissertation proposes a new classification system for warm-season rainfall events that have been found to produce flash flooding, based on the organization of the precipitation as exhibited on radar. This classification system consists of four general groups of events: back-building, linear, scale, and scattered, which each contain four sub-groups of events, for a total of 16 event types. These event types are found to be associated with different patterns of environmental conditions, all of which contain a reasonable supply of moisture, a relatively favorable wind pattern to advect that moisture, and relatively favorable dynamics, either at large scales or small scales, to lift and condense that moisture. Despite the differences in appearance and the regional differences in the Northeast, all event types combined these basic "ingredients" to produce heavy rainfall that led to flash flooding.

While this study has provided answers to the research questions posed in the first chapter of this dissertation, these answers are not definitive, and this research has at the same time produced more questions relating to the structure, frequency, and flash flood potential of different storm types that require still further research to

answer. To close this dissertation, some of these questions related to future work are posed below.

How often do these storm types occur, both in the Northeast and in other regions?

Are some of these storm types more often identified with long-lived heavy precipitation and flash flooding?

How can these storm types be defined and identified by an objective algorithm?

How are fatalities and flood damage related to these storm types? Are flood fatalities and damages more often associated with storm types that produce widespread rainfall, or are they more often a product more localized, high-intensity events?

For large basins and small basins, what storm types produce enough rainfall to generate one-year, two-year, five-year, ten-year, twenty-five year, and fifty-year floods?

In the BBMERGE events, is there a physical connection between the back-building MCS and the approaching convective line, perhaps a gravity wave or gust front, that reinforces the back-building MCS and sustains it until the merging of the two features? Can a computer model shed some light on the possible existence of this connection?

Can computer models show the structure of the thunderstorms and MCSs in SCTRAND events, and are these features truly rooted at different levels depending on the direction in which they are moving?

Can computer models simulate the three-dimensional process by which the two distinct MCSs merge in the SCTMERGE events, and can such a modeling study lend insight into how this merging process occurs?

REFERENCES

Arthur, Ami T., Gina M. Cox, Nathan R. Kuhnert, David L. Slayter, Kenneth W. Howard, 2005: THE NATIONAL BASIN DELINEATION PROJECT. *Bull. Amer. Meteor. Soc.*, **86**, 1443–1452.

Ashley, S. T., W. S. Ashley, 2008: Flood Fatalities in the United States. *J.Appl.Meteor.Climatol.*, **47**, 805-818, doi:10.1175/2007JAMC1611.1.

Bell, G. D., L. F. Bosart, 1989: A 15-Year Climatology of Northern Hemisphere 500 mb Closed Cyclone and Anticyclone Centers. *Mon.Wea.Rev.*, **117**, 2142-2164, doi:10.1175/1520-0493(1989)117<2142:AYCONH>2.0.CO;2.

Bluestein, H. B., M. H. Jain, 1985: Formation of Mesoscale Lines of Pirecipitation: Severe Squall Lines in Oklahoma during the Spring. *J.Atmos.Sci.*, **42**, 1711 1732, doi:10.1175/1520-0469(1985)042<1711:FOMLOP>2.0.CO;2.

Bluestein, H. B., G. T. Marx, and M. H. Jain, 1987: Formation of Mesoscale Lines of Precipitation: Nonsevere Squall Lines in Oklahoma during the Spring. *Mon.Wea.Rev.*, **115**, 2719-2727, doi:10.1175/1520-0493(1987)115<2719:FOMLOP>2.0.CO;2.

Bosart, L. F., F. Sanders, 1981: The Johnstown Flood of July 1977: A Long-Lived Convective System. *J.Atmos.Sci.*, **38**, 1616-1642.

Bradley, A. A., J. A. Smith, 1994: The Hydrometeorological Environment of Extreme Rainstorms in the Southern Plains of the United States. *J.Appl.Meteor.,* **33**, 1418-1431, doi:10.1175/1520-0450(1994)033<1418:THEOER>2.0.CO;2.

Brooks, H. E., D. J. Stensrud, 2000: Climatology of Heavy Rain Events in the United States from Hourly Precipitation Observations. *Mon.Wea.Rev.,* **128**, 1194-1201, doi:10.1175/1520-0493(2000)128<1194:COHREI>2.0.CO;2.

Caracena, F., R. A. Maddox, L. R. Hoxit, and C. F. Chappell, 1979: Mesoanalysis of the Big Thompson Storm. *Mon.Weather Rev.,* **107**, 1-17.

Chappell, C. F., 1993: Dissecting the flash flood forecasting problem. Post-Print Volume, *Third National Heavy Precipitation Workshop*, NOAA Tech. Memo. NWS ER-87, 293-297.

Ciach, G. J., W. F. Krajewski, and G. Villarini, 2007: Product-Error-Driven Uncertainty Model for Probabilistic Quantitative Precipitation Estimation with NEXRAD Data. *J.Hydrometeorol.,* **8**, 1325-1347.

Colman, B. R., 1990: Thunderstorms above Frontal Surfaces in Environments without Positive CAPE. Part I: A Climatology. *Mon.Wea.Rev.,* **118**, 1103-1122, doi:10.1175/1520-0493(1990)118<1103:TAFSIE>2.0.CO;2.

Cope, A.M., 2009: A Climatology of Flash Flood Events for the National Weather Service Eastern Region. NOAA Tech. Memo. NWS ER-103, 85 pp.

Corfidi, S. F., J. H. Meritt, and J. M. Fritsch, 1996: Predicting the Movement of Mesoscale Convective Complexes. *Wea.Forecasting*, **11**, 41-46, doi:10.1175/1520-0434(1996)011<0041:PTMOMC>2.0.CO;2.

Cotton, W. R., 1990: *Storms.* Geophysical Science Series, Vol. 1, Aster Press,158 pp.

Davis, R. S.,1993: AMBER, a prototype flash flood warning system. Preprints, *13th Conf. on Weather Analysis and Forecasting*, Vienna, VA, Amer. Meteor. Soc., 379-383.

Davis, R. S., 2001: Flash Flood Forecast and Detection Methods. *Meteorological Monographs*, **28**, 481-526, doi:10.1175/0065-9401-28.50.481.

Doswell, C. A., H. E. Brooks, and R. A. Maddox, 1996: Flash Flood Forecasting: An Ingredients-Based Methodology. *Weather and Forecasting*, **11**, 560-581.

Droegemeier, K. K., J. D. Smith, S. Businger, C. Doswell, J. Doyle, C. Duffy, E. Foufoula-Georgiou, T. Graziano, L. D. James, V. Krajewski, M. LeMone, D. Lettenmaier, C. Mass, R. Pielke, S. Rutledge, P. Ray, J. Schaake, and E. Zipser, 2000: Hydrological Aspects of Weather Prediction and Flood Warnings: Report of the Ninth Prospectus Development Team of the U.S. Weather Research Program. *Bull.Am.Meteorol.Soc.*, **81**, 2665-2680.

Fritsch, J. M., R. A. Houze, R. Adler, H. Bluestein, L. Bosart, J. Brown, F. Carr, C. Davis, R. H. Johnson, N. Junker, Y. Kuo, S. Rutledge, J. Smith, Z. Toth, J. W. Wilson, E. Zipser, and D. Zrnic, 1998: Quantitative Precipitation Forecasting:

Report of the Eighth Prospectus Development Team, U.S. Weather Research Program. *Bull.Am.Meteorol.Soc.*, **79**, 285-299.

Fritsch, J. M., R. J. Kane, and C. R. Chelius, 1986: The Contribution of Mesoscale Convective Weather Systems to the Warm-Season Precipitation in the United States. *J.Climate Appl.Meteor.*, **25**, 1333-1345, doi:10.1175/1520-0450(1986)025<1333:TCOMCW>2.0.CO;2.

Funk, T. W., 1991: Forecasting Techniques Utilized by the Forecast Branch of the National Meteorological Center During a Major Convective Rainfall Event. *Wea.Forecasting,* **6**, 548-564, doi:10.1175/1520-0434(1991)006<0548:FTUBTF>2.0.CO;2.

Geerts, B., 1998: Mesoscale Convective Systems in the Southeast United States during 1994–95: A Survey. *Wea.Forecasting,* **13**, 860-869, doi:10.1175/1520-0434(1998)013<0860:MCSITS>2.0.CO;2.

Giordano, L. A., J. Michael Fritsch, 1991: Strong Tornadoes and Flash-Flood-Producing Rainstorms During the Warm Season in the Mid-Atlantic Region. *Wea.Forecasting,* **6**, 437-455, doi:10.1175/1520-0434(1991)006<0437:STAFFP>2.0.CO;2.

Houze, R. A., B. F. Smull, and P. Dodge, 1990: Mesoscale Organization of Springtime Rainstorms in Oklahoma. *Mon.Wea.Rev.,* **118**, 613-654, doi:10.1175/1520-0493(1990)118<0613:MOOSRI>2.0.CO;2.

Jessup, S. M., A. T. DeGaetano, 2008: A Statistical Comparison of the Properties of Flash Flooding and Nonflooding Precipitation Events in Portions of New York and Pennsylvania. *Wea.Forecasting*, **23**, 114-130, doi:10.1175/2007WAF2006066.1.

Junker, N. W., R. S. Schneider, and S. L. Fauver, 1999: A Study of Heavy Rainfall Events during the Great Midwest Flood of 1993. *Wea.Forecasting*, **14**, 701-712, doi:10.1175/1520-0434(1999)014<0701:ASOHRE>2.0.CO;2.

Karl, T. R., R. W. Knight, 1998: Secular Trends of Precipitation Amount, Frequency, and Intensity in the United States. *Bull.Amer.Meteor.Soc.*, **79**, 231-241, doi:10.1175/1520-0477(1998)079<0231:STOPAF>2.0.CO;2.

Konrad, C. E., 1997: Synoptic-Scale Features Associated with Warm Season Heavy Rainfall over the Interior Southeastern United States. *Wea.Forecasting*, **12**, 557-571, doi:10.1175/1520-0434(1997)012<0557:SSFAWW>2.0.CO;2.

Konrad, C. E., 2001: The Most Extreme Precipitation Events over the Eastern United States from 1950 to 1996: Considerations of Scale. *J.Hydrometeor*, **2**, 309-325, doi:10.1175/1525-7541(2001)002<0309:TMEPEO>2.0.CO;2.

Lapenta, K. D., B. J. McNaught, S. J. Capriola, L. A. Giordano, C. D. Little, S. D. Hrebenach, G. M. Carter, M. D. Valverde, and D. S. Frey, 1995: The Challenge of Forecasting Heavy Rain and Flooding throughout the Eastern Region of the National Weather Service. Part I: Characteristics and Events.

Wea.Forecasting, **10**, 78-90, doi:10.1175/1520-0434(1995)010<0078:TCOFHR>2.0.CO;2.

Maddox, R. A., F. Canova, and L. R. Hoxit, 1980: Meteorological Characteristics of Flash Flood Events over the Western United States. *Mon.Wea.Rev.*, **108**, 1866-1877, doi:10.1175/1520-0493(1980)108<1866:MCOFFE>2.0.CO;2.

Maddox, R. A., C. F. Chappell, and L. R. Hoxit, 1979: Synoptic and Meso-α Scale Aspects of Flash Flood Events1. *Bull.Am.Meteorol.Soc.*, **60**, 115-123.

Maddox, R. A., L. R. Hoxit, C. F. Chappell, and F. Caracena, 1978: Comparison of Meteorological Aspects of the Big Thompson and Rapid City Flash Floods. *Mon.Weather Rev.*, **106**, 375-389.

National Centers for Environmental Prediction, 2007. North American Regional Reanalysis Homepage. http://www.emc.ncep.noaa.gov/mmb/rreanl/.

NOAA, 2010a: Natural hazard statistics. [Available online at http://www.nws.noaa.gov/om/hazstats.shtml].

NOAA, 2010b: Storm Data. Ashville, NC, NESDIS, National Climatic Data Center. [Available online at http://www4.ncdc.noaa.gov/cgi-win/wwcgi.dll?wwEvent~Storms].

NWS, 2008: National Weather Service Manual 10-950. Definitions and General Terminology. [Available online at http://www.nws.noaa.gov/directives/sym/pd01009050curr.pdf].

Orville, H. D., 1968: Ambient Wind Effects on the Initiation and Development of Cumulus Clouds over Mountains. *J.Atmos.Sci.,* **25**, 385-403, doi:10.1175/1520-0469(1968)025<0385:AWEOTI>2.0.CO;2.

Parker, M. D., R. H. Johnson, 2000: Organizational Modes of Midlatitude Mesoscale Convective Systems. *Mon.Wea.Rev.,* **128**, 3413-3436, doi:10.1175/1520-0493(2001)129<3413:OMOMMC>2.0.CO;2.

Pontrelli, M. D., G. Bryan, and J. M. Fritsch, 1999: The Madison County, Virginia, Flash Flood of 27 June 1995. *Wea.Forecasting,* **14**, 384-404, doi:10.1175/1520-0434(1999)014<0384:TMCVFF>2.0.CO;2.

Rappaport, E. N., 2000: Loss of Life in the United States Associated with Recent Atlantic Tropical Cyclones. *Bull.Amer.Meteor.Soc.,* **81**, 2065-2073, doi:10.1175/1520-0477(2000)081<2065:LOLITU>2.3.CO;2.

Rogash, J. A., J. Racy, 2002: Some Meteorological Characteristics of Significant Tornado Events Occurring in Proximity to Flash Flooding. *Wea.Forecasting,* **17**, 155-159, doi:10.1175/1520-0434(2002)017<0155:SMCOST>2.0.CO;2.

Schiesser, H. H., R. A. Houze, and H. Huntrieser, 1995: The Mesoscale Structure of Severe Precipitation Systems in Switzerland. *Mon.Wea.Rev.,* **123**, 2070-2097, doi:10.1175/1520-0493(1995)123<2070:TMSOSP>2.0.CO;2.

Scofield, R. A., V. J. Oliver, and L. Spayd, 1980: Estimating rainfall from

thunderstorms with warm tops in the infrared imagery. Preprints, *Eighth Conf. on Weather Forecasting and Analysis*, Denver, CO, Amer. Meteor. Soc., 85-92.

Schumacher, R. S., R. H. Johnson, 2005: Organization and Environmental Properties of Extreme-Rain-Producing Mesoscale Convective Systems. *Mon.Wea.Rev.*, **133**, 961-976, doi:10.1175/MWR2899.1.

Schumacher, R. S., R. H. Johnson, 2006: Characteristics of U.S. Extreme Rain Events during 1999–2003. *Weather and Forecasting*, **21**, 69-85.

Spayd, L. E., Jr., and R. A. Scofield, 1983: Operationally detecting flash flood producing thunderstorms which have subtle rainfall signatures in GOES imagery. Preprints, *Fifth Conf. on Hydrometeorology*, Tulsa, OK, Amer. Meteor. Sox., 190-197.

Thiao, W., R. A. Scofield, and J. Robinson, 1993: The relationship between water vapor plumes and extreme rainfall events during the summer season. NOAA Tech. Rep. NESDIS 67, U.S. Department of Commerce, 69 pp.

Tollerud, E. I., D. Rodgers, and K. Brown, 1987: Seasonal, diurnal, and geographic variations in the characteristics of heavy-rain-producing mesoscale convective complexes: A synthesis of eight years of MCC summaries. Edmonton, AB, Canada, Amer. Meteor. Soc., 143-146.

University Corporation for Atmospheric Research, 2010. CISL's NCAR Command

Language. http://www.ncl.ucar.edu/.

U.S. Census Bureau. "State Rankings -- Statistical Abstract of the United States. Resident Population – July 2008." [Available online at http://www.census.gov/statab/rank/rank01.html].

U.S. Census Bureau, 2004: "2000 Census of Population and Housing", *Population and Housing Unit Counts.* PHC-3-1, United States Summary. Washington, DC. [Available online at http://www.census.gov/prod/cen2000/phc3-us-pt1.pdf].

Wilks, D. S., 1995: *Statistical methods in the atmospheric sciences : an introduction.* Academic Press.467 pp.

Winkler, J. A., B. R. Skeeter, and P. D. Yamamoto, 1988: Seasonal Variations in the Diurnal Characteristics of Heavy Hourly precipitation across the United States. *Mon.Wea.Rev.*, **116**, 1641-1658, doi:10.1175/1520-0493(1988)116<1641:SVITDC>2.0.CO;2.

Yoshizaki, M., Y. Ogura, 1988: Two-and Three-Dimensional Modelling Studies of the Big Thompson Storm. *J.Atmos.Sci.*, **45**, 3700-3722.

Young, K. C., 1993: *Microphysical processes in clouds.* Oxford University Press, 427 pp.

Zhang, D., J. M. Fritsch, 1986: Numerical Simulation of the Meso-β Scale Structure

and Evolution of the 1977 Johnstown Flood. Part I: Model Description and Verification. *J.Atmos.Sci.*, **43**, 1913-1944.

Zhang, D., J. M. Fritsch, 1987: Numerical Simulation of the Meso-β Scale Structure and Evolution of the 1977 Johnstown Flood. Part II: Inertially Stable Warm-Core Vortex and the Mesoscale Convective Complex. *J.Atmos.Sci.*, **44**, 2593-2612.

Zhang, D., J. M. Fritsch, 1988: Numerical Simulation of the Mesa-β Scale Structure and Evolution of the 1977 Johnstown Flood. Part III. Internal Gravity Waves and the Squall Line. *J.Atmos.Sci.*, **45**, 1252-1268.